Report No. CDOT-DTD-R-2003-4

THE BEHAVIOR OF FIBER-REINFORCED POLYMER REINFORCEMENT IN LOW TEMPERATURE ENVIRONMENTAL CLIMATES

by
Renée Cusson and Yunping Xi

Department of Civil, Environmental & Architectural Engineering
University of Colorado
Boulder, CO 80309-0428

Sponsored by
Colorado Department of Transportation

December 2002

Colorado Department of Transportation
Research Branch
4201 E. Arkansas Ave.
Denver, CO 80222

The contents of this report reflect the views of the author(s), who is(are) responsible for the facts and accuracy of the data presented herein. The contents do not necessarily reflect the official views of the Colorado Department of Transportation or the Federal Highway Administration. This report does not constitute a standard, specification, or regulation.

EXECUTIVE SUMMARY

Fiber-reinforced polymers (FRP) have been shown to be excellent construction materials in low temperature environments due to their low thermal conductivity to strength ratio, and high strength to density ratio. However, in cold weather climates, high residual stresses can build up within the fibrous composite material due to different coefficients of thermal expansion of the constituent materials. In regions where the environmental temperature may vary from day to day, microcracking and void generation can accentuate these residual stresses. This report focuses on the effects of combined loading history and environmental exposure on the durability of carbon and glass Fiber-reinforced polymer reinforcement bars. Specifically, degradations of FRP bars due to coupled freeze-thaw cycling, tension, and tensile fatigue loading are experimentally investigated. After a series of cyclic environmental preconditioning and mechanical loading, the degradation and variable loading rate dependency of GFRP bars are evaluated from several aspects: strength degradation due to freeze-thaw cycling, static and dynamic tensile strength, elongation, Young's modulus, displacement stiffness, fatigue strength, and failure mode analysis including bar grip failures.

An environmental chamber was used to test the influence of sub-zero ambient temperatures on the mechanical and visco-elastic properties of the rods. Each specimen requiring pre-conditioning was subjected to low temperature thermal cycling at an 8 cycle per day rate. Specimens were exposed to 250 freeze-thaw cycles corresponding to 750 hours of exposure. A total of 105 bars were prepared, 32 of which were pre-conditioned in this manner. Following 250 thermal cycles, the bars were visually examined for the development of cracks and long-term mechanical properties are then investigated. Investigations were made into the variable rate effect on the ultimate tensile strengths and elastic properties of the different FRP reinforcements. Static and dynamic tension tests were performed to determine the ultimate tensile capacities of two types of commercially available GFRP reinforcing bars (3/8"$GFRP_S$, and 3/8" & 1/2"$GFRP_R$) and one type of CFRP bar. Preliminary fatigue tests were performed to establish a definitive program for future study to determine the relationship of load range to number of cycles, and effect of micro-cracking endured during freeze-thaw cycling.

The following conclusions have been made based on analysis of the results:

1) The rate sensitivity of the glass fiber strength is quite apparent in comparisons of ultimate strength results obtained for variable frequency load rates.
2) There were noticeable increases in strength and marked changes in fracture appearance with increasing load rate.
3) Freeze-thaw conditioning does have some deleterious effect on the ultimate strength capabilities of glass fiber polymer reinforcing bars. The degree of deterioration of the FRP bars depends on the temperature ranges and number of freezing-thawing cycles applied. Not more than 10% of deterioration in tensile strength of FRP bars occurred under the temperature conditions (See Section 5.3) applied in the project. Although the temperature conditions were more severe than the actual temperature fluctuations in Colorado, the degradation of tensile strength should be considered properly in structural design.
4) No definitive conclusions could be established based on load control tests, stroke controlled test programs produced more complete failure modes and repeatable load-displacement curves.
5) A basis for fatigue testing up to 2 Hz has been established.
6) A complete experimental system and testing procedures are established for durability testing of FRP materials under environmental and mechanical loadings.

ACKNOWLEDGEMENTS

The financial support provided by the Colorado Department of Transportation (CDOT) for this project is gratefully acknowledged. The writers would like to express their thanks to the Research Branch of CDOT for continuous support and encouragement throughout this study, and specifically to Richard Griffin and Ahmad Ardani of CDOT Research Branch, Michael McMullen of CDOT Bridge Division, and Matt Greer of FHWA for their valuable suggestions and inputs. The writers would also like to thank Hughes Brothers, Inc for donating the Aslan100 GFRP samples, Marshall Industries Composites, Inc for the C-Bar™ GFRP bars, and Mitsubishi Chemical for providing the Leadline™ CFRP products.

TABLE OF CONTENTS

LIST OF FIGURES

LIST OF TABLES

1.0 Introduction

1.1 Background

Several approaches have been taken to investigate the effectiveness of different fiber-reinforced polymers (FRP) as durable reinforcement material for concrete. Many studies worldwide have shown that FRP reinforcing products provide an excellent non-corrosive, lightweight, non-metallic substitute for steel. A variety of structural products and shapes are currently being produced in order to explore the beneficial structural properties of these composite materials. Unfortunately, the mechanical properties of these FRP composites vary from one product to another as a result of varied manufacturing processes. Therefore, detailed material characteristics need to be established for specific loading and atmospheric conditions. Research projects have often focused on the polymer composite's high glass transition temperature (T_g), and the effects of moisture, while variable load rate FRP performance data for cold environments is limited. Preliminary reports bring to our attention the potential benefits of the use of FRP products at low temperatures. Tests outlined by Karbhari and Pope [46] show how off-axis and transverse strength can increase at low temperatures due to matrix hardening. Other low temperature tests mentioned by Karbhari revealed increased strength properties of wound fiberglass composites, and an improvement in the static load response of unfilled polymeric materials. On the other hand, complexities may arise due to water absorption and freeze-thaw cycling. P. K. Dutta [47] realized the importance of considering composite constituents and the negative effects of matrix cracking due to extreme low temperatures. Discrepancies in coefficients of thermal expansion of the constituent elements cause high residual stresses to occur in composites at low temperatures. Comparative low temperature experiments are a limited few and information regarding design of composites in cold climates is developing at a slow rate. The benefits of FRP reinforcement use in cold weather environments may best be seen in rehabilitation of our deteriorating parking structures, bridge decks, and roadway systems. Construction benefits include lower transportation, labor, and maintenance costs. The deteriorating effects of steel reinforced structures in other corrosive environments such as marine sites, waste water plants, and near cooling towers, provide additional opportunities to consider FRP reinforcement. It is therefore essential to develop a firm understanding of the durability possibilities and effects of fiber-reinforced polymers exposed to severe and frequently changing environments.

1.2 Scope

This report focuses on the effects of combined loading history and environmental exposure on the durability of carbon and glass Fiber-reinforced polymer reinforcement bars. Specifically, degradation of FRP bars due to coupled freeze-thaw cycling, tension, and fatigue loading is experimentally investigated. After a series of cyclic environmental preconditioning and mechanical loading, the degradation and variable load rate dependency of GFRP bars is evaluated from these aspects: strength degradation due to freeze-thaw cycling, static and dynamic tensile strength, elongation, Young's modulus, displacement stiffness, fatigue strength, and failure mode analysis including bar failures and grip failures.

The study discusses tests of two types of commercially available E-glass fiber-reinforced polymer rods, and one type of carbon fiber-reinforced polymer rod used in concrete construction. Each specimen type considered is unique in terms of cross-sectional dimensions, composition, and surface deformation patterns. One type of GFRP used is of the production line Aslan100 donated by Hughes Brothers, Inc. These glass-reinforced bars are made of continuous longitudinal E-glass fibers, 70% fibers by weight, and bound by thermosetting vinyl ester (100%) resin matrix. Another type of 3/8"-diameter E-glass fiber concrete reinforcement used was C-Bar™ Deformed FRP Bars manufactured by Marshall Industries Composites, Inc. These bars consist of 35% by volume binding material reinforced with 60% by volume continuous E-glass fibers. Approximately 3% ceramic fibers are included to reinforce the ribbed surface deformations. Pitch-based continuous fiber prestressing bars called Leadline™ were provided by Mitsubishi Chemical of Japan. These bars contain 65% by volume carbon fiber and 35% epoxy resin by volume.

1.3 Organization of the Report

The contents of this report have been organized in the following fashion. Chapter 2 covers the historical development of FRP reinforcement. FRP types, material properties, and durability aspects are addressed. Chapter 3 presents a literature review of current research on the uses and implementation of fiber-reinforced polymer rebar in construction applications worldwide. In Chapter 4, the composite constituent materials are described and the FRP manufacturing processes is outlined. Chapter 5 establishes the experimental plan for the project.

The material types used are described in detail. Material properties such as effective diameter and specific gravity are calculated. Detailed descriptions of specimen preparation, the anchorage grip system, rebar potting layout, and assembly are also included. The environmental conditioning program used for freeze-thaw cycling is outlined. Chapter 6 is comprised of the mechanical testing procedures and data collection. It addresses the importance and effects of the variable rate dependency of glass-reinforced polymers. Preliminary results and failure mode analysis are described. Conclusions of the environmental and mechanical testing results presented in the previous chapter appear in Chapter 7.

2.0 Historical Development of FRP Reinforcement

The selection of FRP reinforcement for structural applications depends on several issues. While corrosion resistance, light weight, and non-magnetic are among the more desirable aspects for choosing fiber plastics, they also exhibit high tensile strength, low mechanical relaxation, good toughness, and high fatigue resistance. Historically, prohibitive initial costs and the extreme care needed in handling these composite materials have restricted widespread development of their use in reinforced concrete designs. Extensive degradation due to marine salts and continued use of de-icing material on roadways and bridges are compelling enough to consider non-corrosive Fiber-reinforced polymer materials. Steel reinforcement may initially be protected against corrosion by the alkalinity of the concrete, but combinations of temperature, moisture, and chlorides ultimately reduce the alkalinity of the concrete. The resulting deterioration of steel reinforcement in concrete structures has allowed FRP to be realized as a possible replacement candidate in particular instances.

Several forms of FRP reinforcement for construction purposes are being manufactured today; from one-dimensional bars and tendons (cables) to two-dimensional gratings and grids. A variety of these elements are shown in Figure 1 [20]. Empirical data on the thermo-mechanical properties of these reinforcements needs to be expanded before safe design practices can take place.

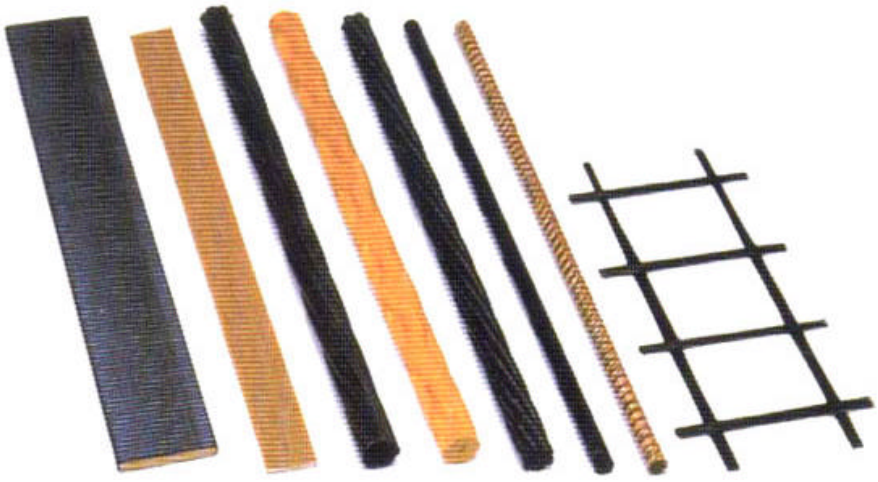

Figure 1: Variable types of FRP reinforcing

The data in Table 1 compare properties of glass and carbon Fiber-reinforced polymer bars and tendons with steel reinforcements. Properties of FRP reinforcements vary with fiber volume, size, and loading grip system used. Unlike steel, tensile strength of FRP bars is a function of bar diameter. Shear lag causes outer diameter fibers to experience more stress than fibers on the inside of the cross-section of the FRP bar. As the diameter of the bar increases, the tensile stress varies across the cross-section due to shear lag developing between the fibers. Ultimately, larger diameter bars could experience reduced strength and inefficiency due to this shear lag phenomenon.

Although the thermal coefficients are dissimilar between each FRP constituent, the coefficient of thermal expansions for glass fiber composite bars tend to have a similar, 6 $x10^{-6}$ in/in/°F, coefficient as concrete. Popular for being lightweight, FRP reinforcing bars have a specific gravity of only 1.5 to 2.4. Nearly four times lighter than steel, lower transportation costs could provide an additional incentive for FRP use in remote and cold weather regions.

Table 1: Property Comparison of Continuous Fiber Composites and Steel

Tensile Propeties	Steel Bar	Steel Tendon	GFRP Bar	GFRP Tendon	CFRP Tendon
Ultimate Strength, ksi	70 - 100	200 - 270	75 - 175	200 - 250	240 - 350
Elastic Modulus, ksi	29,000	27 - 29,000	6 - 8,000	7 - 9,000	22 - 24,000
Specific Gravity	7.9	7.9	1.5 - 2.0	2.4	1.5 - 1.6
Tensile Strain, %	>10	>4	3.5 - 5.0	3.0 - 4.5	1.0 - 1.5
Thermal Coeff. $x10^{-6}$/ºF	Longitudinal: 6.5	6.5	5.5	5.5	0.38 to -0.68

FRP materials display anisotropic response and exhibit high tensile strength in the primary direction of the reinforcing fibers. Ultimately, mechanical properties of FRP bars are highest when measured in the longitudinal direction parallel to the fibers, with close attention paid to loading history, duration, temperature and moisture. Carbon fiber bars and tendons have been tested with ultimate strengths greater than steel. And at about three times greater than glass, stiff carbon fibers allow carbon fiber-reinforced polymer (CFRP) tendons an elastic modulus approaching that of the prestressing steel tendon.

On a whole however, the modulus of elasticity to strength ratio of most FRP products is relatively small compared to steel, and many projects have been carried out in hopes of improving its ductility. Experienced researchers in the field of fiber composites at the University of Missouri-Rolla have recently focused on a new type of FRP bar with increased ductility. Pseudo-ductility was validated for FRP rods composed of different types of fibers that would fail at different times during loading [3]. They have also delved into computer modeling for predicting durability response of composite materials [87]. Similar to the work in Missouri, Drexel University developed hybrid FRP bars that were found to exhibit equivalent bilinear stress-strain characteristics, with a Young's modulus approaching that of steel. Their bars failed in a gradual manner, with a definite yield and an ultimate strength higher than yield [13]. Figure 2 compares the tensile stress-strain behaviour between common reinforcing fibers and steel. The stress-strain behaviour of most fiber/polymer composites approximates that of a linear-elastic brittle material and does not yield. Figure 3 illustrates an approximate stress-strain comparison between FRP reinforcement and some common construction materials. Besides the expected response of FRP in tension, one curve represents the general form of response for ordinary structural-grade steel in tension, and the other is representative of materials for which the relation of stress to strain varies continuously over the range of stress, such as for concrete and wood [80]. Although high ultimate strengths are achievable, the brittle behaviour of FRP inhibits onsite bending and forming of the reinforcement.

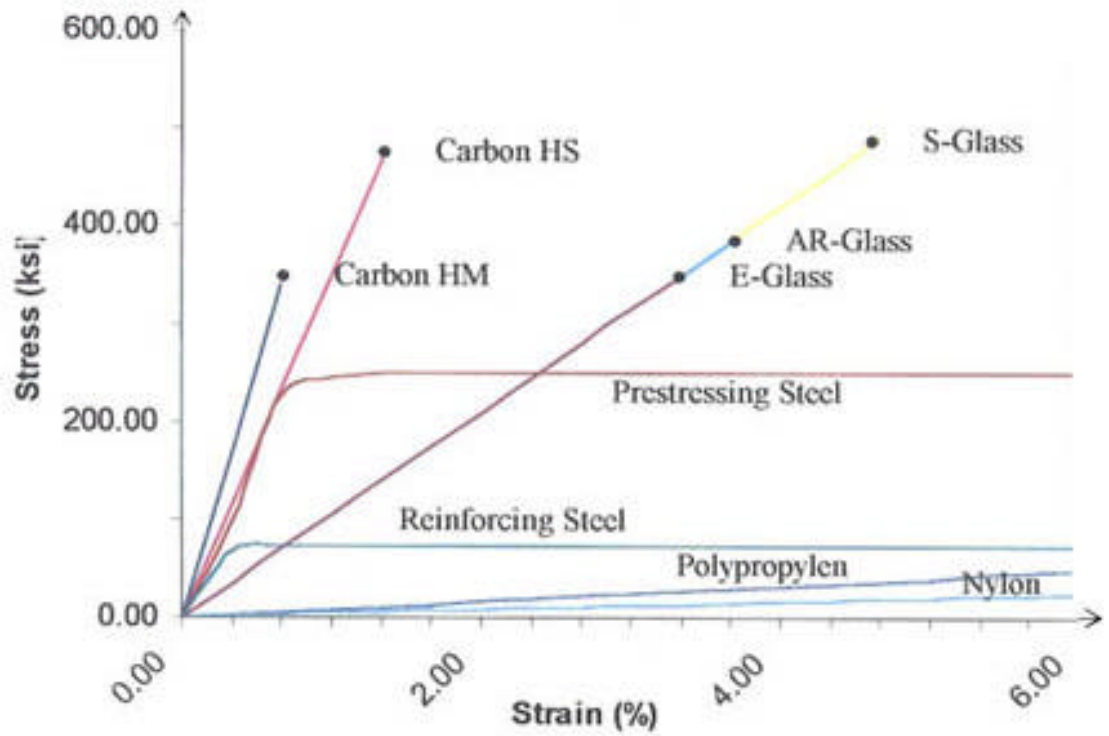

Figure 2: Tensile Stress-Strain Behaviour of Reinforcing Fibers As Compared With Steel.
(Adapted from Gerritse and Schurhoff [53])

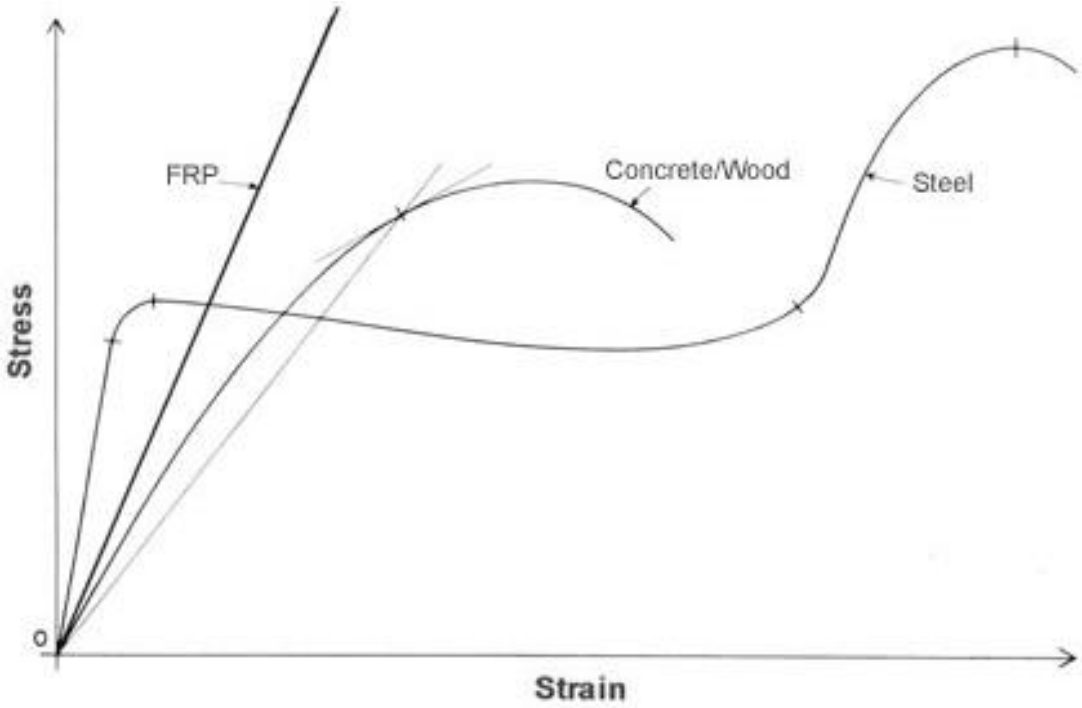

Figure 3: Tensile Stress-Strain Behaviour of Construction Materials.
(Adapted from Ambrose [80])

Extensive long-term durability properties of FRP reinforcing rods are slowly being established for building construction purposes. Realizing this, Hoshijima & Yagi [14] developed two types of composites for durability evaluation. One of the two composites, Leadline^{TM}, was developed as carbon fiber (CF) reinforced plastic rods. The CF rods were manufactured by pultrusion with epoxy resin as the matrix. Lightweight continuous carbon fiber was chosen for its high strength, and durability. Available in two surface types, smooth and etched, the CF rods were applied as tendons and reinforcing bars in concrete. The CF rods were tested for relaxation and creep. By aligning fibers, CF rods were found to have about 1.5 time's greater strength than steel tendons. After a 1000-hour test, creep was also found to be nearly zero at 6500 to 7000 kilograms of force.

In evaluating FRP as reinforcement for concrete bridge decks, Rahman *et al.* strongly emphasized the importance of establishing the capabilities of FRP under frequent freeze-thaw action, in a saline-alkaline environment, undergoing cyclic traffic loads [23]. In the design of highways and bridges that experience repeated dynamic loading, Fiber-reinforced products exhibit excellent internal damping properties resulting in better vibration energy absorption.

Durability aspects of FRP are strongly affected by varying environmental and service load conditions such as: weathering, chemical resistance, wet/dry cycles, and fatigue. Exposure tests considering weatherability, resistance to alkali, and salt water were also conducted on the carbon fiber (CF) rods developed by Hoshijima & Yagi [14]. Alkali resistance of the CF rod was established by a 20-22 day immersion test. Comparing a steel rod and CF rod submersed in an alkaline 3% NaCl + saturated $Ca(OH)_2$ solution at 40ºC (104ºF), resistance of the CF rod was found to be equal to and even greater than that of the steel tendon. After being engaged in a salt water-testing device for one year, five pieces of the CF rod showed no reduction of tensile strength.

Sasaki et al. [27] evaluated the combined effects of long-term durability of FRP cables tested in a maritime exposure test site. Carbon, aramid, glass and vinylon fiber cables were evaluated for tensile strength, modulus, relaxation, under direct sunlight radiation, and saltwater immersion. Each of the six cables was subjected to varying ultraviolet intensity tests either with or without prestressing. The first two cases considering the effects of direct sunlight without prestressing showed no major changes in residual tensile strength. Another study case without

prestressing was submerged in seawater, not directly exposed to UV effects. The composites with the aramid fiber and epoxy resin matrix experienced the most drastic strength reduction, only retaining 49% of the initial value. Also, the glass and vinylon matrices realized strength degradations of 65% and 71% respectively. Most of the prestressed CFRP and AFRP obtained from direct sunlight locations experienced less than 30% relaxation losses, while specimens not directly affected by UV rays underwent losses less than 20%. Ultraviolet rays can degrade the efficiency of the fiber composites due to a chemical reaction in the polymer matrix. When used in design of exposed elements, UV-inhibitors can be added to the resin matrix mix before curing.

3.0 FRP Application Worldwide

In order to establish adequate durability and design data, it is important to consider studies on a variety of factors. The following is a brief illustration of how the significance of FRP reinforcements has been received worldwide.

3.1 Canadian Activities

The Canadian Society of Civil Engineers sparked interest in fiber-reinforced polymer in the 1980's, and a national network, *Technical Committee on Advanced Composite Materials in Bridges and Structures*, was established in 1989. In early 1992, the committee identified several potential topics for concentrated research efforts to be undertaken at universities and research institutions [8]. These research topics include:

- Parking Structures
- Long-Term Material Properties
- Enclosure Systems
- Rehabilitation and Repair
- Bridges

The *Institute for Research in Construction at the National Council* in conjunction with *Public Works Canada* is also conducting inquiries into fiber reinforcement and Fiber-reinforced concrete. Two major universities in Canada, University of Manitoba, and Queen's University in Kingston, have contributed to the establishment of Fiber-reinforced polymer reinforcement for concrete structures. A few of their more recent FRP endeavors include developing design recommendations for FRP reinforced bridge decks, and studying the long-term response of FRP prestressed concrete beams under sustained loading.

3.2 European Activities

The European community has found FRP to be most advantageous as prestressing concrete members. Initially, while post-tensioning, glass fiber composites were being developed in Germany, pre-tensioning, aramid fiber strips and bars were being applied in the Netherlands [35]. Germany boasts the world's first highway bridge using FRP post-tensioning cables, which opened in 1986 [35]. Europe has since established their own conference for composite materials: *International Symposium on Non-Metallic Reinforcement for Concrete Structures.* Many current

FRP applications in Europe are concerned with structural safety; developing externally bonded reinforcement for damaged structures. The European community does financially support a few research programs. The EUROCRETE project, conducted from 1993 to 1997, focused on material development, durability in aggressive environments, structural behavior, and design methods [34]. The first footbridge in Britain using glass FRP reinforcement was built at Chalgrove in Oxfordshire in 1995 as part of the EUROCRETE project. The BRITE/EURAM project intended to accomplish such tasks as: materials research and performance profiling of FRP tensile elements, investigation into the load bearing behavior of prestressed/reinforced FRP concrete members, and design criteria development for FRP reinforced concrete members [34].

Led by Luc Taerwe and Stijn Matthys, the University of Ghent, in Belgium has produced significant studies investigating concrete slabs with different types of FRP grid reinforcements in order to establish acceptable serviceability behavior [36, 37]. Their tests covered ultimate limit states for bending, serviceability limit states, ductility, deformability, and ultimate to service load ratio. Recognizing the importance of fire resistance, they have also considered elevated temperature effects on the thermo-mechanical properties of FRP materials, resins and their interface. Ferrier and Hamelin of Claude Bernard University in Lyon have been interested in the influence of time, temperature, and loading cycles on carbon epoxy reinforcement for concrete structures [10]. They have also considered external bonding of FRP to concrete and interface tested under fatigue loading [11].

3.3 Japanese Activities

Early trial-and-error experimentations in the manufacturing of fiber polymer products began in Japan in the 1970's. Researchers began developing FRP for concrete structures in the 1980's, with the *Society for Research of Composite Materials for Reinforcing Concrete Using Continuous Fibers* (CCC Society) encouraging research activities since 1988. An encouraging number of universities participate in the advancement of composite materials in construction. Approximately twenty universities of civil engineering and ten universities of building engineering are involved in this effort. Most importantly, the Ministry of Construction sponsors the *National Research Project*, which focuses on the advancement of new materials. For the Japanese, the application of fiber-reinforced polymers is divided into two categories: bars and grids for reinforcing and prestressing, and fiber composite sheets for repair and strengthening of

existing structures [12]. In Japan, continuous fiber bars are not allowed to replace reinforcing steel and prestressing steel for load bearing members [38]. These advanced materials have not yet been accepted to replace steel, but rather enhance it. Before this can be an accepted practice, extensive performance evaluation methods need to be developed for fire resistance and durability. Funding for composite materials research in Japan has encouraged them to produce extensive data in almost all the necessary areas. They have a well-established design base for FRP construction. Uomoto, one of the foremost leaders in FRP achievements, and his colleagues have put exhaustive efforts into evaluating tensile strength, creep behavior and fatigue properties of glass, Aramid and carbon fiber rods affected by various chemicals in different temperatures [39, 40, 41]. Also, an innovative project by Sugiyama et al, developed continuous fiber flexible plastic tubing and tested basic properties, load-deflection, and stress concentrations of a U-shaped section [31].

3.4 United States Activities

It is reported that since the 1930's, the US has shown some interest in the advantages of developing non-metallic fiber based reinforcement. Although the U.S. Army Corps of Engineers accomplished the early long glass fiber research in the 1950's and 1960's, it wasn't until the 1980's when there was a surge of interest in capitalizing on the beneficial properties offered by FRP bars and tendons. The National Bureau of Standards, which has since become the National Institute of Standards and Technology, conducted some of the first research into Fiber-reinforced plastic composite rods [6]. Unfortunately even today, unlike their counterparts in Japan and Europe, the US does not have a national coordinated research program, and major corporations are slow to sponsor extensive FRP product development. In the US, the National Science Foundation and the US Department of Transportation's Federal Highway Administration independently sponsor research into performance capabilities of reinforced plastics [5]. In an effort to bring FRP design to the forefront, ASCE began a series of conferences on *Advanced Composites Materials in Civil Engineering Structures* in 1991. Following their lead, in 1993, ACI International sponsored its *First International Symposium on Fiber-reinforced Polymer Reinforcement for Reinforced Concrete Structures*.

Many projects examining FRP reinforcement and composite construction have been carried out by major universities and institutions throughout the country. Current institutional

research covers a wide spectrum of concerns. However, it has been found that recent interests have focused on three areas of development:

- Retrofit and Rehabilitation
- Properties of FRP Reinforcement
- Properties and Performance of FRP Reinforced Concrete

Universities showing significant interest in developing FRP composites through published research and/or established curricula include, but are not limited to:

- West Virginia University
- University of Missouri-Rolla
- University of Wisconsin, Madison
- University of California, San Diego
- University of Kentucky, Lexington
- Pennsylvania State University
- University of Arizona, Tucson
- University of Wyoming
- Iowa State University
- University of Utah
- Oregon State University
- Drexel University

Representatives of the University of West Virginia have shown a remarkable amount of interest in composite material activities. They have worked extensively in developing models to predict long-term creep behavior of polymer and metal matrix composites; fatigue life of hybrid composites; and mechanical properties such as Young's modulus, Poison's ratio, and ultimate strength [9, 78]. They have explored durability aspects mainly regarding glass FRP, producing reports on strength and stiffness properties under harsh conditions; accelerated aging of bars exposed to varying humidity, temperatures and stresses; and design factors for bridges constructed with FRP bars [78, 42, 68]. The University of Arizona has also shown considerable effort in expanding data on fiber-reinforced polymers. Experiments have been done testing Aramid fiber tendons for relaxation, creep and fatigue in varying temperature and chemical environments [25]. Ultimate tensile strength, ultimate strain, elastic modulus, and moisture absorption were evaluated for innovative alkali resistant glass fiber bars exposed to corrosive solutions [26]. Many of the other institutions have focused on such studies as retrofitting concrete structures, concrete behavior prestressed with FRP tendons, bond strength and interface properties.

Europe and Japan have gotten a jump on FRP use in construction; the United States needs to take a more active role at introducing new technology materials into their construction projects. A prime opportunity is available. The bridge infrastructure of the United States is in constant need of repair and rehabilitation. It is reported that 43% of the bridges in the United

States have been identified as being structurally deficient or functionally obsolete due to corrosion [79]. By now a few prototype applications of FRP there have been developed as a replacement for steel reinforcing in highway structures. Between universities, the department of transportation and FHWA, West Virginia has done a considerable amount of work with FRP in highway infrastructure. The vehicular bridge erected across Buffalo Creek in McKinleyville, West Virginia, is considered to be the first vehicular bridge in the United States to use FRP reinforcement in the concrete deck [68]. The bridge was completed in August 1996 and opened to traffic the following month. The bridge is being field monitored and tested for response to loads, aging, and temperature fluctuations. Creative Pultrusion and Martin Marietta Materials have each gone so far as to have designed a composite bridge deck system made of pultruded elements; Superdeck™ and DuraSpan™, respectively.

To remain on the leading edge of technology, it is imperative for future investigations to expand upon the efforts of prior experimental works. There appear to be abundant reports of investigations into bond performance and creep-rupture of reinforcing rods embedded in concrete as well as durability properties at high temperatures. Upon review of much invaluable experimentation, it was realized that particular devotion should be made to further exploring the possible effects of freeze-thaw cycling on the durability of FRP reinforcing bars in highway applications.

4.0 FRP Constituents and Manufacturing Processes

A fiber-reinforced polymer or FRP is an advanced composite, or materials system. It is defined as a solid material which is composed of two or more substances having different physical characteristics in which each substance retains its identity while contributing desirable properties to the whole; a structural material made of plastic within which a fibrous material is embedded [51]; the components remain physically identifiable exhibiting an interface between one another. FRP composites exhibit anisotropic behavior and are often composed of brittle constituents. The successful physical performance of these composites is therefore inherently dependent upon the individual properties of the materials of which they are made.

4.1 Fiber Reinforcement

Structural polymer applications, such as those discussed in this report, efficiently combine the extraordinary strength and stiffness properties of small diameter fibers with a ductile polymer binder, or resin matrix. The fiber component consists of fine thread-like natural or synthetic material characterized by its aspect ratio (fiber length divided by fiber diameter), with length nearly 100 times its diameter. The fibers used in structural FRP composites are continuous and are not to be confused with the short fibers commonly used in fiber-reinforced concrete (FRC).

Fibers may be treated for protection and to aid in saturation during composite manufacture. Experiments performed by Tsushima, *et al*. indicate that fiber surface preparation and treatment can ultimately affect composite material properties. The study looked at the fracture mechanism of CFRP made from fibers with various surface treatment levels and with two kinds of matrix. Their results show that CFRP strength was significantly affected by the fiber surface treatment level. The inter-laminar shear strength increased with an increasing level of surface treatment, however, the longitudinal tensile strength decreased with increasing surface treatment level [71]. This illustrates how every aspect of FRP fabrication can ultimately have an effect on final product characteristics.

Glass, carbon, and aramid are the most commonly employed organic and inorganic substances available for the fibrous load-bearing constituent.

Glass is an amorphous material made from silica (SiO_2). Unlike window or bottle glass, fibers for reinforcing can achieve very high tensile strengths if the surface is protected from

abrasion, moisture and water vapor. In addition to being highly abrasive to one another, moisture has also been found to have a deleterious effect on the overall strength of glass fibers. Physico-chemical absorption produces local areas of corrosion thus reducing strength properties. This strength reduction is thought to be due to a combination of stress corrosion and a reduction in effective surface energy [66]. Stress corrosion is the preferential attack of areas under stress in a corrosive environment, when the environment alone would not have caused corrosion. Therefore, glass fibers are coated with a binder which enhances compatibility with the resin matrix for protection. E-glass, S-glass, and C-glass represent the three main types of glass fibers available. Economical E-glass fibers, commonly referred to as fiberglass, are manufactured from lime-alumina-borosilicate glass developed for its high electrical resistance. E-glass fiber polymers are the most widely used in general commercial applications, comprising 80-90% of commercial glass fiber production [22]. Performing well at high temperatures, high strength S-glass fiber polymers are about 1/3 stronger than E-glass but expensive to produce, and are prevalent mostly in military applications. Exhibiting excellent resistance to corrosion, C-glass composites are useful where acidic materials and chemically aggressive environments present problems.

Three natural resources supply the production of structural carbon fibers: pitch, a by-product of petroleum distillation; PAN, polyacrylonitrile; and rayon. *High modulus* and *high strength* are the two types of carbon fiber available. Characteristics for these two carbon type fibers are compared with those of E-glass roving in Table 2 shown below. In general, carbon fibers tend to exhibit high stiffness and good resistance to chemical attack, but have low toughness and impact resistance. Carbon fibers may often exhibit a slightly negative coefficient of thermal expansion, meaning they contract upon heating, increasing in negativity with higher modulus fibers. Carbon fibers may also be referred to as graphite. In graphite fibers, the carbon has been *graphitized* and has a carbon content of greater than 99%.

The most widely used *organic* fibers for structural reinforcing applications belong to a class of liquid crystal polymers. In the family of nylons, aramid fibers are useful in corrosive environments, and have high thermal stability. These fibers are less dense than carbon fibers and have a lower Young's modulus. And while carbon and glass fibers have excellent creep resistance, aramid fibers exhibit good fatigue and abrasion resistance. Aramid fibers are less

brittle than glass or carbon and although they do not need any surface treatments, they do not bond as well to matrices.

Table 2: Typical Properties of FRP Fiber Types

Tensile Propeties	E-Glass	Aramid	Carbon-PAN		Carbon-pitch
			high strength	high modulus	high modulus
Ultimate Strength, ksi	275-500	504 - 525	505 - 1,030	360 - 565	305 - 350
Elastic Modulus, ksi	10,500	6, - 27,000	33,360 - 42,640	42,640 - 85,280	75,420 - 139,235
Specific Gravity	~2.5	~1.3	~1.8	~1.75	~1.75
Tensile Strain, %	2.4 - 5.6	1.86 - 8.75	1.6 - 1.8	0.7	0.3
Poissons Ratio	0.2	0.38	-0.2	-0.2	N/A
Density lb/in^3	0.094	0.052	0.065	0.063	0.063
Thermal Coeff. $x10^{-6}/^oF$	Longitudinal: 9.0	-2.0 to -4.0		Carbon: 0.0 to -2.0	

N/A: Not Available

4.2 Matrix Polymers

Polymers are plastics whose molecular structure consists of a chain of one or more repeating units of atoms. The two classifications of polymer matrices are: thermoplastic and thermosetting. While molecules remain linear, thermoplastic polymers can be repeatedly softened at high temperatures. Thermoset plastics are used for structural purposes for their ability to undergo a chemical reaction when cured. Molecules of these polymers become highly cross-linked at high temperatures and the matrix becomes an infusible and insoluble material.

Affecting mechanical, chemical, and thermal properties of FRP composites, the thermoset matrix resin serves a variety of purposes. It protects the fibers from environmental degradation, provides lateral support against compression buckling, and allows the transfer of stresses from the bar surface to interior fibers. Although strong, the reinforcing fibers can be brittle and not all fibers may be capable of resisting the applied stress. The matrix helps redistribute the load and can absorb energy by deforming under stress. Besides stiffness, the matrix polymer also allows the composite good thermal stability and chemical resistance. To enhance structural and aesthetic characteristics, the polymer matrix resin is combined with filler, catalyst, and additives (ultraviolet inhibitors, dies, release agents, etc.). Still, for structural

applications, the resin matrix makes up only a small portion of the total volume of the FRP composite.

Some common thermosetting matrix resins include epoxy, polyester (Ortho/Iso), and vinyl ester. Table 3 shows a property comparison of these thermosetting resins. The Composites Institute estimates that approximately 85% of U.S. composite production is based on unsaturated polyester resins [1].

Vinyl ester resin is used in the bars of this study. It is one of the commercially available types of unsaturated polyesters. A di-epoxide is reacted with acrylic acid and the product cured by polymerizing the vinyl groups to form the cross-linked vinyl ester resin. A vinyl ester resin matrix provides better mechanical performance than costly polyesters, doesn't absorb as much water, and doesn't shrink as much when cured. The compatibility of a particular resin with the reinforcing fibers is also a concern. Compatibility is measured by the wet-out, or degree of saturation. Strengths will be lower if the wet-out is deficient [72]. Vinyl ester resins tend to saturate the fibers more efficiently resulting in higher strengths, while epoxies require much higher fiber content. Vinyl esters also bond well to glass to increase the resistance of these fibers in aggressive chemical environments.

Table 3: Various Properties of FRP Matrix Resins

Tensile Propeties	Epoxy	Polyester	Vinyl Ester
Ultimate Strength, ksi	8 - 20	3 - 15	11.5 - 13
Elastic Modulus, ksi	360 - 595	305 - 595	460 - 490
Tensile Strain, %	1.0 - 9.0	1.0 - 6.0	3.9 - 5.2
Poissons Ratio	0.37	0.35-0.40	0.373
Density lb/in^3	.040 - .047	.036 - .052	.038 - .040
Thermal Coeff. $x10^{-6}/^oF$	Longitudinal: 25 - 45	30 - 55	15 - 35

N/A: Not Available

4.3 Manufacturing Processes

Design and manufacturing processes have significant influences on resulting composite properties. When investigating FRP as reinforcing, it needs to be emphasized that there are two

factors influencing testing results. The thermo-mechanical properties of the composite material can rely on both its chemical composition as well as the process by which the composite is produced. Quality control during manufacture plays a critical role in developing a product's final characteristics.

Several composite processing methods exist. Pultrusion is one of the most popular methods for producing linear composite elements with the primary reinforcing fibers in the longitudinal direction. Pultrusion is a continuous filament molding process incorporating fiber reinforcement with thermosetting resin matrices. Figure 4 shows the pultrusion process as illustrated by Creative Pultrusions, Inc. [52]. Using guide plates for aligning the reinforcing material in the proper locations, continuous fibers are drawn through a low viscosity liquid state polymer solution of resin, filler, catalyst and other additives. Once all fibers are wet-out, they are drawn into a steel die and cast with the desired cross-section properties. The molecules of the thermosetting resin become highly cross-linked as the composite is heated at elevated temperatures, and a solid polymer product emerges. As fiber orientation can be strongly influenced by the material flow during the molding process, the reinforcement-to-matrix ratio and content are carefully controlled. Close dimensional tolerances can be obtained in this process.

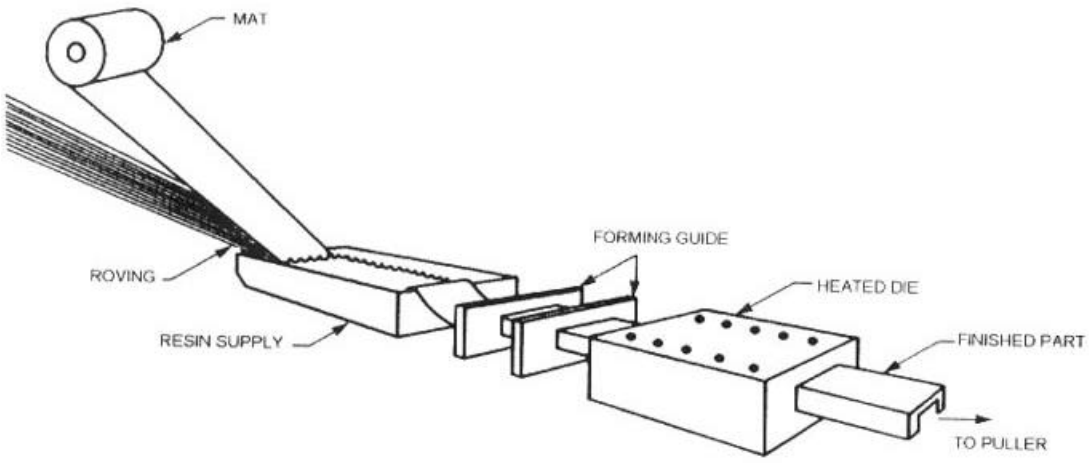

Figure 4: The Pultrusion Process

Material type, fiber and matrix volume fractions, and manufacturing processes all can have an effect on the elastic properties of FRP bars. Investigations into manufacturing a more ductile hybrid composite can help increase its strength and low elastic modulus. One area to

consider with FRP is that properties such as tensile strength and elastic modulus are dependent upon the direction of measurement in relation to the direction of the fibers. These mechanical properties are proportional to the amount of fiber by volume oriented in the direction of measurement. Although anisotropic, preferential directional strengthening of the fibers during this manufacturing procedure provides FRP composites a design advantage over steel.

Geometrical shape and surface texture can also be manipulated. FRP rods are a typical product produced by the pultrusion process. A secondary process occurs to add surface deformations if required for adequate bond properties. A helical fiber over-winding, protruding ribs, or a sand coating can be added to the smooth outer layer of resin. FRP reinforcing bars are available as smooth, braided, spiral wound, and as a twisted-rod strand, just to name a few. While these surface characteristics are beneficial, one must be aware that by simply increasing bar diameter can decrease its ultimate strength. In reduced cross-sections, increasing fiber volume can increase strength properties.

5.0 Experimental Plan

5.1 Materials and Specimen Preparation

5.1.1 Product Line

The present study discusses tests of two types of commercially available E-glass fiber-reinforced polymer rods, and one type of carbon fiber-reinforced polymer rod used in concrete construction. Each specimen type considered is unique in terms of cross-sectional dimensions, composition, and surface deformation patterns.

One type of GFRP used is of the production line Aslan100 by Hughes Brothers, Inc. These glass-reinforced bars are made of continuous longitudinal E-glass fibers, 70% fibers by weight, and bound by thermosetting vinyl ester (100%) resin matrix. The bars are wrapped with a clear helical glass fiber chord, surface coated with resin, and rolled in sand to provide enhanced bond properties. Hughes Brothers, Inc. differentiates between production lines by the color of the helical wrap. The bars used in this study are of the "clear" helical wrap production run made May, 2000. Two sizes of these bars were available for testing, 3/8"diameter and 1/2" diameter. These rough coated bars are denoted as 3/8"$GFRP_R$ and 1/2"$GFRP_R$, respectively.

Another type of 3/8"-diameter E-glass fiber concrete reinforcement used was C-Bar™ Deformed FRP Bars manufactured by Marshall Industries Composites, Inc. These deformed bars are cast with a smooth clear urethane modified vinyl ester resin with "lugs" or protruded surface deformations. These surface texture undulations provide a mechanical interlock to inhibit longitudinal movement when bonded to concrete. These bars consist of 35% by volume binding material reinforced with 60% by volume continuous E-glass fibers. Approximately 3% ceramic fibers are included to reinforce the ribbed surface deformations. The maximum average spacing of the ribs is 0.225 inches, 0.030 inches high. A limited number of 1/2"-diameter bars of this type were also available. These bars with the smooth resin surface are denoted as 3/8"$GFRP_S$ and 1/2"$GFRP_S$.

Linearly oriented coal tar pitch-based continuous fiber prestressing bars called Leadline™ were provided by Mitsubishi Chemical of Japan. These are epoxy-impregnated 3/8" nominal diameter carbon rods with a helical wrap nearly flush with the bar surface. Leadline™ is designed to be used as prestressing reinforcement. These bars contain 65% by volume carbon fiber and 35% epoxy resin by volume. In Figure 5 a sample of each type bar used is shown

along side a #4 steel rebar for comparison. Table 4 summarizes the tensile properties for each of these type bars as supplied by the manufacturers.

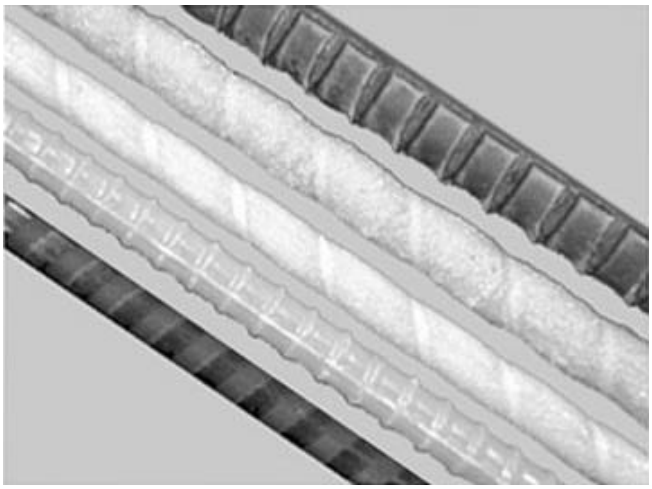

Figure 5: GFRP & CFRP Samples Used

Table 4: Material Properties As Supplied By the Manufacturer

Tensile Propeties		**Aslan100: $GFRP_R$**		**C-Bar: $GFRP_S$**		**LEADLINE: CFRP**	
Ultimate Strength	3/8'	110 ksi	(825 MPa)	121 ksi	(840 MPa)	455 ksi	(3140 MPa)
	1/2'	100 ksi	(860 Mpa)	116 ksi	(800 MPa)		
Elastic Modulus		5,920 ksi	(40.8 Gpa)	6,000 ksi	(42 GPa)	21,320 ksi	(147 GPa)
Specific Gravity		2.00	-	1.90	-	1.60	-
Thermal Coeff. $x10^{-6}/°F$		Longitudinal: 5.04	-	4.50	-	0.38 to -0.68	-

5.1.2 Effective Diameter

The mean diameter and area of each type bar was determined. ASTM D3916 [55] suggests a micrometer be used to measure the minimum and average bar thickness at "several points along its length." However, this method is impractical for the deformed and sand coated bars used in this study due to their irregular surface structure. Therefore, the average diameter of each bar was determined from the mass, length, and water displacement properties as suggested by Castro and Carino [44]. Eight-inch and twelve-inch samples were used to calculate the effective diameter for each bar type. Three to five samples of each size were used to obtain an appropriate measure of density. A micrometer was used to accurately measure the average

lengths of each sample. The minimum and mean cross-sectional areas and diameters calculated for each specimen type are included in Table 5. A complete list of measured data is included in the appendix.

Table 5: Effective Diameter, Area, and Density of Test Specimens

	DIAMETER (in)		**AREA** (in^2)		**DENSITY**	
Bar Type	Minimum	Average	Minumum	Average	(g/cm^3)	(lb/in^3)
3/8" CFRP	0.359	0.369	0.101	0.107	1.744	0.063
3/8" GFRPs	0.369	0.388	0.107	0.118	1.947	0.070
3/8" GFRPr	0.376	0.390	0.111	0.119	2.046	0.074
1/2" GFRPr	0.503	0.515	0.199	0.208	1.999	0.072
1/2" GFRPs	-	0.5[1]	-	0.196[1]	-	-

[1] Samples were not available for this type bar to determine precise values.

5.1.3 Specific Gravity

The specific gravity is a property that can easily be measured. The specific gravity of a solid can be utilized to identify a particular material, to follow physical changes, or to indicate a degree of uniformity within a sample batch. A representative sample of bars was taken from the testing materials. Data collection followed steps outlined in ASTM D 792-00, *Standard Test Methods for Density, and Specific Gravity of Plastics by Displacement* [62]. A balance with a precision of 0.001 g was used throughout the procedure. The specific gravity of each sample was calculated as follows.

$$SG = \frac{a}{(a + w - b)}$$

a = weight of specimen in air (without wire or sinker)

b = weight of specimen immersed in water (with sinker)

w = weight of wire and sinker

Table 6 outlines the results obtained for each type material available. At nearly a quarter of the weight of steel, the reduced weight of FRP bars allow for significant benefits in lower transportation costs and decreased handling and installation time.

Table 6: Specific Gravity of Test Specimens

Bar Type	WEIGHT (lb/ft)	WEIGHT (g/mm)	SPECIFIC GRAVITY Minumum	SPECIFIC GRAVITY Average
3/8" CFRP	0.084	0.118	1.70	1.74
3/8" GFRPs	0.096	0.147	1.85	1.95
3/8" GFRPr	0.108	0.158	1.92	2.05
1/2" GFRPr	0.180	0.271	1.89	2.00
1/2" GFRPs[1]	-	-	-	-

[1] Samples were not available for this type bar.

5.2 Anchorage and Grip System

Since high compressive stresses and mechanical damage can occur due to surface serrations of traditional wedge-shaped grips, the FRP bars used cannot be tested using the same gripping techniques as used for steel. For experiments of this study, MTS 647.50 hydraulic wedge grips were used. It is necessary to encase the ends of the FRP specimen in an anchorage system to distribute the grip stresses so they are not concentrated at critical points on the bar. Figure 6 illustrates how the lateral compressive forces of the gripping system would be applied to each end of the bar. An accurately designed anchoring device must be able to develop the full strength of the bar allowing for failure to occur in the gage length of the specimen.

Initially, bars were cut 40 inches in length, however, due to coupled loading and conditioning restraints, maximum specimen length was limited to 24 inches, independent of bar diameter. The free-length is the unsupported distance between the end anchorage grips. The average free-length for the 40-inch specimens was 16.00 inches, and 24-inch samples averaged a free-length of 11.34 inches.

The tubular anchorage system developed for this project, as shown in Figure 7, requires each end of the reinforcing bar be embedded into an RB4-40 (Schedule 40) Steel Pipe with Randustrial M-183 Bolt Anchor Immersible Sulfaset expanding cement filler.

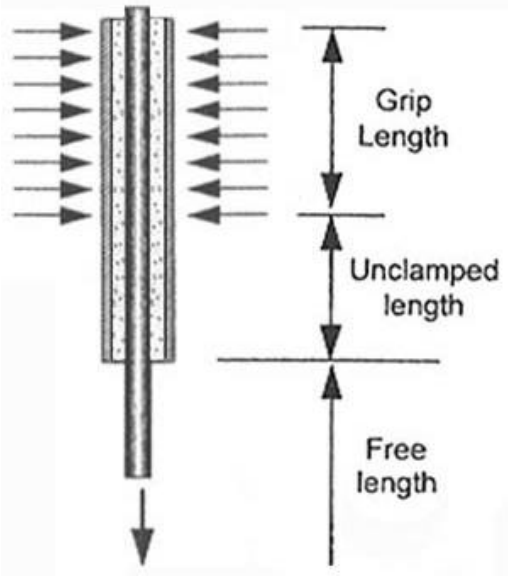

Figure 6: Grip System
(Adapted from Castro & Carino [44])

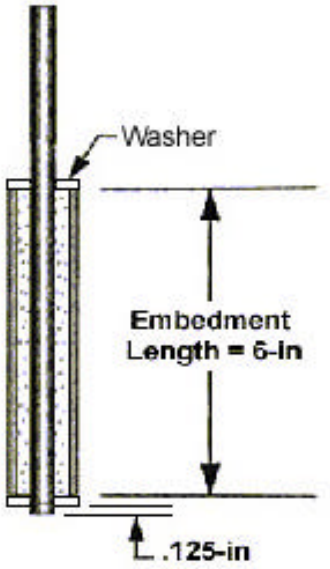

Figure 7: Rebar Potting Layout

Two wooden assembly racks were designed to accommodate the preparation of 14 bars at a time. Figure 8 shows the wooden frame able to support an arrangement of 11 bars. Each specimen type was cut 24 inches in length and the cement rebar potting procedure was guided by the specifications for *Anchorage of FRP Rebar for Tensile Testing* as outlined by Hughes Brothers, Inc [45]. To minimize eccentricity when loading, washers and tape are used to position each bar concentric with the steel pipe while curing. Samples were secured in the assembly rack as shown.

Figure 8: Assembly rack

The large 1/2"-dia specimens used 1" inner-diameter uncoated carbon steel pipe with .133" wall thickness. For the small 3/8"-dia specimens, 3/4" inner-diameter uncoated carbon steel pipe with .113" wall thickness was used. The cementitious grout was mixed to produce a water-to-cement ratio of 0.37. The mixture was "spooned" into the pipe and continuously tamped to release any entrapped air. Tape was also used to cap each tube in order to hold each bar in position and contain the grout or epoxy. The filler material was allowed to cure for 24 hours before inverting the samples to assemble the other end. Samples completed with the cementitious grout were allowed to cure for a minimum of 1 week before pre-conditioning and 28 days before testing. Each prepared specimen is labeled with an identifying number and the dates of assembly. The 3D drawing in Figure 9 illustrates the final bar and anchor layout.

Figure 9: 3-D View of Bar and Anchor Layout

To ensure the bar will not pullout from the tube when loaded (Figure 10), an adequate embedment length needs to be established. Due to the restriction on specimen length, the maximum embedment lengths for the 40-in and 24-in specimens ranged from 24 to 32 times and 12 to 16 times the bar diameter, respectively. The free-length-to-diameter ratios for the bars vary from 24-43 depending on bar size. Initial tensile tests show these lengths to be sufficient for GFRP specimens; however, the anchorage system for CFRP samples needed to be redesigned. Therefore, a limited number CFRP and GFRP samples were made with anchorages filled with epoxy. The epoxy grips were assembled in a similar manner as described previously. Many different gripping systems have been devised, but researchers have solely adopted no specific system.

Figure 10: Bar and Epoxy Pullout

5.3 Conditioning Program

5.3.1 Freeze-Thaw Cycling

Temperature induced stresses can be a major concern for concrete reinforced structures in regions of drastic temperature changes. In an FRP-concrete composite system, self-equilibrating stresses develop in two cases: differential thermal expansion and contraction of the FRP and concrete, and when the distribution of temperature over the cross-section of the FRP is non-linear. The self-equilibrating stresses due to non-linear temperature distributions occur because each fiber in the cross-section is restrained against free expansion by being monolithic with adjacent fibers [76]. In the longitudinal direction, GFRP rebar tends to have a coefficient of thermal expansion similar to hardened concrete; however, CFRP tends to be significantly less, even negative. In the transverse direction, GFRP can experience coefficients 5-8 times greater than concrete [81]. In low temperatures, this can cause bursting stresses to buildup in the concrete surrounding the reinforcement and negatively affect the bond characteristics and break down concrete cover.

The FRP material within itself can experience difficulties in low temperature conditions due to water absorption and matrix cracking initiated by freeze-thaw cycling. Initially, it may be thought that since the fibers in reinforced polymers are generally least sensitive to the environment, the longitudinal tensile strength would not be significantly affected by temperature effects. However, attention to the interaction of the constituent materials under variable temperature conditions is necessary.

The importance of composite make up is realized by considering the negative effects of matrix cracking. "Microcracking and void generation can occur in composite materials during freeze-thaw cycling due to mismatched coefficients of thermal expansion of constituent elements [47]." Tests conducted by Dutta [47], where FRP samples were subjected to 150 freeze-thaw cycles from +73.4ºF to -40ºF (+23ºC to -40ºC), showed that the tensile strength of glass-epoxy FRP was reduced by about 10% because of freeze-thaw cycling. And although similar tests on carbon-epoxy composites did not show any significant reduction in tensile strength or elastic modulus, thermal cycling did produce significant degradation of off-axis properties for CFRP.

Additional studies attribute crack accumulation and failure to water absorption in void generations. Verghese, *et al.* [50&77], investigated the effect of temperature cycling of polymer composite materials in a water bath. They found that although it is virtually impossible to freeze water in a highly cross-linked amorphous polymer like vinyl ester, in the composite system, interfacial crack dimensions exist that are large enough to facilitate the freezing of water during aging. Verghese, *et al.* believes that it is this mechanism then of freezing and the associated volume increase during transition that leads to the propagation of cracks and accumulation of damage [77]. Comparisons between resins affected by moisture and freeze-thaw cycling performed by Karbhari and Pope [46], show that vinyl ester resins have an advantage at combating these deleterious effects in cold weather applications.

Another aspect of concern relating to the physical behaviour of the matrix resin during temperature fluctuations exists. Reinforcing fibers exhibit greatest strength and mechanical properties when perfectly aligned. Curing of the polymer resin matrix can cause micro-buckling of the fibers to occur. At low temperatures, increased stiffness does not allow the matrix to yield under applied tensile load, restricting fiber realignment. Resulting load distribution is not uniform. Some fibers will carry more of the load than others, and failure may occur prematurely, initiating progressive failure in other fibers.

The uncertainties in the area of low temperature usage need to be further examined as advanced fiber composites provide benefits of low ratio of thermal conductivity to modulus or strength, and high ratio of modulus or strength to density.

The possible effects of low temperature conditions are analyzed in the subsequent study. The following procedure outlines the pretreatment used to standardize the temperature and humidity requirements of each “conditioned” specimen prior to testing. Development of the

conditioning program was guided by ASTM Standards: D 618; *Standard Practice for Conditioning Plastics for Testing* [56], and C 666; *Standard Test Method for Resistance of Concrete to Rapid Freezing and Thawing* [57]. The freezing and thawing procedure applied to the FRP bars follows similar methods applied to concrete, in order to appropriately measure durability effects on FRP as reinforcing for concrete applications.

An environmental chamber, manufactured by Russells Technical Products and shown in Figure 11, is used to test the influence of sub-zero ambient temperatures on the mechanical and visco-elastic properties of the rods. The intent of this study is to consider short-term axial tension for ultimate strength, Young's modulus, and elongation obtained at ambient temperature and –20°F (-29°C) with a tolerance maintained within $\pm$3°F.

Figure 11: Environmental Chamber

The refrigeration equipment provides continuous, reproducible cycles within a desired temperature range, and was designed specifically for the university to be operated simultaneously while loading specimens in the MTS testing apparatus. The preconditioning program developed for this research is a result of the first attempt at successful operation of this new machinery. Much time was spent analyzing the freeze-thaw cycling capabilities of the equipment. Extensive timing tables were established that outlined the time required for the environmental chamber to achieve each desired temperature level within acceptable tolerance. Since this research has begun, the environmental chamber has been incorporated into other research projects investigating the effects of freeze-thaw on concrete specimens.

After extensive research into previous experiments done on temperature effects of FRP reinforcements was concluded, there seemed to be a lack of abundant data for FRP in the low temperature range between -20ºF to 60ºF. Each specimen requiring pre-conditioning was thus subjected to low temperature thermal cycling between 68°F (20°C) and –20°F (-29°C) temperature excursions with a 1-hour hold at –20°F and 20-minute hold at 68°F, achieving an 8

cycle per day rate. Figure 12 graphically represents the cycling procedure for a 12-hour period. Specimens were exposed to 250 freeze-thaw cycles corresponding to 750 hours of exposure. A total of 105 bars were prepared, thirty-two of which were pre-conditioned in this manner: 1-40" CFRP sample, 15-3/8"GFRP$_S$, 4-3/8"GFRP$_R$, 11-1/2"GFRP$_R$, and 1-1/2"GFRP$_S$. Additional 3/8"GFRP$_R$ bars are available for future testing. Specimens that were not subjected to freeze-thaw cycling were stored in the structures testing laboratory at room temperature and relative humidity.

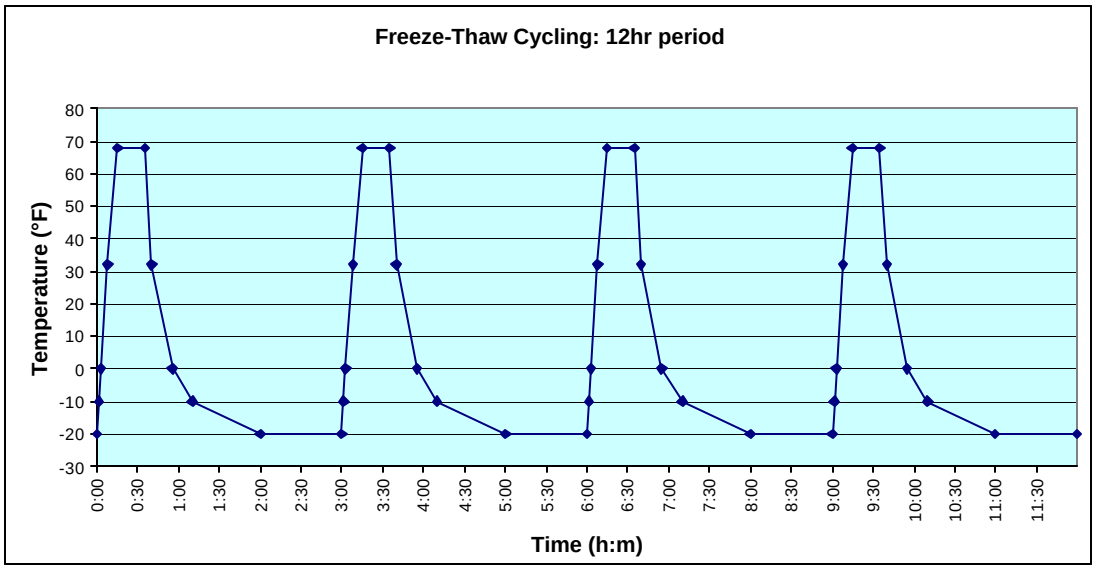

Figure 12: 12-Hr Freeze-Thaw Cycling Program

6.0 Test Methods and Results

Mechanical properties of fiber-reinforced plastics cannot be evaluated by the standard test methods developed for traditional construction materials. Exact testing procedures for these materials are still being developed, taking into consideration loading conditions and material characteristics as obtained from the manufacturer. The following are standard durability test methods often applied to fiber-reinforced polymers. Non-destructive evaluation techniques can also be useful. Of those listed, the durability test methods covered in this report include tension, fatigue, and chemical resistance.

- Tension test
- Creep failure test
- Flexural tension test
- Thermal expansion test
- Chemical resistance test
- Long-term relaxation test
- Horizontal shear strength test
- High cycle tensile fatigue test

Following 250 thermal cycles, the bars were visually examined for the development of cracks and long-term mechanical properties were then investigated. Investigations were made into the variable rate effect on the ultimate tensile strengths and elastic properties of the different FRP reinforcements. Preliminary fatigue tests were performed to establish a definitive program for future study to determine the relationship of load range to number of cycles, and effect of micro-cracking endured during freeze-thaw cycling.

A minimum of 3 specimens was considered for each test and environmental combination. In many cases, several samples were available for testing in each category, with improper failure modes eliminated from the cumulative results.

6.1 Non-Destructive Evaluation

A preliminary non-destructive inspection for the detection of flaws and matrix cracking due to freeze-thaw preconditioning was undertaken. A 50X microscope was used to develop digital images examining surface deformation and cracking. A sample of these images is shown in Figures 14 and 15.

Figure 14: Microscopic View of GFRPr Bar

Figure 15: Microscopic View of GFRPr Bar

6.2 Tensile Tests

6.2.1 Static Tension

To evaluate axial tensile strength, at least three samples of each type bar were tested for each procedure. Test methods followed the guidelines set forth in ASTM: D 3916, *Standard Test Method for Tensile Properties of Pultruded Glass-Fiber-Reinforced Plastic Rod* [55]. Similar methods can be applied to the evaluation of carbon fiber bars, but may not be adequate at the high level of stress required for tensile failure. In order to accurately calculate tensile strength and modulus of elasticity, the effective bar diameters were measured as outlined previously.

Initial static tension tests were performed with the Tinius Olsen testing apparatus shown in Figure 16. The ultimate tensile capacities of two types of commercially available GFRP

reinforcing bars (3/8"$GFRP_S$, and 3/8" & 1/2"$GFRP_R$) and one type of CFRP bars were examined. The FRP bars are positioned in the testing machine as shown in Figure 17. The anchorages are held in steel wedge shaped grips that apply sufficient lateral pressure to prevent slippage during loading. Load is applied in the longitudinal direction parallel with the fibers. The specimen is loaded axially until fracture occurs or there is a sudden drop in load capacity. This testing apparatus did not have data acquisition capability. As suggested in ACI Committee 440's report [83], if the test machine is not equipped with either load or displacement control, a timing device may be used to observe the time taken to apply a known increment of stress. This procedure was followed, and it was calculated that the specimens were loaded at approximately 250 lbs/sec. A preliminary analysis of the failure mode was made and the bar was released. A total of 23 FRP bars were tested in axial tension in this manner. Of these, there were 3 unconditioned carbon fiber bars, 9 unconditioned glass fiber bars, 1 conditioned carbon bar, and 10 conditioned glass bars. The nominal ultimate tensile strength is calculated by dividing the maximum load carried before failure by the original minimum cross-sectional area.

Figure 16: Tinius Olsen Machine

Figure 17: 24-Inch FRP Bar in Tensile Testing Apparatus

6.2.2 Static Tension Results

Several comparisons were made with the data collected from the ultimate tensile strength tests performed on the Tinius Olsen machine. The average ultimate tensile strengths for all bars tested using the Tinius Olsen testing apparatus are listed in Table 7.

It was intended to examine the variability of test results between the 40-in and 24-in specimens to determine whether the free-length or grip length of the test specimen has an effect on the outcome. Figures 18 & 19 graphically compare the results obtained for each 24-inch and 40-inch specimen, unconditioned and conditioned, respectively. However, there were not enough 40-inch specimens tested to arrive at an adequate conclusion. In most cases, the ultimate strengths of the 40-inch specimens were found to be higher than the average strengths of the 24-inch bars. This was not the case in all of the tests; discrepancies could be due to variability in loading rate. Preliminary results show the average strength of 40-inch unconditioned CFRP bars tested by the Tinius Olsen machine is 483,168 psi, a 14% greater ultimate strength than the 24-inch unconditioned CFRP bars. The average ultimate tensile strength of the carbon fiber bars are about 4-times stronger than the glass fiber bars. The average strengths of the 24-inch and 40-inch unconditioned 3/8" $GFRP_S$ specimens were 118,458 psi, and 119,159 psi, respectively. The average strength of the 24-inch unconditioned 3/8" $GFRP_R$ specimens was 109,309 psi.

Table 7: Results of Static Tensile Tests

Load Rate	Bar Type	Tensile Load 24" Maximum (lbs)	Tensile Strength Nominal (psi)	COV (%)	SD	Tensile Load 40" Maximum (lbs)	Tensile Strength Nominal (psi)	COV (%)	SD
UNCONDITIONED:									
0.01 Hz Frequency:	3/8" CFRP	41,975	415,594	5.000%	21003	48,800	483,168	-	-
0.01 Hz Frequency:	3/8" $GFRP_S$	12,675	118,458	1.116%	1322	12,750	119,159	-	-
0.01 Hz Frequency:	3/8" $GFRP_R$	12,133	109,309	1.259%	1376				
0.01 Hz Frequency:	1/2" $GFRP_R$	14,938	75,063	4.852%	3642				
0.01 Hz Frequency:	1/2" $GFRP_S$					20,000	102,041	-	-
CONDITIONED:									
0.01 Hz Frequency:	3/8" CFRP					47,375	469,059	-	-
0.01 Hz Frequency:	3/8" $GFRP_S$	11,625	108,645	2.443%	2654				
0.01 Hz Frequency:	3/8" $GFRP_R$	11,733	105,706	1.812%	1916				
0.01 Hz Frequency:	1/2" $GFRP_R$					23,500	118,342	0.300%	355
0.01 Hz Frequency:	1/2" $GFRP_S$					19,000	96,939	-	-

[1]Graph Included

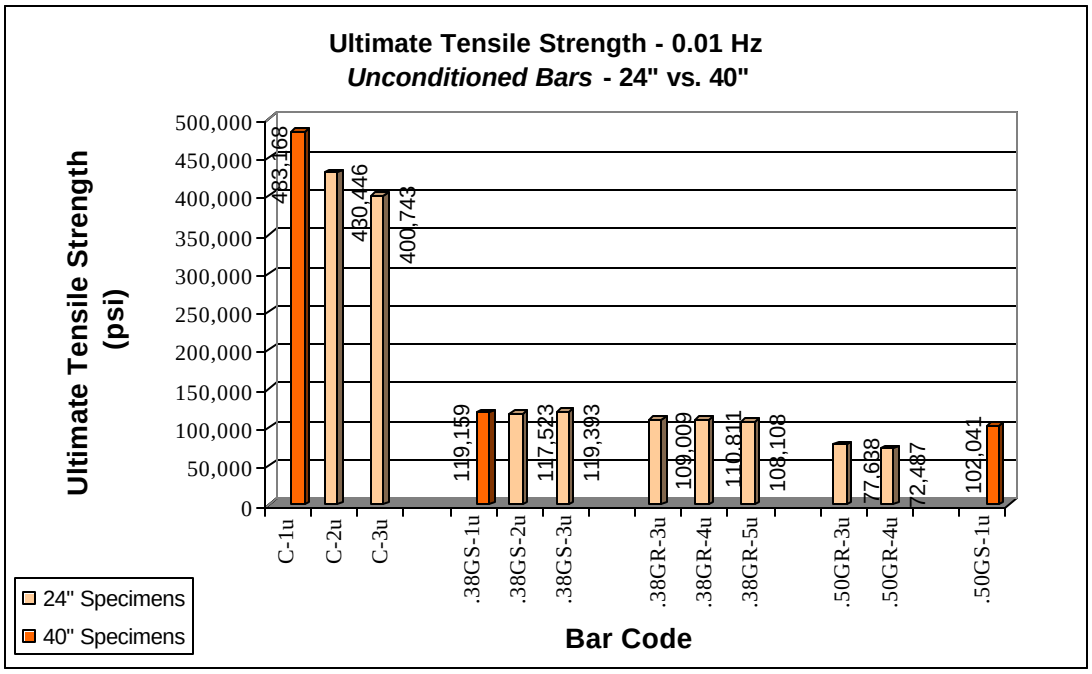

Figure 18: Results of Initial Tensile Tests for Unconditioned Specimens

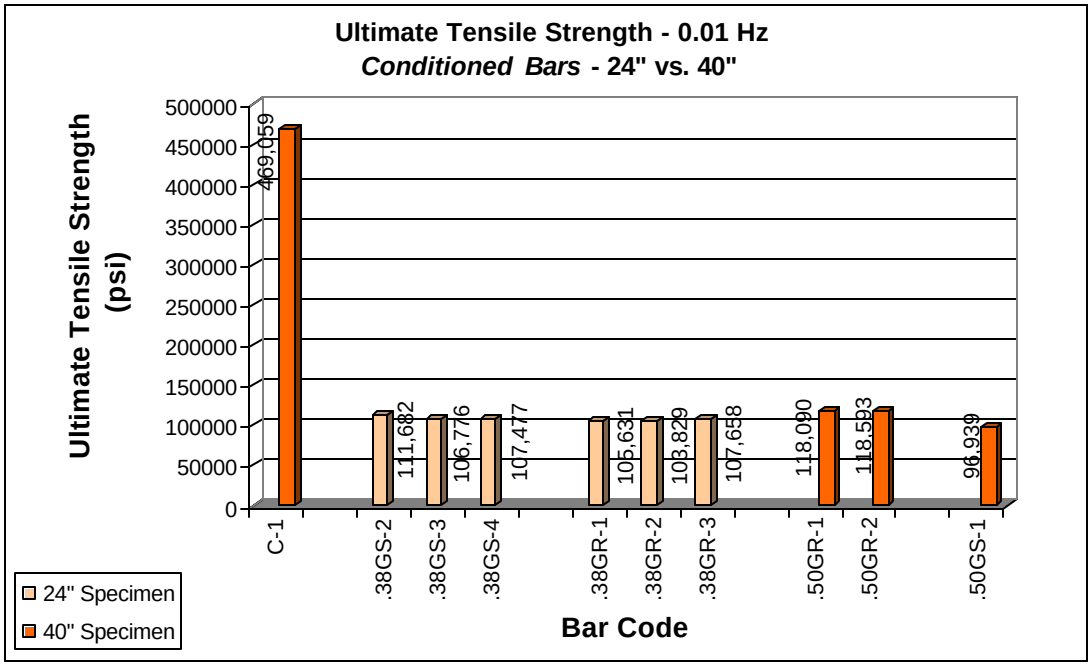

Figure 19: Results of Initial Tensile Tests for Conditioned Specimens

The descriptions of each bar are coded as follows.
.38GS-1u = (bar dia)(fiber type)(surface texture)-(# this type bar)(unconditioned)
EX: .38GS-2u =The second unconditioned 3/8"-dia smooth surface glass fiber bar tested.

Another comparison considers the average ultimate tensile strengths of *unconditioned* versus *conditioned* specimens. Figure 20 graphically compares the tensile strengths obtained from the tested unconditioned and conditioned bars. An environmental chamber was used to condition a sample of test specimens through 250 freeze-thaw cycles as outlined in the experimental plan. For unconditioned specimens, initial tests show the 3/8"$GFRP_S$ rods (average strength, 118,692 psi) have a slightly higher strength capacity than the 3/8"$GFRP_R$ (average strength, 109,309 psi) and 1/2"$GFRP_R$ (average strength, 75,063 psi). Each of these bars experienced adequate failure within the gage length, with no slippage within the anchorage. However, full distribution of stresses in the 3/8-inch specimens was not realized before failure since several of the specimens in this group had hard cores remaining. The 1/2"$GFRP_R$ bars tested at this loading rate experienced considerable fiber failure, but a greater cross-sectional area reduces its ultimate strength comparatively.

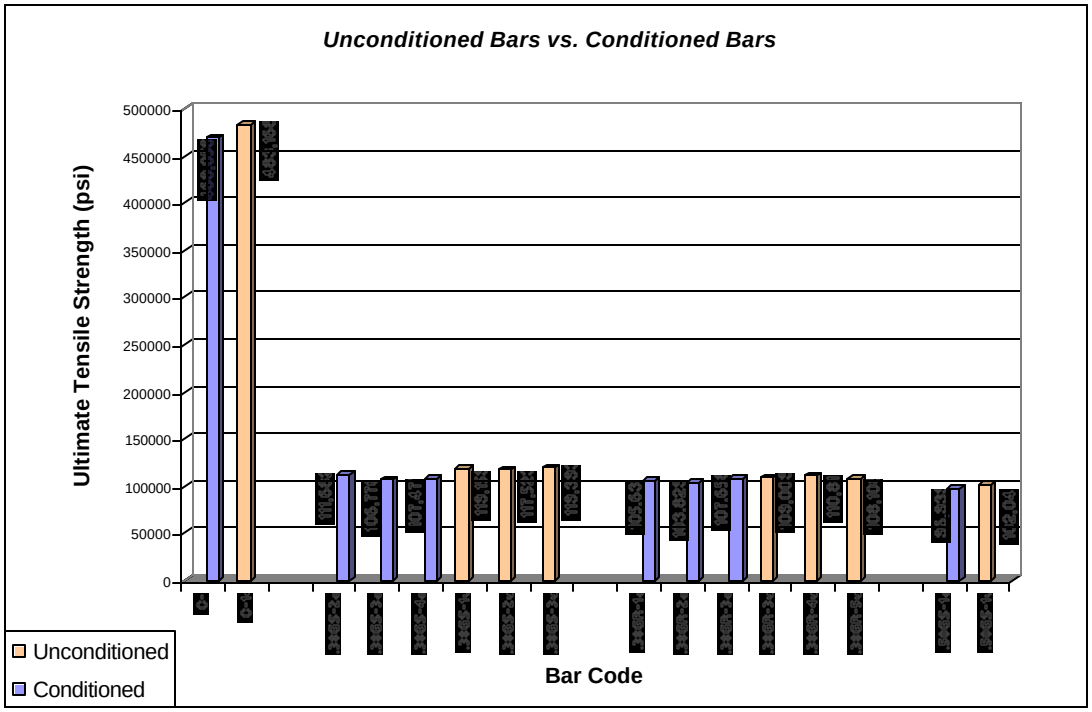

Figure 20: Comparison of Results of Initial Tensile Tests

For glass fiber bars, the 3/8"$GFRP_S$ specimens realized the greatest reduction of strength between unconditioned and conditioned bars tested. The average ultimate strength of these conditioned GFRP bars decreased by nearly 10,000 psi, an 8% reduction in strength. The average ultimate strength of the conditioned 3/8"$GFRP_R$ bars was found to be approximately

3600 psi lower than the tested unconditioned specimens, a 3% decrease. The ½"GFRP$_S$ bars also show similar results, with a 5% decrease in strength noticed in the conditioned specimens.

The most valid results for considering tensile strength are obtained from specimens in which failure occurs in the free-length of the bar. In the initial tests, all carbon fiber bars exhibited failure near or within the cement casing of the grips. Figure 21 shows how the first unconditioned CFRP bar tested experienced complete fracture at the grip surface. Figure 22 illustrates how the fibers began to fray within the free-length of this conditioned specimen before failure occurred due to pullout. Figure 23 shows the effects of the strong lateral pressures required to hold on to the carbon fiber specimens at high tensile loads.

Figure 21: Uncond. CFRP Failure

Figure 22: CFRP

Figure 23: Crushed CFRP Grips

Figure 24 shows a common occurrence in the carbon fiber bars tested. The cement binder did not provide adequate bond strength to prevent pullout from the anchorage before failure in the free-length of the specimen could occur. A supplementary anchorage system was designed using epoxy.

Figure 24: Unconditioned CFRP Grip Failure

6.2.3 Dynamic Tension

Additional mechanical testing was performed on a 110-kip rated universal servo hydraulic testing machine. The MTS machine used is shown in Figure 25**.** MTS 647.50 hydraulic wedge grips were used. Through the use of the TestStar/TestWareSX software, this apparatus provides computer operated programming and data acquisition capabilities.

Figure 25: MTS Testing Apparatus

After initial static tensile tests were completed, fatigue tests were designed at 80% of what was believed to be the average ultimate strengths of the reinforcement bars tested. Concern was raised after initial fatigue tests did not fail after 1,000,000 cycles. After deeper investigation into the reasoning behind this phenomenon, the rate dependency of glass-fiber FRP

reinforcement was made apparent. Unlike carbon and aramid fiber FRP bars, the strength of glass fiber bars is strongly rate dependent; as the loading or strain rate increases, tensile strength increases.

6.2.4 Glass Fiber-Reinforced Polymers

Past research into fatigue properties of fiber composites has often focused on high modulus carbon and aramid fiber bars. However, it is important to realize that composite materials containing E-glass fiber reinforcement tend to be much more sensitive to tensile or cyclic fatigue loading in the fiber direction than composites reinforced with other fibers. The effect of loading frequency on the mechanical properties of most continuous fiber FRP products appears to be negligible when tested in the longitudinal direction parallel to the reinforcing fibers. Properties of glass fiber polymer reinforcements, on the other hand, have shown a significant rate dependency. It is also apparent that there are no conclusive reasons for this phenomenon. Curtis [65] mentions that one theory suggests the rate effect is due to the environmental sensitivity of the glass fibers, rather than any viscoelastic effect. He refers to studies that have shown the rate effect to change when the environment surrounding the glass fibers is changed. Studies performed by Mandell [85] agree with the hypothesis that tensile fatigue failure in glass composites appears to be a fiber dominated failure mode, rather than matrix or interfacial cracking.

6.2.5 Variable Rate Tension Tests

The significance of the previous theories on the current study was evaluated. In his work on the fatigue behaviour of fiber-resin composites, J.F. Mandell realized that it is very important to consider the loading frequency of glass reinforcements because of the time sensitivity of the glass fiber strength, and the ultimate strength results obtained at low displacement rates are usually significantly below those experienced at fatigue rates [85]. A new tensile testing program was then developed to established appropriate ultimate strength values based on the following concept. In order for an adequate cyclic fatigue testing procedure to be designed, the ultimate strengths of the GFRP materials need to be obtained at a rate equivalent to the time to failure consistent with one half-cycle of the proposed fatigue test. This became the aim of the variable rate tension tests performed.

It was established that a strength comparison would be made between three loading frequencies; 0.1 Hz, 1.0 Hz and 10 Hz. Initial dynamic tension tests showed that failure times corresponding to one half-cycle at loading rates of 0.1 in/sec, 1.0 in/sec and 10 in/sec would occur at approximately 5.0, 0.5 and 0.05 seconds respectively. Samples from three of the different type bars available, 3/8"GFRP$_S$, 3/8"GFRP$_R$, and 1/2"GFRP$_R$, were investigated in this manner.

The dynamic tensile tests of this project represent the first attempt made by the structural engineering group at the university to operate the MTS machine in tension. Therefore, many of the tests performed revolved around optimizing the testing program to provide the best failure modes at appropriate failure times. Successful failure of tensile tests was only achievable up to a 2 Hz frequency, corresponding to a 0.25 second failure rate. This does not imply that the MTS machine is not capable of running at frequencies above 2 Hz. Initial fatigue tests, designed based on ultimate strengths obtained with the Tinius Olsen machine, were successfully run at 5 Hz. The maximum load applied in these fatigue tests was 10,000 lbs. The problem exists when establishing what percent of ultimate bar strength the 10,000 lbs is equivalent, if adequate dynamic tensile strength values are not obtainable for 5 Hz.

In an attempt to obtain 1/2-cycle ultimate strength failures at times corresponding to frequencies above 2 Hz, several loading programs were considered. Initial tests were performed in load control, both as a ramp rate in lbs/sec, and as frequency, in Hz (cycles/sec). It was then realized that better performance results were realized by application of stress in stroke control, applied as a ramp rate in in/sec of displacement. Therefore, each desired failure time corresponded to loading rates of approximately 0.1 in/sec, 1.0 in/sec and 10 in/sec. Between the two control application methods, the quickest failure observed still only occurred at 0.20 seconds. Data was thus accumulated for a series of specimens at 2 Hz rather than 10 Hz as initially planned. Additional materials are available to continue testing tensile failure of 3/8"GFRP$_R$ specimens at 2 Hz in order to establish a representative ultimate strength value for fatigue design.

6.2.6 Failure Mode Analysis

Upon completion of each test, initial personal reactions were recorded as well as initial visual descriptions of the failure mode. The bar was removed from the testing apparatus and a more detailed failure analysis was catalogued.

A JVC digital video camera was also used to capture failures of a group of samples for each load rate. The failure modes of 10-3/8"$GFRP_S$ specimens were analyzed in this manner. Figure 26 shows a frame captured from one of these video clips. This procedure aided in the visual inspection of failure mode. Each clip could be slowed down in order to record such aspects as: which grip initiated failure, was fiber failure gradual or instantaneous, how many bursts of failure did the sample endure before complete fracture, etc.

Figure 26: Video Still Frame

The fiber-break propagation model infers that as each fiber breaks, the redistribution of stress leads to additional stress on neighboring fibers. This process was visually evident upon examining the filmed failures. As the specimens were loaded, outer diameter fibers would initiate failure. Often initial fiber breaks occurred at the surface of the anchorage grip. Fiber breakage accumulated rapidly, often accompanied by bursts of energy release causing total fiber failure. In several cases, when the ultimate strength was reached and load capacity returned to zero, a hard center core of fiber/matrix material remained. Although bars tested at higher frequencies registered greater strengths, it was apparent these bars failed in tension before the stress could be distributed throughout all fibers of the cross-section. Bars tested at 0.1 Hz

loading performed better in this manner and experienced a greater number of fiber breaks. For the 3/8”-diameter specimens tested at 0.1 Hz, 5 out of 7 experienced nearly complete fiber failure, with the bar being completely severed in two.

There were significant differences noticed between bars of different cross-sectional diameter. The 1/2”-diameter GFRP specimens tested at low frequencies experienced several bar pullouts from the anchorage system. Since the chemical bond between the concrete filler and the FRP bar is extremely low, mechanical interlock becomes the primary means of stress transfer. The lack of this mechanical interlock would seem to explain the majority of bar pullouts in the sand coated 1/2”$GFRP_R$ specimens. All grip slippages of this size occurred in the top grip. Grip failures of this type are shown in the left specimens of Figure 27. However, Nanni [69] suggests that the bond of deformed FRP rods (such as the ribbed $GFRP_S$ bars in this study) is generally lower than that of equal diameter deformed steel bars and when FRP bars are sand coated, the opposite is true. In response to the number of bar pullouts that were experienced in the 1/2”$GFRP_R$ specimens with the cement anchor system, a series of additional tests were performed on these type bars with epoxy grips. Although the epoxy grips did provide comparable strength values, all of these bars pulled out of the epoxy grips. Several of the 1/2”$GFRP_R$ specimens also experienced severe fiber-matrix debonding in the grip region. This phenomenon is shown in the right specimens of Figure 27. It is apparent that for these bars the ultimate strength was not reached before the fiber-matrix interfacial bond strength was exceeded.

Figure 27: 1/2”$GFRP_R$

Unlike the previous responses exhibited by the 1/2”-diameter bars, all of the bars pre-conditioned in freeze-thaw cycling, experienced complete fiber failure. These failures are shown in Figures 28 & 29 below. Still, overall, the conditioned strengths were less than those realized in unconditioned specimens.

Figure 28: 1/2”GFRP$_R$

Figure 29: 1/2”GFRP$_R$

Nearly all 3/8” GFRP$_S$ specimens experienced complete bar failure. Two common failure modes are shown in Figure 30. The 3/8”GFRP$_S$ bars were the only type tested that did not experience any pullouts of the bar from the anchorage. A couple of these type bars did, however, experience shearing of the fiber-matrix interface in the grip region. A sample of those grips experiencing fiber-matrix slippage are shown in the grips on the left side of Figure 31. This was common among 3/8”-diameter bars; 50% of those tested at 1Hz to 2Hz experienced this failure mode. Welsh [82] suggests that although failures at intermediate strain rates will be dominated by glass fiber strength, there is a greater tendency for debonding between the fibers and resin matrix to cause failure at high rates of strain.

Figure 30: 3/8”GFRP$_S$

Figure 31: 3/8”GFRP$_S$ & 3/8”GFRP$_R$

The grips shown on the right side of Figure 31 show how the 3/8” GFRP$_R$ bars pulled out of the epoxy filled anchorages. Although the epoxy filled grips realized equal if not greater strengths than the grout filled grips, all of the bars tested with the epoxy grip system experienced bar pullout.

6.2.7 Variable Rate Tension Results

The time sensitivity of the glass fiber strength is quite apparent in comparing the ultimate strength results obtained for variable frequency load rates. Figures 32-34 visually illustrate the strong load rate dependence of each type bar. Tables 8 & 9 contain all data collected for each loading rate, unconditioned and conditioned specimens respectively. Figure 35 shows the overall rate dependant trend of each type bar considered.

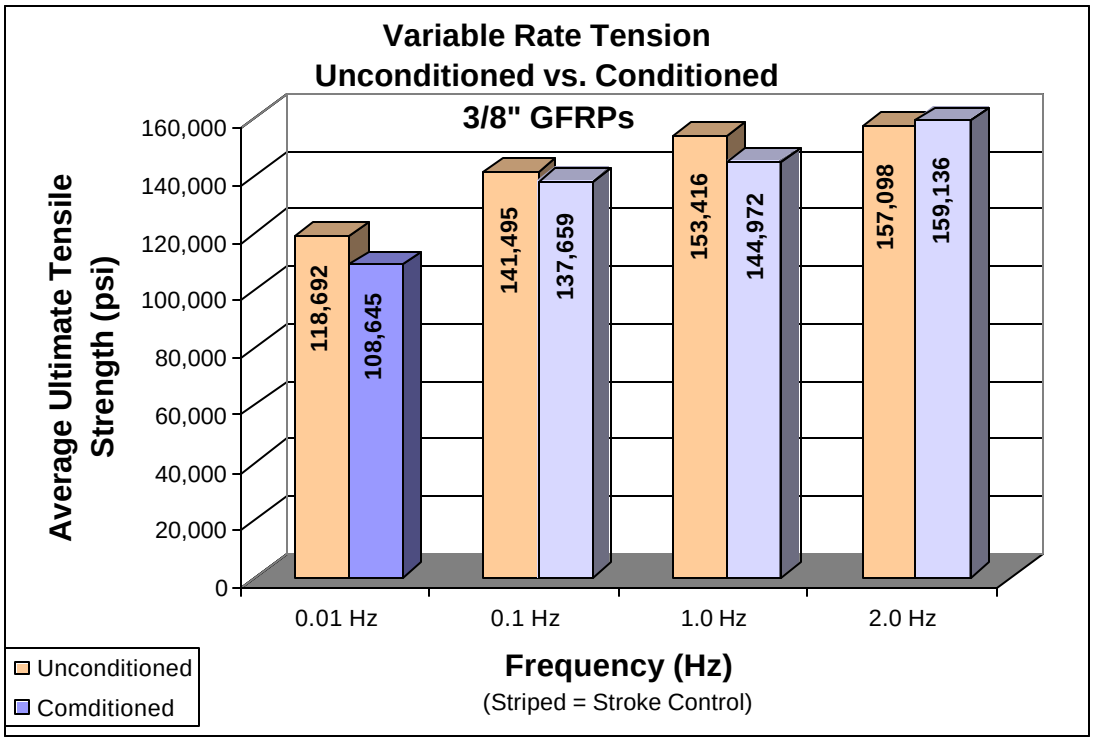

Figure 32: Variable Rate Tension 3/8" $GFRP_S$

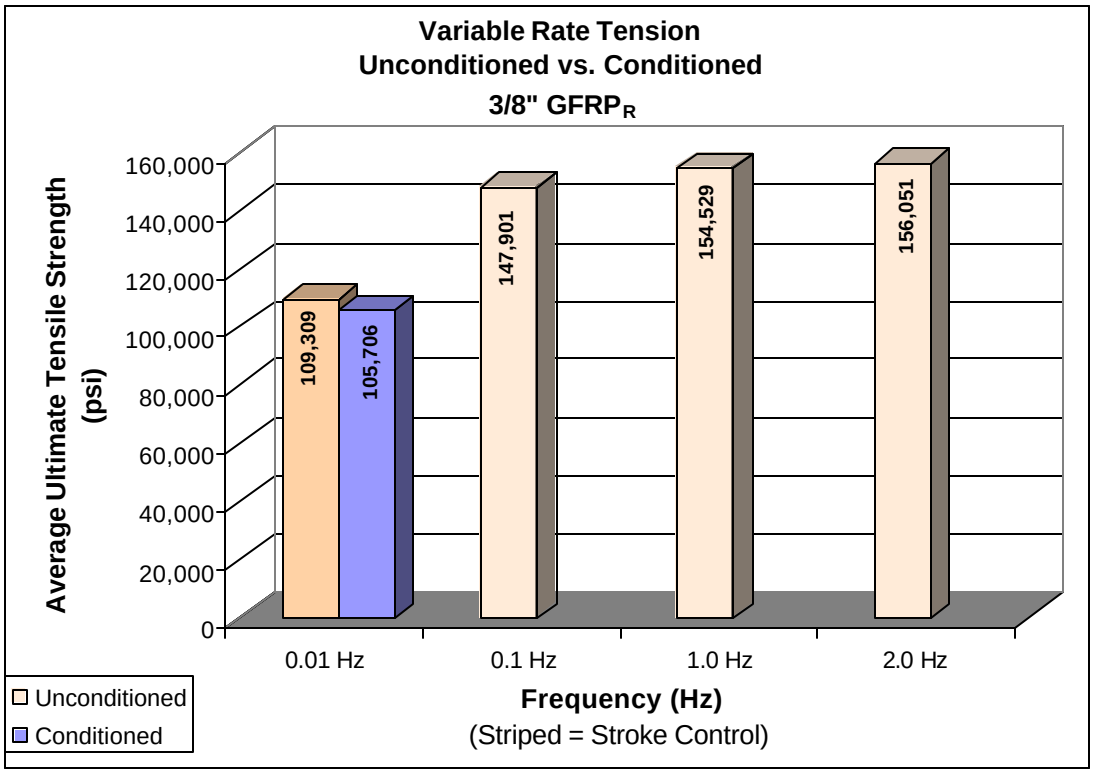

Figure 33: Variable Rate Tension 3/8" $GFRP_R$

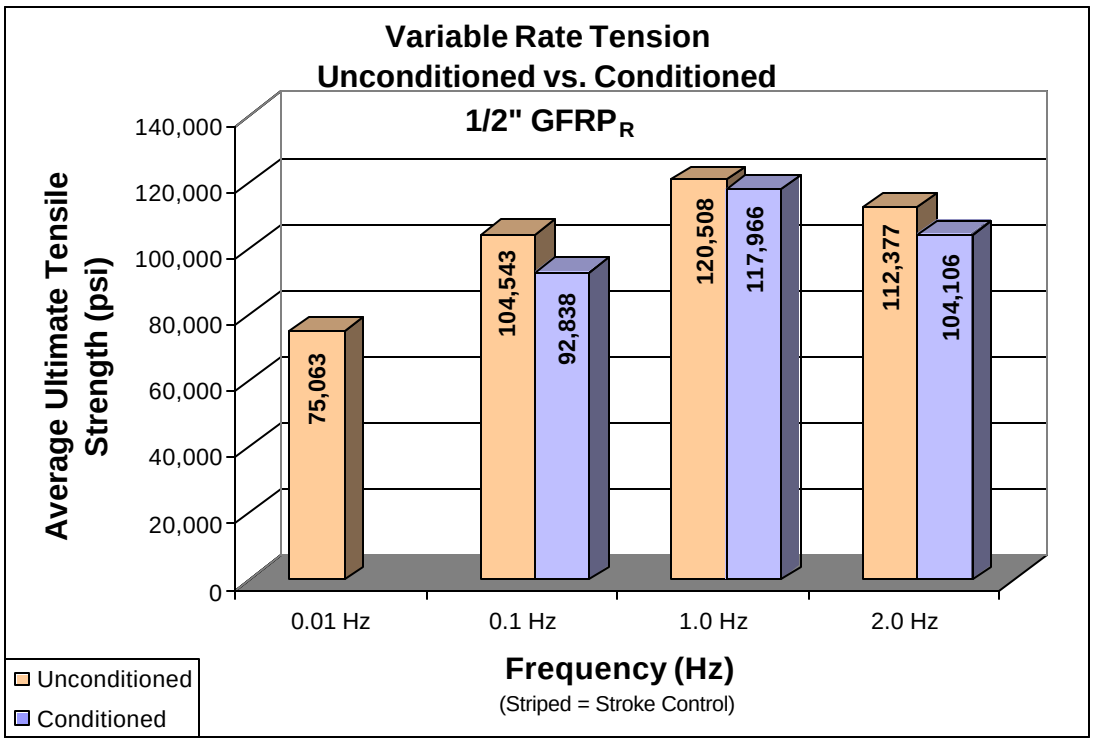

Figure 34: Variable Rate Tension 1/2" GFRP$_R$

Table 8: Average Ultimate Tensile Strengths for Unconditioned Specimens

		Average 24" Tensile Load		Average Tensile Strength			Average 40" Tensile Load		Average Tensile Strength		
Load Rate	**Bar Type**	Extension (in)	Maximum (lbs)	Nominal (psi)	COV (%)	SD	Extension (in)	Maximum (lbs)	Nominal (psi)	COV (%)	SD
0.01 Hz frequency:	3/8" CFRP	-	*41,975*	*415,594*	*5.054%*	*21003*	-	48,800	483,168	0.000%	0
0.01 Hz frequency:	3/8" $GFRP_S$	-	12,700	118,692	0.858%	1018	-	12,750	119,159	0.000%	0
0.1 Hz frequency:	3/8" $GFRP_S$	0.433	15,140	141,495	3.415%	4833					
1.0 Hz frequency:	3/8" $GFRP_S$	0.447	16,416	153,416	2.744%	4210					
2 Hz frequency:	3/8" $GFRP_S$	0.450	16,810	157,098	3.908%	6139					
0.01 Hz frequency:	3/8" GFRPr	-	12,133	109,309	1.259%	1376	-				
0.1 Hz frequency:	3/8" GFRPr	0.594	16,417	147,901	1.222%	1808					
1.0 Hz frequency:	3/8" GFRPr	0.503	17,153	154,529	9.249%	14292					
2 Hz frequency:	3/8" GFRPr	0.497	17,322	156,051	9.554%	14909					
0.01 Hz frequency:	1/2" GFRPr	-	*14,938*	*75,063*	*4.852%*	*3642*					
0.1 Hz frequency:	1/2" GFRPr	*0.540*	*21,097*	*106,013*	*5.703%*	*6046*					
1.0 Hz frequency:	1/2" GFRPr	*0.481*	*21,681*	*108,947*	*10.044%*	*10943*					
2 Hz frequency:	1/2" GFRPr	*0.411*	*22,363*	*112,377*	*0.000%*	*0*					
0.01 Hz frequency:	1/2" GFRPs						-	20,000	102,041	0.000%	0

[1]Italic: *Anchoraae failures.*
[2]Graph Included

Table 9: Average Ultimate Tensile Strengths for Conditioned Specimens

		24" Average Tensile Load		24" Average Tensile Strength			40" Average Tensile Load		40" Average Tensile Strength		
Load Rate	**Bar Type**	Extension (in)	Maximum (lbs)	Nominal (psi)	COV (%)	SD	Extension (in)	Maximum (lbs)	Nominal (psi)	COV (%)	SD
0.01 Hz frequency:	3/8" CFRP						-	47,375	469,059	0.000%	0
0.01 Hz frequency:	3/8" $GFRP_S$	-	11,625	108,645	2.443%	2654					
0.1 Hz frequency:	3/8" $GFRP_S$	0.410	14,730	137,659	2.332%	3210					
1.0 Hz frequency:	3/8" $GFRP_S$	0.437	15,512	144,972	1.130%	1639					
2 Hz frequency:	3/8" $GFRP_S$	0.469	17,028	159,136	3.375%	5371					
0.01 Hz frequency:	3/8" GFRPr										
0.1 Hz frequency:	3/8" GFRPr										
1.0 Hz frequency:	3/8" GFRPr										
2 Hz frequency:	3/8" GFRPr										
0.01 Hz frequency:	1/2" GFRPr						-	23,550	118,342	0.300%	355
0.1 Hz frequency:	1/2" GFRPr	*0.285*	*18,475*	*92,838*	*4.620%*	*4290*					
1.0 Hz frequency:	1/2" GFRPr	*0.396*	*23,475*	*117,966*	*2.376%*	*2803*					
2 Hz frequency:	1/2" GFRPr	*0.362*	*20,717*	*104,106*	*0.000%*	*0*					
0.01 Hz frequency:	1/2" GFRPs						-	19,000	96,939	0.000%	0

[1]Italic: *Anchoraae failures.*
[2]Graph Included

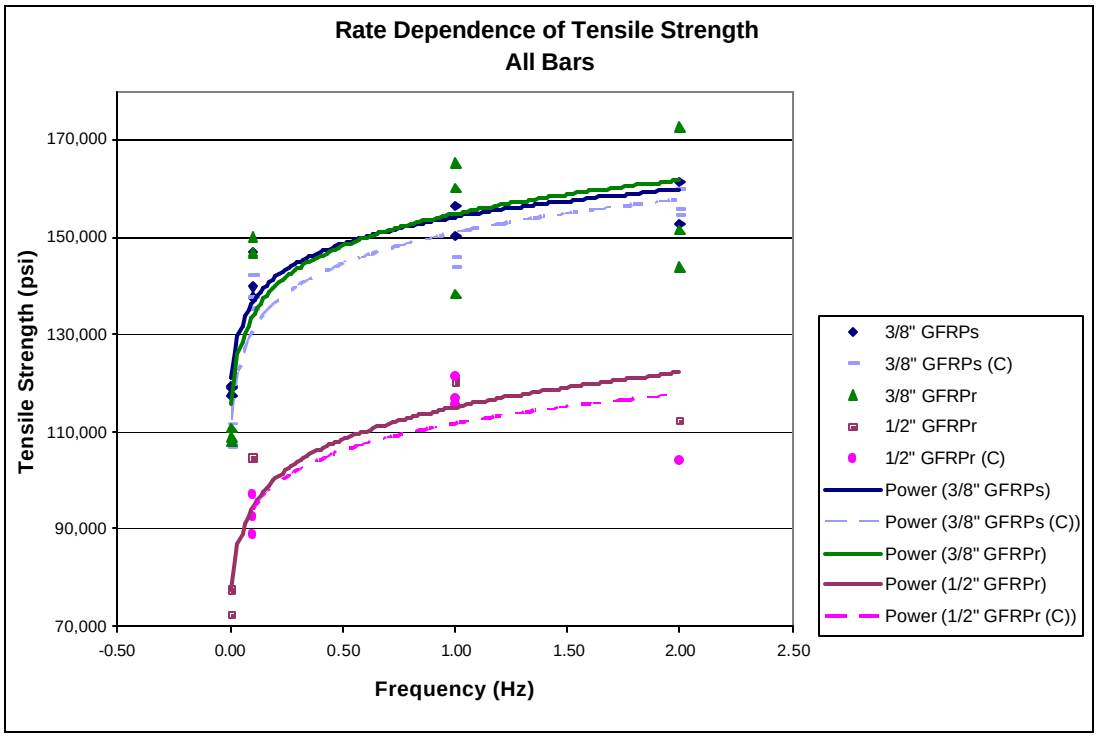

Figure 35: Rate Dependence of Glass Fiber-Reinforced Polymer Bars

Static tensile strengths measured with the Tinius Olsen machine are significantly less than those recorded at fatigue rates. And although the data obtained from the static tests does follow the trend of load rate increase, Shah [84] points out that the correlation of tests results obtained from different types of machines is very poor. Freeze-thaw pre-conditioned specimens experienced at least a 3% decrease in strength in all cases, except for the 2Hz, 3/8"GFRPs (Figures 36-39). Due to the fact that there were only 2 unconditioned samples available for testing as opposed to 4 conditioned specimens, it is supposed that if the sample number increased for the unconditioned case, a similar trend would be evident. The greatest ultimate strengths of all type bars considered were realized by the 3/8"GFRPr. No definitive conclusions can be made on whether load control or stroke control produces greater ultimate strengths. Stroke control loading has been seen to provide better failure modes and repeatable displacement stiffness curves.

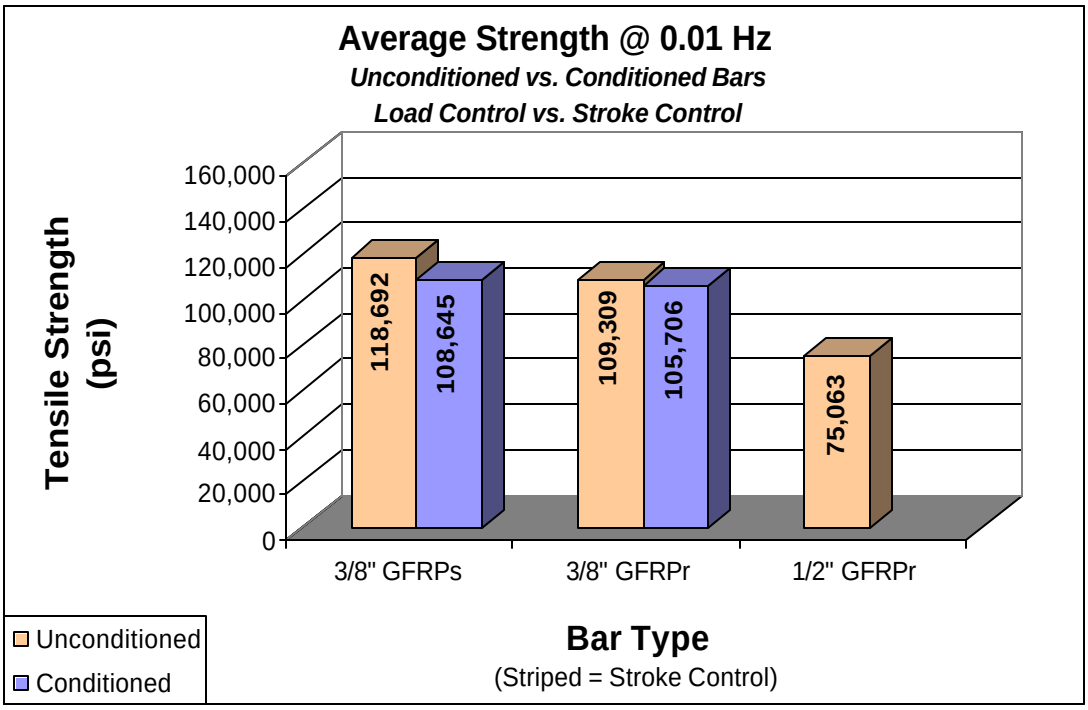

Figure 36: Average Strength at 0.01 Hz

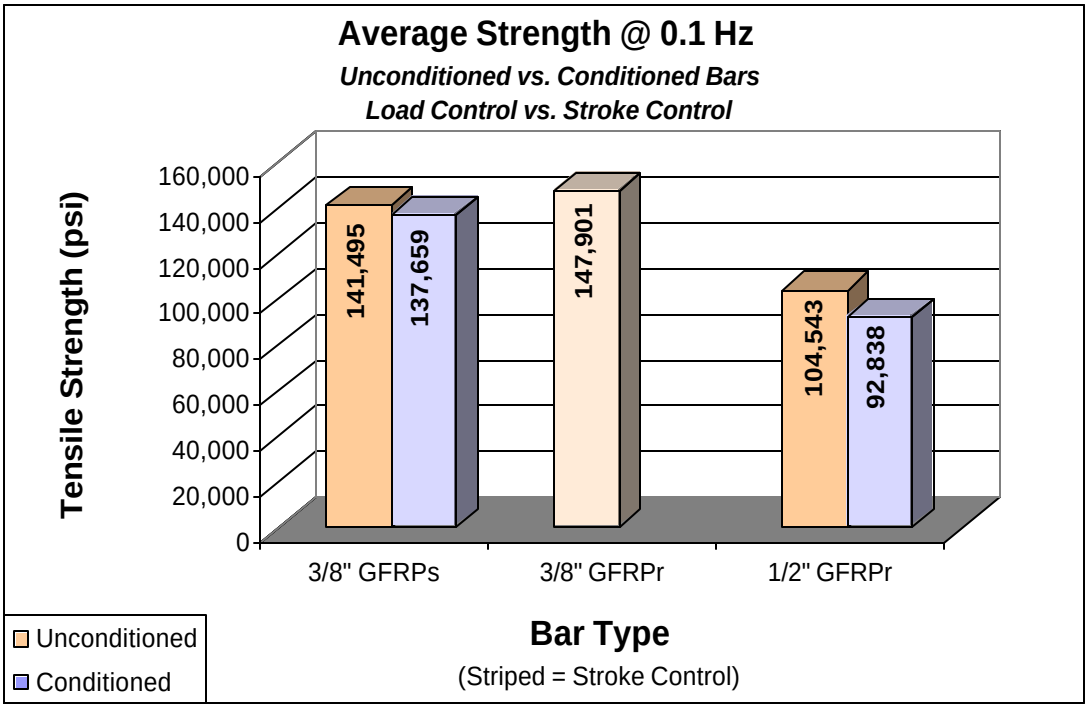

Figure 37: Average Strength at 0.1 Hz

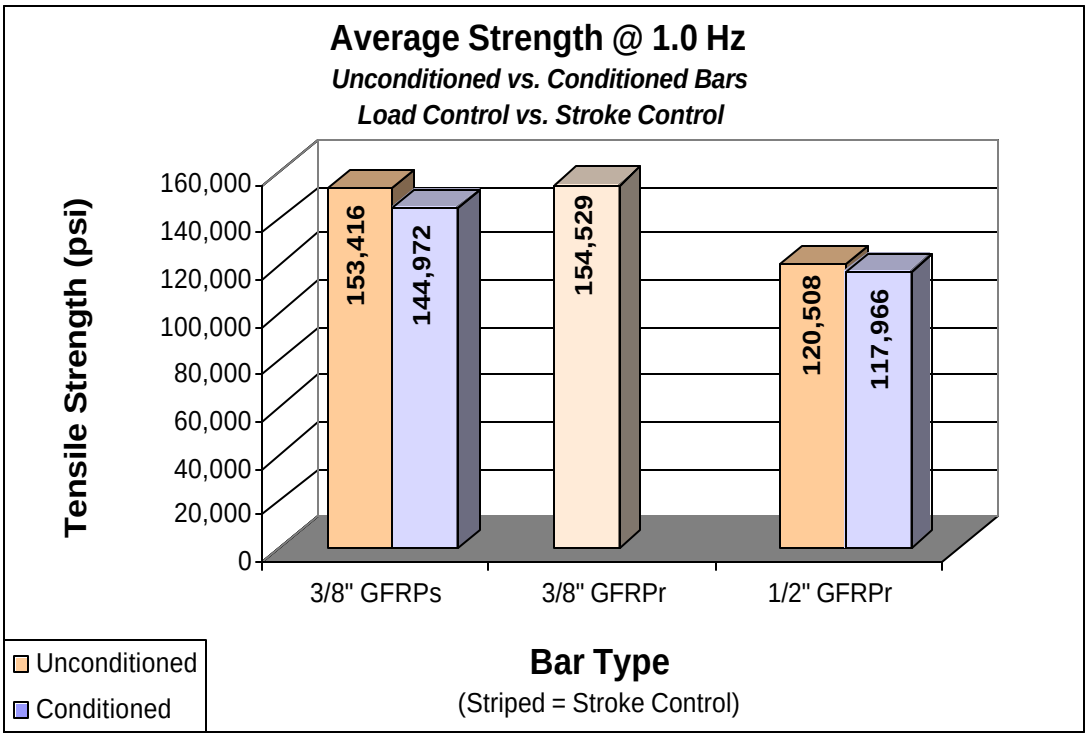

Figure 38: Average Strength at 1.0 Hz

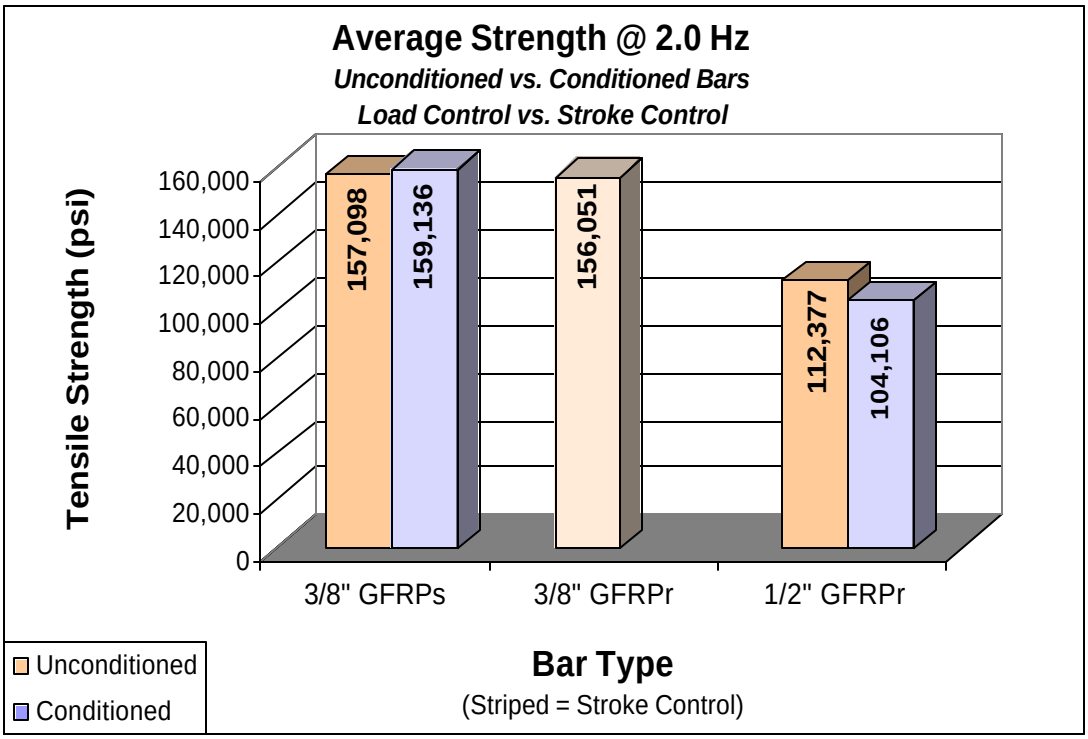

Figure 39: Average Strength at 2.0 Hz

6.2.8 Elastic Modulus

As mentioned earlier, several factors can affect the elasticity of fiber-reinforced products. The elastic modulus of glass fiber polymer rods subjected to variable tension tests was evaluated for each rate of loading. Specimens were loaded uniaxially and load and displacement data was recorded continuously until failure. Data acquisition was obtained at increments of 0.005 to 0.0005 seconds depending on predicted time to failure. Most of the tests resulted in a load-displacement relationship linear up to failure as shown in Figure 40. In these cases, sudden failure resulted in rapid unloading of the specimen.

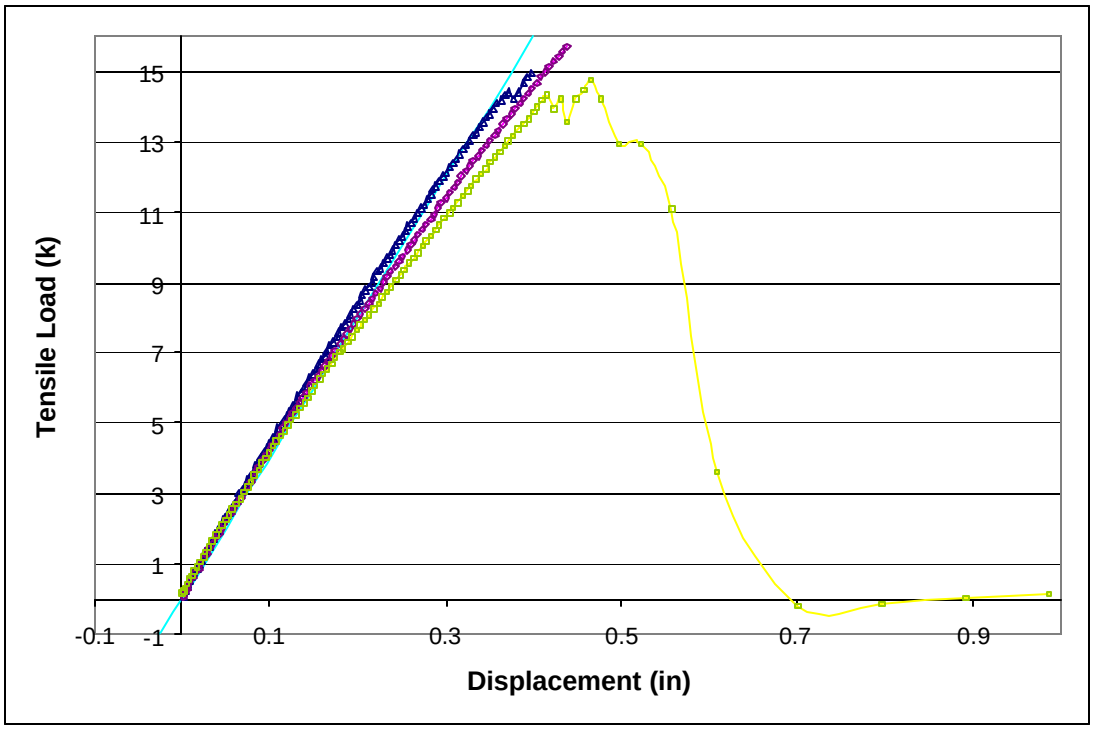

Figure 40: Linear elastic behaviour to failure.

The linear portion up to failure was considered in calculating the elastic modulus. The axial stress for each data point was calculated by dividing the load value by the specimen's original cross-sectional area. The average initial cross-sectional area within the gage length of the specimen, as listed in Table 5, is used for this calculation. Strain values were calculated similarly by dividing displacement values for each data point by the original length of the specimen.

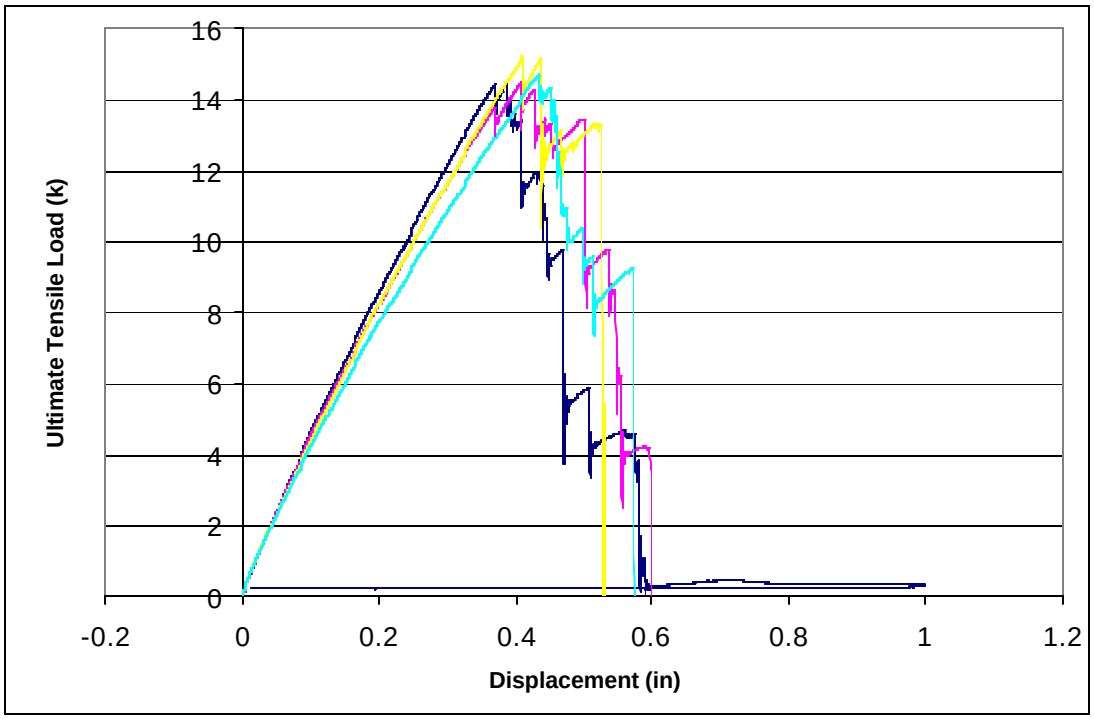

Figure 41: Linear behaviour with a non-linear region of cyclic load reductions after failure.

Other load-displacement relationships indicate that after ultimate strength was achieved, response leads into a non-linear region of cyclic load reductions. Figure 41 illustrates several samples exhibiting this behaviour.

Stress-strain curves and load-displacement stiffness curves were drawn for each set of loading frequencies, as well as for each bar type. Young's modulus was calculated based on the least squares method and least squares regression lines were generated. The stress-strain diagram is shown in Figure 42. Stiffness values of fiber-reinforced polymers are usually in the range of 1/5 to 2/3 that of steel (29 x 10^6 psi). The displacement stiffness for each set of specimens was also calculated and illustrated in Figure 43.

6.2.9 Elongation

Elongation inspection was conducted for each set of specimens tested in tension. The percent elongation at break of each specimen was determined by dividing the extension at rupture by the original gage length of the specimen and multiplying by 100. Elongation and Tensile Modulus values are included in Table 10. A complete list of results for each of the worksheets is included in appendix B.

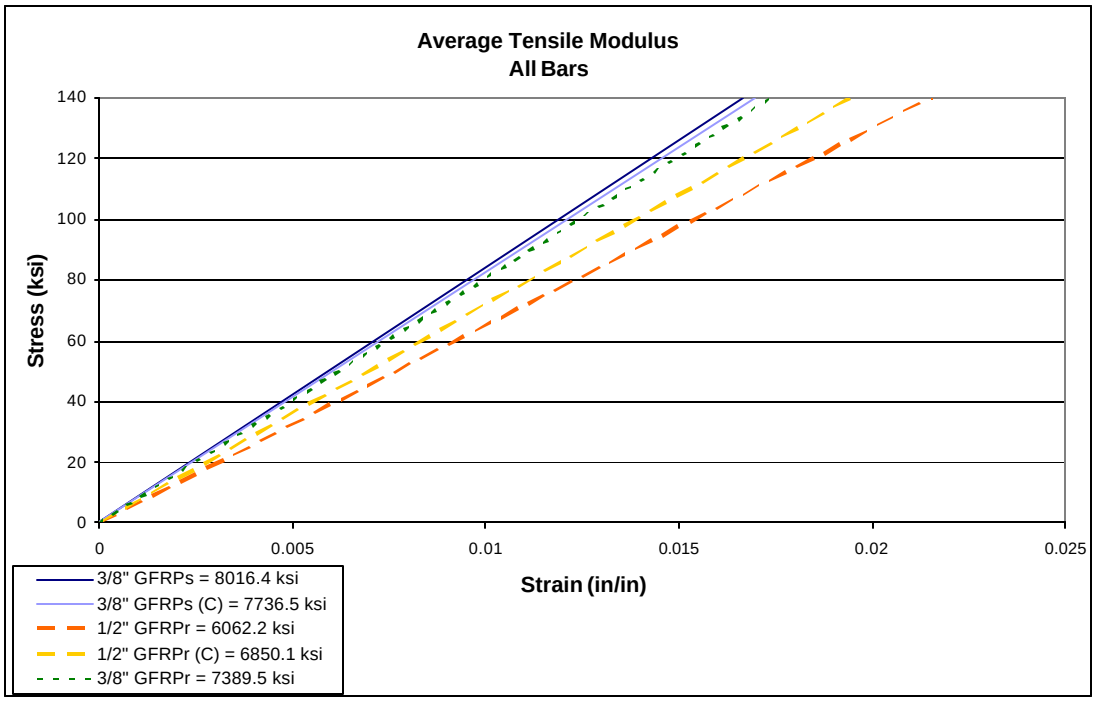

Figure 42: Average Tensile Modulus

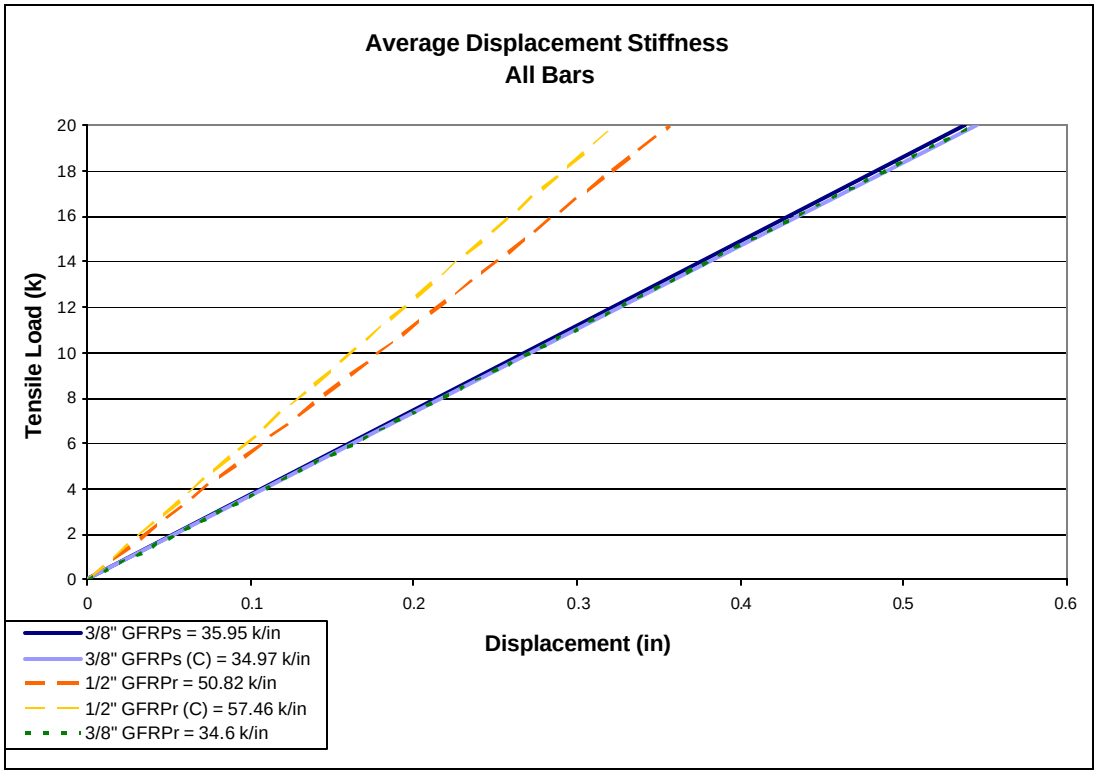

Figure 43: Average Displacement Stiffness

6.3 Fatigue Tests

Generally, fiber-reinforced polymer bars tend to exhibit good fatigue resistance. Anchorage tests conducted at the University of Wyoming indicated that carbon, aramid, and E-glass rods could easily sustain 100,000 cycles of load between 60-70% of their ultimate tensile capacity [6]. As the glass fibers were found to break during fatigue, the glass fiber bars lost stiffness as the number of cycles increased, as opposed to carbon and aramid fiber rods, which gained stiffness as the number of cycles increased. Uomoto *et al.* examined the fatigue properties of vinyl ester GFRP and CFRP rods with a 55% fiber volume fraction [25]. Their experiments showed the fatigue strength of polymer composites to be directly related to the type of fiber, and it can be expressed by the amplitude, mean stress, and number of cycles.

6.3.1 Tension-Tension Fatigue

Many variables can ultimately affect the total number of cycles to failure: stress levels, stress rate, mode of cycling, process history, material composition, and environmental conditions. The fatigue processes which reduce strength in advance composite materials are generally very complex, involving the accumulation of many damage modes.

The mechanisms of cyclic fatigue degradation of E-glass fiber-reinforced polymers have proven more difficult to establish than carbon or Aramid composites. J.F. Mandell has conducted many studies on the fatigue behaviour of GFRP. In one study [85] he illustrates that cyclic fatigue degradation and failure of single glass strand is primarily due to fiber-fiber interaction, as opposed to matrix cracking.

Fatigue test specifications include load range, load rate and number of cycles. When designing a fatigue test program it is important to specify each of the following parameters: mean stress, stress amplitude and cyclic frequency. Each parameter is established so that fatigue failure of the test specimen shall occur in a manner similar to the material of comparable structural component.

Table 10: Elongation and Tensile Modulus

Bar #	Code	Type	Failure Load	Failure Stress		Extension at Rupture	Original Length			Elongation	Corr. Coef.	Displacement Stiffness	Tensile Modulus	Corr. Coef.
			Maximum	Nominal				SD	COV		R^2		Slope, M	R^2
UNCONDITIONED:			(lbs)	(psi)		(in)	(in)		(%)	(%)		(lb/in)	(ksi)	
0.1 Hz frequency:		3/8" GFRPs	15,140	141,495	**Avg.**	0.433	23.75	0.1402	7.70%	1.82%	0.990	35.910	8006.3	0.990
1.0 Hz frequency:		3/8" GFRPs	16,416	153,416	**Avg.**	0.447	23.69	0.0500	2.66%	1.88%	0.997	35.885	7999.0	0.996
2 Hz frequency:		3/8" GFRPs	16,810	157,098	**Avg.**	0.450	23.75	0.0100	53.00%	1.90%	0.998	37.274	8283.6	0.998
									3/8" GFRPs Type Average[2]:			**35.951**	**8016.4**	
0.1 Hz frequency:		3/8" GFRPr	16,417	147,901	**Avg.**	0.594	23.71	0.4431	17.65%	2.51%	0.989	34.456	7371.8	0.989
1.0 Hz frequency:		3/8" GFRPr	17,153	154,529	**Avg.**	0.503	23.86	0.2836	13.44%	2.11%	0.988	35.199	7580.5	0.988
2 Hz frequency:		3/8" GFRPr	17,322	156,051	**Avg.**	0.497	23.81	0.3101	14.84%	2.09%	0.988	32.129	6919.0	0.988
									3/8" GFRPr Type Average[2]:					
0.1 Hz frequency:		1/2" GFRPr	21,097	106,013	**Avg.**	0.540	23.72	0.5119	22.45%	2.28%	0.990	52.229	6229.9	0.990
1.0 Hz frequency:		1/2" GFRPr	21,681	108,947	**Avg.**	0.481	23.72	0.1977	9.74%	2.03%	0.981	48.146	5729.1	0.980
2 Hz frequency:		1/2" GFRPr	22,363	112,377	**Avg.**	0.411	23.88	0.0000	0.00%	1.72%	0.992	51.126	6135.1	0.992
									1/2" GFRPr Type Average[2]:			**50.818**	**6062.2**	
CONDITIONED:														
0.1 Hz frequency:		3/8" GFRPs	14,730	137,659		0.410	23.64	0.0889	5.14%	1.73%	0.987	34.910	7694.1	0.985
1.0 Hz frequency:		3/8" GFRPs	15,512	144,972		0.437	23.85	0.0707	3.86%	1.83%	0.993	35.281	7874.3	0.992
2 Hz frequency:		3/8" GFRPs	17,028	159,136		0.469	23.75	0.1080	5.48%	1.97%	0.990	34.058	7570.1	0.990
									3/8" GFRPs Type Average[2]:			**34.968**	**7736.5**	
0.1 Hz frequency:		1/2" GFRPr	18,475	92,838		0.285	23.71	0.2255	18.79%	1.20%	0.991	56.900	6776.0	0.992
1.0 Hz frequency:		1/2" GFRPr	23,475	117,966		0.396	23.81	0.0406	2.45%	1.66%	0.990	59.135	7075.4	0.985
2 Hz frequency:		1/2" GFRPr	20,717	104,106		0.362	23.75	0.0000	0.00%	1.52%	0.996	55.044	6569.4	0.996
									1/2" GFRPr Type Average[2]:			**57.463**	**6850.1**	

[1]Graph Included

[2]Type Average is the result of a graph inclusive of all data points, not the average of the three rate values.

Fatigue tests are carried out with a 110-kip servo hydraulic testing machine. The MTS machine has the ability to perform fatigue tests in load, stroke, or strain control. In position control, the displacement is cycled between preselected maximum and minimum values, independent of the load developed within the test piece. Strain control emulates position control but can filter out errors associated with movement within the grips or supports [65]. Figure 44 illustrates placement of the specimen within the environmental test chamber during loading. Figure 45 shows the chamber closed in operating position around the MTS. In the load control test set, sinusoidal cyclic stress is applied between predetermined maximum and minimum limits. Initial tests were designed to apply fatigue loading cycles at a test frequency of 5 Hz repeated 2-million times on specimens maintained at –20°F (-4ºC). These results were to be compared to those at room temperature to determine the effect of cyclic loading on endurance limit at low temperature. In preliminary tests, the MTS machine was used in load control with a feedback loop to sustain a cyclic load pattern. In this method, as the test material is damaged in fatigue, greater displacements result, allowing the test piece to support the applied load. Table B9, which outlines all fatigue tests completed, is included in appendix B.

Figure 44: MTS testing apparatus.

Figure 45: MTS testing apparatus.

The post fatigue performance of three 1/2"$GFRP_R$ bars was investigated. When failure of tested specimens did not occur after a specified number of cycles, the static strength was measured. The first two examples are 3/8"$GFRP_S$ specimens cycled at 5 Hz between 40%-50% of the expected ultimate strength. The first of these successfully completed 985,000 cycles before power was lost in the laboratory. The residual strength of this test specimen was found at 0.01 Hz to be 137,346 psi. The second specimen was cycled at 5 Hz repeated 765,374 times. The recorded residual strength of this bar at 0.01 Hz was 122,252 psi. The third trial was a 3/8"$GFRP_R$ specimen cycled at 5 Hz at roughly 20-25% of its ultimate strength. This bar was removed after 500 cycles and tested to have remaining strength at 2 Hz of 154,505 psi. In each of these cases, load capacity was not significantly reduced. Static strength should be reduced with increasing number of cycles. However, failure of the FRP bars will not occur if cycled at less than 60% of their ultimate strength.

7.0 Conclusions

The effect of the rate of loading on the tensile strength properties of glass fiber polymer reinforcements was investigated in order to establish a basis for cyclic fatigue loading procedures. The following conclusions have been made based on analysis of the test results:

1. The rate sensitivity of the strength of glass fiber reinforcing bars is quite apparent in comparisons of ultimate strength results obtained for variable loading rates.
2. There were noticeable increases in strength and marked changes in fracture appearance with increased loading rate.
3. Freeze-thaw conditioning does have some deleterious effect on the ultimate strength of glass fiber polymer reinforcing bars.
4. No definitive conclusions could be established based on load control test, stroke controlled test programs produced more complete failure modes and repeatable load-displacement curves.
5. A basis for fatigue testing up to 2 Hz has been established.
6. A complete experimental system and testing procedures are established for durability testing of FRP materials under environmental and mechanical loadings.

In order for FRP reinforcing bars to be successfully implemented in roadway construction projects, it is essential to develop a firm understanding of the durability properties of FRP bars and effects of exposure to severe and frequently changing environments. Preliminary results in this report show that freeze-thaw exposure may have a deleterious effect on the fatigue cycling program. The degree of deterioration of the FRP bars depends on the temperature ranges and number of freezing-thawing cycles applied. Not more than 10% of deterioration in tensile strength of FRP bars occurred under the temperature conditions (See Section 5.3) applied in the project. Although the temperature conditions were more severe than the actual temperature fluctuations in Colorado, the degradation of tensile strength should be considered properly in structural design.

For future researches, concurrent load and freeze-thaw cycling tests would illustrate a more definitive relationship between conditioning and load deterioration. The carbon fiber-reinforced bars need a more effective grip system to be developed in order to test CFRP properties systematically. Additional testing is desired to adequately establish a consistent

testing method for ultimate tensile capacities of the rate-dependant glass fiber reinforcements. A comprehensive fatigue program also needs to be established to determine the effect of cyclic loading on endurance limit at low temperatures.

REFERENCES

(1.) ACI Committee 440. State-of-the-Art Report on Fiber-Reinforced Plastic Reinforcement for Concrete Structures. Detroit: ACI, 1996.

(2.) BANK, Lawrence C. *Properties of FRP Reinforcements for Concrete,* Fiber-Reinforced-Plastic Reinforcement for Concrete Structures: Properties and Applications. Ed. by Antonio Nanni. New York: Elsevier, 1993.

(3.) BELARBI, Abdeldjelil, K. CHANDRASHEKHARA and Steve E. WATKINS. *Performance Evaluation of Fiber-Reinforced Polymer Reinforcing Bar Featuring Ductility and Health Monitoring Capability*, Fourth International Symposium on Fiber-Reinforced Polymer Reinforcement for Reinforced Concrete Structures (SP-188). Ed. by Antonio Nanni, Charles Dolan, Sami Rizkalla. Farmington Hills: ACI International, 1999.

(4.) BLONTROCK, Hendrik, Luc TAERWE and Stijn MATTHYS. *Properties of Fiber-reinforced Plastics at Elevated Temperatures with Regard to Fire Resistance of Reinforced Concrete Members*, Fourth International Symposium on Fiber-Reinforced Polymer Reinforcement for Reinforced Concrete Structures (SP-188). Ed. by Antonio Nanni, Charles Dolan, Sami Rizkalla. Farmington Hills: ACI International, 1999.

(5.) DOLAN, Charles W. *FRP Prestressing in the U.S.A.*, Concrete International, 21:21-24. October, 1999.

(6.) DOLAN, Charles W. *FRP Development in the United States,* Fiber-Reinforced-Plastic Reinforcement for Concrete Structures: Properties and Applications. Ed. by Antonio Nanni. New York: Elsevier, 1993.

(7.) DOLAN, Charles and H.R. HAMILTON. *Design Recommendations for Concrete Structures Prestressed with FRP Tendons*, Final Draft, 1: 1-100. May, 2000.

(8.) ERKI, M.A. and S.H. RIZKALLA. *A Canadian Perspective on R&D, Design/Codes and Technical Committees*, Fiber-Reinforced-Plastic Reinforcement for Concrete Structures: Properties and Applications. Ed. by Antonio Nanni. New York: Elsevier, 1993.

(9.) FAZA, S.S. and H.V.S. GANGARAO. *Glass FRP Reinforcing Bars for Concrete,* Fiber-Reinforced-Plastic Reinforcement for Concrete Structures: Properties and Applications. Ed. by Antonio Nanni. New York: Elsevier, 1993.

(10.) FERRIER, E. and P. HAMELIN. *Influence of Time-Temperature-Loading on Carbon Epoxy Reinforcement for Concrete Structures*, Fourth International Symposium on Fiber-Reinforced Polymer Reinforcement for Reinforced Concrete Structures (SP-188). Ed. by Antonio Nanni, Charles Dolan, Sami Rizkalla. Farmington Hills: ACI International, 1999.

(11.) FERRIER, E., P. HAMELIN and P. NASSERI. *Fatigue Behavior of Composite Reinforcement for Concrete Structures,* Fourth International Symposium on Fiber-Reinforced Polymer Reinforcement for Reinforced Concrete Structures (SP-188). Ed. by Antonio Nanni, Charles Dolan, Sami Rizkalla. Farmington Hills: ACI International, 1999.

(12.) FUKUYAMA, Hiroshi. *FRP Composites in Japan,* Concrete International, 21:29-32. October, 1999.

(13.) HARRIS, Harry, Win SOMBOONSONG and Frank KO. *New Ductile Hybrid FRP Reinforcing Bar for Concrete Structures,* Journal of Composites for Construction, 2:28-37. February, 1998.

(14.) HOSHIJIMA, Tokitaro and Kensuke YAGI. *Properties of CFRP Composites for Concrete Structures,* Fiber Composites in Infrastructure: Proceedings of the First International Conference on Composites in Infrastructure, 227-241. January, 1996.

(15.) KASKI, Greg, and Charles DOLAN. *Creep Rupture of Fiber-Reinforced Polymer Prestressing Tendons under Curvature,* Fourth International Symposium on Fiber-Reinforced Polymer Reinforcement for Reinforced Concrete Structures (SP-188). Ed. by Antonio Nanni, Charles Dolan, Sami Rizkalla. Farmington Hills: ACI International, 1999.

(16.) MASHIMA, M., and K. IWAMOTO. *Bond Characteristics of FRP Rod and Concrete After Freezing and Thawing Deterioration*, Fiber-Reinforced-Plastic Reinforcement for Concrete Structures: International Symposium. Ed. Antonio Nanni and Charles Dolan. Detroit: ACI, 1993.

(17.) MUKAE, K., S. KUMAGAI, H. NAKAI, and H. ASAI. *Characteristics of Aramid FRP Rods*, Fiber-Reinforced-Plastic Reinforcement for Concrete Structures: International Symposium. Ed. Antonio Nanni and Charles Dolan. Detroit: ACI, 1993.

(18.) NANNI, Antonio (ed.), Fiber-Reinforced-Plastic Reinforcement for Concrete Structures: Properties and Applications. Ed. by Antonio Nanni. New York: Elsevier, 1993.

(19.) NANNI, Antonio. *FRP Reinforcement for Prestressed and Non-Prestressed Concrete Structures*, Fiber-Reinforced-Plastic Reinforcement for Concrete Structures: Properties and Applications. Ed. by Antonio Nanni. New York: Elsevier, 1993.

(20.) NANNI, Antonio and Charles DOLAN (eds.), Fiber-Reinforced-Plastic Reinforcement for Concrete Structures: International Symposium. Detroit: ACI, 1993.

(21.) NANNI, Antonio, Charles DOLAN and Sami RIZKALLA (eds.), Fourth International Symposium on Fiber-Reinforced Polymer Reinforcement for Reinforced Concrete Structures (SP-188). Farmington Hills: ACI International, 1999.

(22.) OLSON, Ryan. Temperature and Moisture Effects on FRP Reinforcing Products, Final Report, CVEN 5161.

(23.) RAHMAN, A.H., D. A. TAYLOR, C. Y. KINGSLEY. *Evaluation of FRP as Reinforcement for Concrete Bridges*, Fiber-Reinforced-Plastic Reinforcement for Concrete Structures: International Symposium. Ed. Antonio Nanni and Charles Dolan. Detroit: ACI, 1993.

(24.) RIZKALLA, Sami and Pierre LABOSSI ÈRE. *Structural Engineering in FRP in Canada*, Concrete International, 21:25-28. October, 1999.

(25.) SAADATMANESH, Hamid and Fares E. TANNOUS. *Long-Term Behavior of Aramid Fiber-Reinforced Plastic (AFRP) Tendons*, ACI Materials Journal, 96:297-305. May-June, 1999.

(26.) SAADATMANESH, Hamid and Fares E. TANNOUS. *Durability of AR Glass Fiber-Reinforced Plastic Bars*, Journal of Composites for Construction, 3:12-19. February, 1999.

(27.) SASAKI, Iwao, Itaru NISHIZAKI, Hiroyuki SAKAMOTO, Kiyoshi KATAWAKI and Yukihiro KAWAMOTO. *Durability Evaluation of FRP Cables by*

Exposure Tests, Non-Metallic (FRP) Reinforcement for Concrete Structures: Proceedings of the Third International Symposium, 2: 131-137. October, 1997.

(28.) SEKIJIMA, Kenzo, Yasushi OTSUKA and Tomohiro KONNO. *Durability of Fiber-Reinforced Polymer Reinforcement Embedded in Concrete,* Fourth International Symposium on Fiber-Reinforced Polymer Reinforcement for Reinforced Concrete Structures (SP-188). Ed. by Antonio Nanni, Charles Dolan, Sami Rizkalla. Farmington Hills: ACI International, 1999.

(29.) SHEHATA, Emile, Ryan MORPHY and Sami RIZKALLA. *Fiber-reinforced Polymer Reinforcement for Concrete Structures,* Fourth International Symposium on Fiber-Reinforced Polymer Reinforcement for Reinforced Concrete Structures (SP-188). Ed. by Antonio Nanni, Charles Dolan, Sami Rizkalla. Farmington Hills: ACI International, 1999.

(30.) SONOBE, Yasuhisa. *An Overview of R&D in Japan,* Fiber-Reinforced-Plastic Reinforcement for Concrete Structures: Properties and Applications. Ed. by Antonio Nanni. New York: Elsevier, 1993.

(31.) SUGIYAMA, Tetsuya, Saki TOMITA, Satoshi KOUZAKI, Yasuhiko SATO, Tamon UEDA, and Akira KOBAYASHI. *Development of Continuous Fiber Flexible Reinforcement,* Fourth International Symposium on Fiber-Reinforced Polymer Reinforcement for Reinforced Concrete Structures (SP-188). Ed. by Antonio Nanni, Charles Dolan, Sami Rizkalla. Farmington Hills: ACI International, 1999.

(32.) SVECOVA, Dagmar and Ghani RAZAQPUR. *Fiber-Reinforced Polymer Prestressed Tension Elements as Reinforcement for Concrete*, Fourth International Symposium on Fiber-Reinforced Polymer Reinforcement for Reinforced Concrete Structures (SP-188). Ed. by Antonio Nanni, Charles Dolan, Sami Rizkalla. Farmington Hills: ACI International, 1999.

(33.) TAERWE, Luc (ed.), Non-Metallic (FRP) Reinforced for Concrete Structures: Proceeddings of the Second International RILEM Symposium (FRPRCS-2). New York: E & FN Spon, 1995.

(34.) TAERWE, Luc. *FRP Developments and Applications in Europe,* Fiber-Reinforced-Plastic Reinforcement for Concrete Structures: Properties and Applications. Ed. by Antonio Nanni. New York: Elsevier, 1993.

(35.) TAERWE, Luc and Stijn Matthys. *FRP for Concrete Construction: Activities in Europe*, Concrete International, 21:33-36. October, 1999.

(36.) TAERWE, Luc and Stijn Matthys. *Concrete Slabs Reinforced with FRP Grids. I: One-Way Bending*, Journal of Composites for Construction, 4:145-153. August, 2000.

(37.) TAERWE, Luc and Stijn Matthys. *Concrete Slabs Reinforced with FRP Grids. II: Two-Way Bending*, Journal of Composites for Construction, vol. 4, August, 2000.

(38.) TANANO, Hiroyuki, Yoshihiro MASUDA and F. TOMOSAWA. Characteristics and Performance Evaluation Methods of Continuous Fiber Bars-State of the Art Studies on Fire Properties and Durability of Continuous Fiber-reinforced Concrete in Japan, Fourth International Symposium on Fiber-Reinforced Polymer Reinforcement for Reinforced Concrete Structures (SP-188). Ed. by Antonio Nanni, Charles Dolan, Sami Rizkalla. Farmington Hills: ACI International, 1999.

(39.) UOMOTO, Taketo and F. KATSUKI. Prediction of Deterioration of FRP Rods Due to Alkali Attack, Non-Metallic (FRP) Reinforced for Concrete Structures: Proceedings of the Second International RILEM Symposium (FRPRCS-2). Ed. by Luc Taerwe. New York: E & FN Spon, 1995.

(40.) UOMOTO, Taketo and Tsugio NISHIMURA. *Deterioration of Aramid, Glass, and Carbon Fibers Due to Alkali, Acid, and Water in Different Temperatures,* Fourth International Symposium on Fiber-Reinforced Polymer Reinforcement for Reinforced Concrete Structures (SP-188). Ed. by Antonio Nanni, Charles Dolan, Sami Rizkalla. Farmington Hills: ACI International, 1999.

(41.) UOMOTO, Taketo and Tsugio NISHIMURA, H OHGA. *Static and Fatigue Strength of FRP Rods for Concrete Reinforcement,* Non-Metallic (FRP) Reinforced for Concrete Structures: Proceedings of the Second International RILEM Symposium (FRPRCS-2). Ed. by Luc Taerwe. New York: E & FN Spon, 1995.

(42.) VIJAY, P.V. and H.V.S. GANGARAO. *Accelerated and Natural Weathering of Glass Fiber-Reinforced Plastic Bars,* Fourth International Symposium on Fiber-Reinforced Polymer Reinforcement for Reinforced Concrete Structures (SP-188). Ed. by Antonio Nanni, Charles Dolan, Sami Rizkalla. Farmington Hills: ACI International, 1999.

(43.) ERKI, M.A. and S.H. RIZKALLA. *Anchorages for FRP Reinforcing*, Concrete International, 54-57. June, 1993.

(44.) CASTRO, Protasio, and Nicholas CARINO. *Tensile and Nondestructive Testing of FRP Bars*, Journal of Composites for Construction, 2:17-26. February, 1998.

(45.) HUGHES BROS. ARTICLE

(46.) KARBHARI, Vistasp M. and Gregory Pope. *Impact and Flexure Properties of Glass/Vinyl Ester Composites in Cold Regions*, Journal of Cold Regions Engineering, no. 1, 8:1-20, March 1994.

(47.) DUTTA, P.K. *Structural Fiber Composite Materials for Cold Regions*, Journal of Cold Regions Engineering, no. 3, 2:124-132, September 1988.

(48.) KARBHARI, V.M. and D.A. ECKEL. *Effect of Cold Regions Climate on Composite Jacketed Concrete Columns*, Journal of Cold Regions Engineering, no. 3, 8:73-86, September 1994.

(49.) DUTTA, P.K., D. HUI. *Low-Temperature and Freeze-Thaw Durability of Thick Composites*, Composites Engineering, no. ¾, 27:371-380, August 1995.

(50.) HARAMIS, J., K.N.E. VERGHESE, and J.J. LESKO. *Freeze-Thaw Durability of Composites for Civil Infrastructure (938)*, Technical Papers of the Annul Technical Conference-Society of Plastics Engineers (SPE) Incorporated, 58th, 3:3184-3188, May 2000.

(51.) http://www.merriam-webster.com/cgi-bin/dictionary

(52.) Creative Pultrusions, Inc. *The New and Improved Putex® Pultrusion Global Design Manual of Standard and Custom Fiber-reinforced Polymer Structural Profiles*, Alum Bank, PA, 2000.

(53.) GERRITSE, A. and H.J. SCHURHOFF. *Prestressing with Aramid Tendons*, Proceedings, 10th FIP Congress, New Delhi, 7pp, 1986.

(54.) ASTM Committee D-20. *Standard Test Method for Tensile Properties of Plastics*; D 638. ASTM, West Conshohocken, PA, 2000.

(55.) ASTM Committee D-20. *Standard Test Method for Tensile Properties of Putruded Glass-Fiber-Reinforced Plastic Rod*; D 3916. ASTM, West Conshohocken, PA, 1994.

(56.) ASTM Committee D-20. *Standard Practice for Conditioning Plastics for Testing*; D 618. ASTM, West Conshohocken, PA, 2000.

(57.) ASTM Committee C-9. *Standard Test Method for Resistance of Concrete to Rapid Freezing and Thawing*; C 666. ASTM, West Conshohocken, PA, 1997.

(58.) ASTM Committee D-20. *Standard Test Method for Tensile, Compressive, and Flexural Creep and Creep-Rupture of Plastics*; D 2990. ASTM, West Conshohocken, PA, 1995.

(59.) ASTM Committee D-30. *Standard Test Method for Tensile Properties of Polymer Matrix Composite Materials*; D 3039. ASTM, West Conshohocken, PA, 2000.

(60.) ASTM Committee E-28. *Standard Test Method for Poisson's Ratio at Room Temperature*; E 132. ASTM, West Conshohocken, PA, 1997.

(61.) ASTM Committee E-28. *Standard Test Method for Young's Modulus, Tangent Modulus, and Chord Modulus*; E 111. ASTM, West Conshohocken, PA, 1997.

(62.) ASTM Committee D-20. *Standard Test Method for Density and Specific Gravity (Relative Density) of Plastics by Displacement*; D 792. ASTM, West Conshohocken, PA, 2000.

(63.) MANDELL, J.F., F.J. McGARRY, A.J.Y. HSIEH, C.G. LI. *Tensile Fatigue of Glass Fibers and Composites with Conventional and Surface Compresed Fibers*, Research Report R84-4, Massachusetts Institute of Technology, Cambridge, MA, 1984.

(64.) MANDELL, J.F., F.J. McGARRY, D.D. HUANG. *Tensile Fatigue Performance of Glass Fiber Dominated Composites*, Research Report R80-4, Massachusetts Institute of Technology, Cambridge, MA, 1980.

(65.) CURTIS, P.T. *Fatigue*, Mechanical Testing of Advanced Fibre Composites, ed. J.M. Hodgkinson, Woodhead Publishing Limited, Cambridge, England, 2000.

(66.) CATHERALL, J. A. *Fibre Reinforcement*, Mills & Boon Limited, London, 1973.

(67.) COOMARASAMY, A. and S. GOODMAN. *Investigation of the Durability Characteristics of Fibre Reinforced Plastic (FRP) Materials in Concrete Environment*, Proceedings of the American Society for Composites-12th Technical Conference, pp. 296-305, Dearborn, Michigan, October 1997.

(68.) THIPPESWAMY, Hemanth, Jason FRANCO, and Hota GANGARAO. *FRP Reinforcement in Bridge Decks,* Concrete International, **27**:839-849. October, 2000.

(69.) NANNI, Antonio. *Flexural Behaviour and Design of RC Members Using FRP Reinforcement,* Journal of Structural Engineering, **119**:11, 3344-3359, November, 1993.

(70.) BAKIS, C.E., A. NANNI, J.A. TEROSKY, and S.W. KOEHLER. *Self-Monitoring, Pseudo-Ductile, Hybrid FRP Reinforcement Rods for Concrete Applications,* Composites Science and Technology, **61**:815-823, 2001.

(71.) TSUSHIMA, Eiki, Jun TAKAYASU, and Isao KIMPARA. *Fracture Mechanism for High-Modulus Pitch-Based CFRP,* Advances in Fiber Composite Materials. Ed. by T. Fukuda, Z. Maekawa and T. Fujii, Elsevier Science and The Society of Materials Science. Japan, pp. 1-23, 1994.

(72.) SMITH, Clinton. *Pultrusion Fundamentals*, http://www.cfa-hq.org/documents/PultrusionFundamentals.doc.

(73.) http://www.psrc.usm.edu/macrog/composit.htm. Department of Polymer Science, University of Southern Mississippi, 1996.

(74.) NGUYEN, Tinh, E. BYRD, D. ALSHED, K. AOUADI and Joannie CHIN. *Water at the Polymer/Substrate Interface and Its Role in the Durability of Polymer/Glass Fiber Composites,* Durability of Fibre Reinforced Polymer (FRP) Composites for Construction (CDCC'98): First International Conference. Ed. by B. Benmokrane, H. Rahman. Canada, pp. 451-462, August, 1998.

(75.) Hughes Brothers, Inc. http://hughesbros.com/RebMain.html, 2001.

(76.) ELBADRY, Mamdouh, Hany ABDALLA, and Amin GHALI. *Effects of Temperature on the Behaviour of Fiber-reinforced Polymer Reinforced Concrete Members: Experimental Studies,* Canadian Journal of Civil Engineering, **27**:993-1004. 2000.

(77.) VERGHESE, K., J. HARAMIS, S. PATEL, J. SENNE, S. Case, and J. LESKO. *Enviro-Mechanical Durability of Polymer Composites,* Long Term Durability of Structural Materials. Ed. by P.J.M. Monteiro, K.P. Chong, J. Larsen-Basse, K. Komvopoulos. Elsevier Science Ltd., pp. 159-170, 2001.

(78.) BARBERO, Ever. *West Virginia University (WVU) Research Activities on Composite Materials,* http://www2.cemr.wvu.edu/~ejb/rao.html

(79.) http://www.new-technologies.org/ECT/Civil/superdeck.htm. *Modular FRP Composites Bridge Deck*, Emerging Construction Technologies.

(80.) AMBROSE, James. *Building Structures,* John Wiley & Sons, New York, 1993.

(81.) ELBADRY, Mamdouh, Hany ABDALLA, and Amin GHALI. *Effects of Temperature on the Behaviour of Fiber-reinforced Polymer Reinforced Concrete Members: Experimental Studies,* Canadian Journal of Civil Engineering, **27**:993-1004. 2000.

(82.) WELSH, L.M. and J. HARDING. *Dynamic Tensile Response of Unidirectionally-Reinforced Carbon Epoxy and Glass Epoxy Composites,* Proceedings of the 5th International Conference on Composite Materials ICCM-V, TMSAIME, pp. 1517-1531, 1985.

(83.) ACI Committee 440. Recommended Test Methods for FRP Rods and Sheets. Detroit: ACI, September, 2001.

(84.) SHAH, Vishu. *Handbook of Plastics Testing Technology*. John Wiley & Sons:New York, 1998.

(85.) MANDELL, J.F. *Fatigue Baehaviour of Fibre-Resin Composites,* Developments in Reinforced Plastics 2: Properties of Laminates, Ed. By G. Pritchard, Applied Science Publishers, New York, 1982.

(86.) ARMENAKAS, A.E. and C.A. SCIAMMARELLA. *Response of Glass-Fiber-Reinforced Epoxy Specimens to High Rates of Tensile Loading,* Experimental Mechanics, pp. 433-440, October, 1973.

(87.) ROY, S. *Computer Models for Predicting Durability,* Reinforced Plastics Durability, Ed. By G. Pritchard, Woodhead Publishing Limited, England, 1999.

APPENDIX A: Material Properties

Table A1: Properties of FRP as Compared with Steel

Tensile Propeties	Steel Bar	Steel Tendon	GFRP Bar	GFRP Tendon	CFRP Tendon
Ultimate Strength, ksi	70 - 100	200 - 270	75 - 175	200 - 250	240 - 350
Elastic Modulus, ksi	29,000	27 - 29,000	6 - 8,000	7 - 9,000	22 - 24,000
Specific Gravity	7.9	7.9	1.5 - 2.0	2.4	1.5 - 1.6
Tensile Strain, %	>10	>4	3.5 - 5.0	3.0 - 4.5	1.0 - 1.5
Thermal Coeff, $x10^{-6}/^oF$	Longitudinal: 6.5	6.5	5.5	5.5	0.38 to -0.68

Table A2: Properties of Reinforcing Fibers

Tensile Propeties	E-Glass	Aramid	Carbon-PAN		Carbon-pitch
			high strength	high modulus	high modulus
Ultimate Strength, ksi	275-500	504 - 525	505 - 1,030	360 - 565	305 - 350
Elastic Modulus, ksi	10,500	6, - 27,000	33,360 - 42,640	42,640 - 85,280	75,420 - 139,235
Specific Gravity	~2.5	~1.3	~1.8	~1.75	~1.75
Tensile Strain, %	2.4 - 5.6	1.86 - 8.75	1.6 - 1.8	0.7	0.3
Poissons Ratio	0.2	0.38	-0.2	-0.2	N/A
Density lb/in^3	0.094	0.052	0.065	0.063	0.063
Thermal Coeff, $x10^{-6}/^oF$	Longitudinal: 9.0	-2.0 to -4.0		Carbon: 0.0 to -2.0	

N/A: Not Available

Table A3: Properties of Polymer Resin Matrix

Tensile Propeties	Epoxy	Polyester	Vinyl Ester
Ultimate Strength, ksi	8 - 20	3 - 15	11.5 - 13
Elastic Modulus, ksi	360 - 595	305 - 595	460 - 490
Tensile Strain, %	1.0 - 9.0	1.0 - 6.0	3.9 - 5.2
Poissons Ratio	0.37	0.35-0.40	0.373
Density lb/in^3	.040 - .047	.036 - .052	.038 - .040
Thermal Coeff, $x10^{-6}/^oF$	Longitudinal: 25 - 45	30 - 55	15 - 35

N/A: Not Available

Table A4: Properties of FRP as Supplied by the Manufacturer

Tensile Propeties		Aslan100: $GFRP_B$		C-Bar: $GFRP_S$		LEADLINE: CFRP	
Ultimate Strength	3/8'	110 ksi	(825 MPa)	121 ksi	(840 MPa)	455 ksi	(3140 MPa)
	1/2'	100 ksi	(860 Mpa)	116 ksi	(800 MPa)		
Elastic Modulus		5,920 ksi	(40.8 Gpa)	6,000 ksi	(42 GPa)	21,320 ksi	(147 GPa)
Specific Gravity		2.00	-	1.90	-	1.60	-
Thermal Coeff. $x10^{-6}/^oF$		Longitudinal: 5.04	-	4.50	-	0.38 to -0.68	-

Tables A5: Properties Calculated by Effective Diameter Method

Bar Type	DIAMETER (in)		AREA (in^2)		DENSITY	
	Minimum	Average	Minumum	Average	(lb/in^3)	(g/cm^3)
3/8" CFRP	0.359	0.369	0.101	0.107	0.063	1.744
3/8" GFRPs	0.369	0.388	0.107	0.118	0.070	1.947
3/8" GFRPr	0.376	0.390	0.111	0.119	0.074	2.046
1/2" GFRPr	0.503	0.515	0.199	0.208	0.072	1.999
1/2" GFRPs	-	0.5[1]	-	0.196[1]	-	-

[1] Samples were not available for this type bar to determine precise values

Table A6: Calculated Weight and Specific Gravity

Bar Type	WEIGHT		SPECIFIC GRAVITY	
	(lb/ft)	(g/mm)	Minumum	Average
3/8" CFRP	0.084	0.118	1.70	1.74
3/8" GFRPs	0.096	0.147	1.85	1.95
3/8" GFRPr	0.108	0.158	1.92	2.05
1/2" GFRPr	0.180	0.271	1.89	2.00
1/2" GFRPs[1]	-	-	-	-

[1] Samples were not available for this type bar

Table A7: Catalogue of All Bars Tested

Pre-Conditioning:		UNCONDITIONED		Code Description:		.38GS-1u = (bar dia)(fiber type)(surface texture)-(# this type)(unconditioned)					
				DIAMETER (in)		AREA (in^2)		TOTAL LENGTH (in)		FREE LENGTH (in)	
Bar #	**Code**	**Type**		Minimum	Average	Minumum	Average	Initial	Final	Initial	Final
A	C-1u	3/8" CFRP	Ö	0.359	0.366	0.101	0.105	N/A	39.50	N/A	15.25
8	C-2u	3/8" CFRP	Ö	0.359	0.366	0.101	0.105	N/A	25.00	N/A	12.69
9	C-3u	3/8" CFRP	Ö	0.359	0.366	0.101	0.105	N/A	24.50	N/A	12.38
B	.38GS-1u	3/8" $GFRP_S$	Ö	0.369	0.383	0.107	0.115	N/A	40.00	N/A	16.00
6	.38GS-2u	3/8" $GFRP_S$	Ö	0.369	0.383	0.107	0.115	N/A	24.00	N/A	11.88
12	.38GS-3u	3/8" $GFRP_S$	Ö	0.369	0.383	0.107	0.115	N/A	24.13	N/A	12.00
39	.38GS-4u	3/8" $GFRP_S$	Ö	0.369	0.383	0.111	0.119	N/A	24.25	N/A	12.13
49	.38GS-5u	3/8" $GFRP_S$	Ö	0.369	0.383	0.107	0.115	23.75	24.38	11.31	12.25
50	.38GS-6u	3/8" $GFRP_S$	Ö	0.369	0.383	0.107	0.115	23.88	24.63	11.31	12.19
51	.38GS-7u	3/8" $GFRP_S$	Ö	0.369	0.383	0.107	0.115	23.81	N/A	11.25	N/A
52	.38GS-8u	3/8" $GFRP_S$	Ö	0.369	0.383	0.107	0.115	23.69	N/A	11.25	N/A
53	.38GS-9u	3/8" $GFRP_S$	Ö	0.369	0.383	0.107	0.115	23.88	25.00	11.38	12.38
54	.38GS-10u	3/8" $GFRP_S$	Ö	0.369	0.383	0.107	0.115	23.69	N/A	11.19	N/A
55	.38GS-11u	3/8" $GFRP_S$	Ö	0.369	0.383	0.107	0.115	23.69	24.38	11.25	11.94
56	.38GS-12u	3/8" $GFRP_S$	Ö	0.369	0.383	0.107	0.115	23.69	24.63	11.25	12.19
57	.38GS-13u	3/8" $GFRP_S$	Ö	0.369	0.383	0.107	0.115	23.69	23.75	11.25	11.25
58	.38GS-14u	3/8" $GFRP_S$	Ö	0.369	0.383	0.107	0.115	23.63	N/A	11.13	N/A
59	.38GS-15u	3/8" $GFRP_S$	Ö	0.369	0.383	0.107	0.115	23.75	N/A	11.25	N/A
11	.38GR-1u	3/8" $GFRP_R$	Ö	0.376	0.390	0.111	0.119	N/A	24.00	N/A	11.90
13	.38GR-2u	3/8" $GFRP_R$	Ö	0.376	0.390	0.111	0.119	N/A	24.25	N/A	11.88
28	.38GR-3u	3/8" $GFRP_R$	Ö	0.376	0.390	0.111	0.119	24.00	24.50	11.75	12.25
29	.38GR-4u	3/8" $GFRP_R$	Ö	0.376	0.390	0.111	0.119	24.00	24.00	11.88	11.88
37	.38GR-5u	3/8" $GFRP_R$	Ö	0.376	0.390	0.111	0.119	23.75	24.13	11.31	11.69
38	.38GR-6u	3/8" $GFRP_R$	Ö	0.376	0.390	0.111	0.119	N/A	23.75	N/A	11.19
40	.38GR-8u	3/8" $GFRP_R$	Ö	0.376	0.390	0.111	0.119	23.75	24.75	11.25	12.25
60	.38GR-9u	3/8" $GFRP_R$	Ö	0.376	0.390	0.111	0.119	23.75	24.69	11.19	12.13
61	.38GR-10u	3/8" $GFRP_R$	Ö	0.376	0.390	0.111	0.119	23.75	24.31	11.31	11.87
62	.38GR-11u	3/8" $GFRP_R$	Ö	0.376	0.390	0.111	0.119	23.81	24.81	11.31	12.31
63	.38GR-12u	3/8" $GFRP_R$	Ö	0.376	0.390	0.111	0.119	23.75	24.69	11.25	12.19

N/A: An initial reading was not taken before test or total failure prevented a final reading to be taken.

Table A8: Catalogue of All Bars Tested

Pre-Conditioning:		UNCONDITIONED		Code Description:	.38GS-1u = (bar dia)(fiber type)(surface texture)-(# this type)(unconditioned)					
			DIAMETER (in)		AREA (in^2)		TOTAL LENGTH (in)		FREE LENGTH (in)	
Bar #	**Code**	**Type**	Minimum	Average	Minumum	Average	Initial	Final	Initial	Final
78	.38GR-13u	3/8" $GFRP_R$ Ö	0.376	0.390	0.111	0.119	23.75	24.63	11.19	12.31
79	.38GR-14u	3/8" $GFRP_R$ Ö	0.376	0.390	0.111	0.119	23.63	25.00	11.13	12.75
80	.38GR-15u	3/8" $GFRP_R$ Ö	0.376	0.390	0.111	0.119	23.75	24.63	11.25	12.31
81	.38GR-16u	3/8" $GFRP_R$ Ö	0.376	0.390	0.111	0.119	24.13	N/A	11.56	N/A
82	.38GR-17u	3/8" $GFRP_R$ Ö	0.376	0.390	0.111	0.119	23.69	N/A	11.19	N/A
83	.38GR-18u	3/8" $GFRP_R$ Ö	0.376	0.390	0.111	0.119	23.88	N/A	11.38	N/A
84	.38GR-19u	3/8" $GFRP_R$ Ö	0.376	0.390	0.111	0.119	N/A	24.25	N/A	12.13
85	.38GR-20u	3/8" $GFRP_R$ Ö	0.376	0.390	0.111	0.119	23.75	N/A	11.44	N/A
86	.38GR-21u	3/8" $GFRP_R$ Ö	0.376	0.390	0.111	0.119	23.81	N/A	11.50	N/A
87	.38GR-22u	3/8" $GFRP_R$	0.376	0.390	0.111	0.119	23.75		11.38	
88	.38GR-23u	3/8" $GFRP_R$	0.376	0.390	0.111	0.119	23.75		11.38	
7	.50GR-1u	1/2" $GFRP_R$ Ö	0.503	0.515	0.199	0.208	N/A	23.75	N/A	11.96
10	.50GR-2u	1/2" $GFRP_R$ Ö	0.503	0.515	0.199	0.208	N/A	24.00	N/A	11.88
41	.50GR-3u	1/2" $GFRP_R$ Ö	0.503	0.515	0.199	0.208	23.81	24.31	11.25	11.75
42	.50GR-4u	1/2" $GFRP_R$ Ö	0.503	0.515	0.199	0.208	23.75	24.19	11.25	11.69
64	.50GR-5u	1/2" $GFRP_R$ Ö	0.503	0.515	0.199	0.208	23.75	N/A	11.19	N/A
65	.50GR-6u	1/2" $GFRP_R$ Ö	0.503	0.515	0.199	0.208	23.69	24.63	11.06	12.00
66	.50GR-7u	1/2" $GFRP_R$ Ö	0.503	0.515	0.199	0.208	23.75	N/A	11.19	N/A
67	.50GR-8u	1/2" $GFRP_R$ Ö	0.503	0.515	0.199	0.208	23.69	24.63	11.13	12.25
68	.50GR-9u	1/2" $GFRP_R$ Ö	0.503	0.515	0.199	0.208	23.63	N/A	11.06	N/A
69	.50GR-10u	1/2" $GFRP_R$ Ö	0.503	0.515	0.199	0.208	23.75	N/A	11.13	N/A
70	.50GR-11u	1/2" $GFRP_R$ Ö	0.503	0.515	0.199	0.208	23.88	N/A	11.25	N/A
71	.50GR-12u	1/2" $GFRP_R$ Ö	0.503	0.515	0.199	0.208	23.63	N/A	11.00	N/A
72	.50GR-13u	1/2" $GFRP_R$ Ö	0.503	0.515	0.199	0.208	23.75	N/A	11.13	N/A
73	.50GR-14u	1/2" $GFRP_R$ Ö	0.503	0.515	0.199	0.208	23.75	N/A	11.13	N/A
74	.50GR-15u	1/2" $GFRP_R$ Ö	0.503	0.515	0.199	0.208	23.69	N/A	11.00	N/A
75	.50GR-16u	1/2" $GFRP_R$ Ö	0.503	0.515	0.199	0.208	23.94	N/A	11.31	N/A
76	.50GR-17u	1/2" $GFRP_R$ Ö	0.503	0.515	0.199	0.208	23.81	N/A	11.19	N/A
77	.50GR-18u	1/2" $GFRP_R$ Ö	0.503	0.515	0.199	0.208	23.69	N/A	11.06	N/A
C	.50GS-1u	1/2" $GFRP_S$ Ö	0.500	0.500	0.196	0.196	N/A	40.00	N/A	16.00

Table A9: Catalogue of All Bars Tested

Pre-Conditioning:		**CONDITIONED**		Temperature Cycle (°F) -20°F - 68°F		CycleTime 3 hr/cycle; 24 hr/day		# Cycles 250			
				DIAMETER (in)		**AREA** (in^2)		**TOTAL LENGTH** (in)		**FREE LENGTH** (in)	
Bar #	**Code**	**Type**		Minimum	Average	Minumum	Average	Initial	Final	Initial	Final
1	C-1	3/8" CFRP	Ö	0.356	0.362	0.100	0.103	40.00	N/A	16.00	N/A
2	.38GS-1	3/8" $GFRP_S$	Ö	0.369	0.383	0.107	0.115	40.00	N/A	16.00	N/A
19	.38GS-2	3/8" $GFRP_S$	Ö	0.369	0.383	0.107	0.115	23.88	24.44	11.50	12.00
20	.38GS-3	3/8" $GFRP_S$	Ö	0.369	0.383	0.107	0.115	24.00	24.00	11.81	11.81
21	.38GS-4	3/8" $GFRP_S$	Ö	0.369	0.383	0.107	0.115	24.00	24.00	11.88	11.88
27	.38GS-5	3/8" $GFRP_S$	Ö	0.369	0.383	0.107	0.115	23.94	23.94	11.63	11.63
30	.38GS-6	3/8" $GFRP_S$	Ö	0.369	0.383	0.107	0.115	23.94	24.81	11.50	12.63
31	.38GS-7	3/8" $GFRP_S$	Ö	0.369	0.383	0.107	0.115	23.06	N/A	11.63	N/A
32	.38GS-8	3/8" $GFRP_S$	Ö	0.369	0.383	0.107	0.115	23.81	24.44	11.38	12.00
33	.38GS-9	3/8" $GFRP_S$	Ö	0.369	0.383	0.107	0.115	23.75	24.44	11.50	12.13
34	.38GS-10	3/8" $GFRP_S$	Ö	0.369	0.383	0.107	0.115	23.69	24.31	11.25	11.88
35	.38GS-11	3/8" $GFRP_S$	Ö	0.369	0.383	0.107	0.115	23.75	25.13	11.31	11.88
36	.38GS-12	3/8" $GFRP_S$	Ö	0.369	0.383	0.107	0.115	23.75	N/A	11.25	N/A
46	.38GS-13	3/8" $GFRP_S$	Ö	0.369	0.383	0.107	0.115	23.81	24.63	11.31	12.31
47	.38GS-14	3/8" $GFRP_S$	Ö	0.369	0.383	0.107	0.115	23.63	N/A	11.13	N/A
48	.38GS-15	3/8" $GFRP_S$	Ö	0.369	0.383	0.107	0.115	23.88	N/A	11.38	N/A
4	.50GR-1	1/2" $GFRP_R$	Ö	0.503	0.515	0.199	0.208	40.00	N/A	16.00	N/A
5	.50GR-2	1/2" $GFRP_R$	Ö	0.503	0.515	0.199	0.208	40.00	N/A	16.00	N/A
22	.50GR-3	1/2" $GFRP_R$	Ö	0.503	0.515	0.199	0.208	23.88	23.13	11.63	11.88
14	.50GR-4	1/2" $GFRP_R$	Ö	0.503	0.515	0.199	0.208	23.38	24.19	11.19	12.00
15	.50GR-5	1/2" $GFRP_R$	Ö	0.503	0.515	0.199	0.208	24.00	24.69	11.63	12.69
16	.50GR-6	1/2" $GFRP_R$		0.503	0.515	0.199	0.208	23.44		11.00	
23	.50GR-7	1/2" $GFRP_R$	Ö	0.503	0.515	0.199	0.208	23.75	24.00	11.13	11.94
24	.50GR-8	1/2" $GFRP_R$	Ö	0.503	0.515	0.199	0.208	23.75	N/A	11.19	N/A
43	.50GR-9	1/2" $GFRP_R$	Ö	0.503	0.515	0.199	0.208	23.81	24.38	11.25	12.25
44	.50GR-10	1/2" $GFRP_R$	Ö	0.503	0.515	0.199	0.208	23.81	24.63	11.25	12.44
45	.50GR-11	1/2" $GFRP_R$	Ö	0.503	0.515	0.199	0.208	23.81	N/A	11.19	N/A

N/A: An initial reading was not taken before test or total failure prevented a final reading to be taken.

Table A10: Catalogue of All Bars Tested

Pre-Conditioning:	**CONDITIONED**			Temperature Cycle (°F)		CycleTime		# Cycles			
				-20°F - 68°F		3 hr/cycle; 24 hr/day		250			
				DIAMETER (in)		**AREA** (in^2)		**TOTAL LENGTH** (in)		**FREE LENGTH** (in)	
Bar #	**Code**	**Type**		Minimum	Average	Minumum	Average	Initial	Final	Initial	Final
17	.38GR-1	3/8" $GFRP_R$	Ö	0.376	0.390	0.111	0.119	23.88	24.44	11.63	12.63
18	.38GR-2	3/8" $GFRP_R$	Ö	0.376	0.390	0.111	0.119	23.88	24.38	11.50	12.00
25	.38GR-3	3/8" $GFRP_R$	Ö	0.376	0.390	0.111	0.119	24.00	24.25	11.63	11.88
26	.38GR-4	3/8" $GFRP_R$	Ö	0.376	0.390	0.111	0.119	24.00	24.44	11.88	24.06
3	.50GS-1	1/2" $GFRP_S$	Ö	0.500	0.500	0.196	0.196	40.00	N/A	16.00	N/A

Pre-Conditioning:	**CHEMICAL BATH**			Solution				Time	pH	Temperature	
				0.6 M KOH + 0.2M NaOH + sat'd $Ca(OH)_2$				18 months	13.5_i - 12.45_f	21.8°C	(71.24°F)
				DIAMETER (in)		**AREA** (in^2)		**TOTAL LENGTH** (in)		**FREE LENGTH** (in)	
Bar #	**Code**	**Type**		Minimum	Average	Minumum	Average	Initial	Final	Initial	Final
93	C-1cb	3/8" CFRP	Ö	0.359	0.366	0.101	0.105	23.63	N/A	11.19	N/A
94	C-2cb	3/8" CFRP	Ö	0.359	0.366	0.101	0.105	23.13	N/A	10.31	N/A
95	C-3cb	3/8" CFRP	Ö	0.359	0.366	0.101	0.105	23.63	N/A	11.38	N/A
96	.38GS-1cb	3/8" $GFRP_S$	Ö	0.369	0.383	0.107	0.115	23.94	N/A	11.69	N/A
97	.38GS-2cb	3/8" $GFRP_S$	Ö	0.369	0.383	0.107	0.115	24.00	N/A	11.69	N/A
98	.38GS-3cb	3/8" $GFRP_S$	Ö	0.369	0.383	0.107	0.115	23.88	N/A	11.56	N/A
99	.50GR-1cb	1/2" $GFRP_R$		0.503	0.515	0.199	0.208	23.81		11.50	
100	.50GR-2cb	1/2" $GFRP_R$		0.503	0.515	0.199	0.208	23.69		11.38	
101	.50GR-3cb	1/2" $GFRP_R$		0.503	0.515	0.199	0.208	23.69		11.38	
102	.50GS-1cb	1/2" $GFRP_S$		0.503	0.515	0.199	0.208	23.88		11.56	
103	.50GS-2cb	1/2" $GFRP_S$		0.500	0.500	0.196	0.196	24.19		11.75	
104	.50GS-3cb	1/2" $GFRP_S$		0.500	0.500	0.196	0.196	24.00		11.69	
105	.50GS-4cb	1/2" $GFRP_S$		0.500	0.500	0.196	0.196	24.13		11.81	

N/A: An initial reading was not taken before test or total failure prevented a final reading to be taken.

Table A11: Measurements for Effective Diameter and Specific Gravity

Bar #	Bar Type	Length (mm)	Length (in)	Weight (g)	Weight (lbs)	Volume (mL)	Volume (in^3)	Density (g/cm^3)	Density (lb/in^3)	Area (mm^2)	Area (in^2)	Diameter (mm)	Diameter (in)	SG
9	.38CFRP	190	*7.470*	22.356	*0.049*	13.0	*0.793*	1.720	*0.062*	69	*0.106*	9	*0.368*	1.72
13	.38CFRP	191	*7.516*	22.589	*0.050*	12.5	*0.763*	1.807	*0.065*	65	*0.101*	9	*0.359*	1.81
14	.38CFRP	193	*7.594*	22.807	*0.050*	13.0	*0.793*	1.754	*0.063*	67	*0.104*	9	*0.365*	1.75
15	.38CFRP	194	*7.625*	22.896	*0.050*	13.5	*0.824*	1.696	*0.061*	70	*0.108*	9	*0.371*	1.70
										Avg:	***0.107***	***Avg:***	***0.369***	**1.74**
										Min:	***0.101***	***Min:***	***0.359***	
10	.38GFRP$_S$	202	*7.960*	29.546	*0.065*	16.0	*0.976*	1.847	*0.067*	79	*0.123*	10	*0.395*	1.85
11	.38GFRP$_S$	201	*7.930*	29.709	*0.065*	16.0	*0.976*	1.857	*0.067*	79	*0.123*	10	*0.396*	1.86
12	.38GFRP$_S$	203	*8.010*	29.920	*0.066*	14.0	*0.854*	2.137	*0.077*	69	*0.107*	9	*0.369*	2.14
										Avg:	***0.118***	***Avg:***	***0.388***	**1.95**
										Min:	***0.107***	***Min:***	***0.369***	
5	.38GFRP$_R$	202	*7.960*	31.682	*0.070*	15.0	*0.915*	2.112	*0.076*	74	*0.115*	10	*0.383*	2.11
6	.38GFRP$_R$	203	*8.000*	31.594	*0.070*	14.0	*0.854*	2.257	*0.082*	69	*0.107*	9	*0.369*	2.26
7	.38GFRP$_R$	203	*8.010*	31.856	*0.070*	14.5	*0.885*	2.197	*0.079*	71	*0.110*	10	*0.375*	2.20
18	.38GFRP$_R$	204	*8.035*	32.705	*0.072*	17.0	*1.037*	1.924	*0.070*	83	*0.129*	10	*0.405*	1.92
19	.38GFRP$_R$	202	*7.956*	32.649	*0.072*	16.5	*1.007*	1.979	*0.071*	82	*0.127*	10	*0.401*	1.98
										Avg:	***0.118***	***Avg:***	***0.387***	**2.09**
										Min:	***0.107***	***Min:***	***0.369***	
I	.38GFRP$_R$	304	*11.988*	47.688	*0.105*	24.0	*1.465*	1.987	*0.072*	79	*0.122*	10	*0.394*	1.99
II	.38GFRP$_R$	304	*11.956*	47.345	*0.104*	23.8	*1.449*	1.993	*0.072*	78	*0.121*	10	*0.393*	1.99
III	.38GFRP$_R$	302	*11.906*	47.059	*0.104*	22.5	*1.373*	2.091	*0.076*	74	*0.115*	10	*0.383*	2.09
IV	.38GFRP$_R$	306	*12.056*	47.545	*0.105*	24.5	*1.495*	1.941	*0.070*	80	*0.124*	10	*0.397*	1.94
V	.38GFRP$_R$	304	*11.984*	47.454	*0.105*	24.0	*1.465*	1.977	*0.071*	79	*0.122*	10	*0.394*	1.98
										Avg:	***0.121***	***Avg:***	***0.392***	**2.00**
										Min:	***0.115***	***Min:***	***0.383***	
										8"-12" Avg:	***0.119***	***Avg:***	***0.390***	**2.05**
										8"-12" Min:	***0.111***	***Min:***	***0.376***	
1	.5GFRP$_R$	206	*8.100*	55.237	*0.122*	26.0	*1.587*	2.124	*0.077*	126	*0.196*	13	*0.499*	2.12
2	.5GFRP$_R$	204	*8.030*	55.059	*0.121*	27.0	*1.648*	2.039	*0.074*	132	*0.205*	13	*0.511*	2.04
3	.5GFRP$_R$	204	*8.050*	54.323	*0.120*	26.5	*1.617*	2.050	*0.074*	130	*0.201*	13	*0.506*	2.05
16	.5GFRP$_R$	193	*7.596*	54.608	*0.120*	27.5	*1.678*	1.986	*0.072*	143	*0.221*	13	*0.530*	1.99
17	.5GFRP$_R$	204	*8.025*	54.969	*0.121*	28.0	*1.709*	1.963	*0.071*	137	*0.213*	13	*0.521*	1.96
										Avg:	***0.207***	***Avg:***	***0.514***	**2.03**
										Min:	***0.196***	***Min:***	***0.500***	
VI	.5GFRP$_R$	305	*12.025*	81.957	*0.181*	42.5	*2.594*	1.928	*0.070*	139	*0.216*	13	*0.524*	1.93
VII	.5GFRP$_R$	303	*11.938*	79.326	*0.175*	40.0	*2.441*	1.983	*0.072*	132	*0.204*	13	*0.510*	1.98
IIV	.5GFRP$_R$	304	*11.969*	80.849	*0.178*	40.5	*2.471*	1.996	*0.072*	133	*0.206*	13	*0.513*	2.00
IX	.5GFRP$_R$	303	*11.938*	79.886	*0.176*	39.5	*2.410*	2.022	*0.073*	130	*0.202*	13	*0.507*	2.02
X	.5GFRP$_R$	304	*11.984*	80.479	*0.177*	42.5	*2.594*	1.894	*0.068*	140	*0.216*	13	*0.525*	1.89
										Avg:	***0.209***	***Avg:***	***0.516***	**1.96**
										Min:	***0.202***	***Min:***	***0.507***	
										8"-12" Avg:	***0.208***	***Avg:***	***0.515***	**2.00**
										8"-12" Min:	***0.199***	***Min:***	***0.503***	

APPENDIX B: Mechanical Testing Results

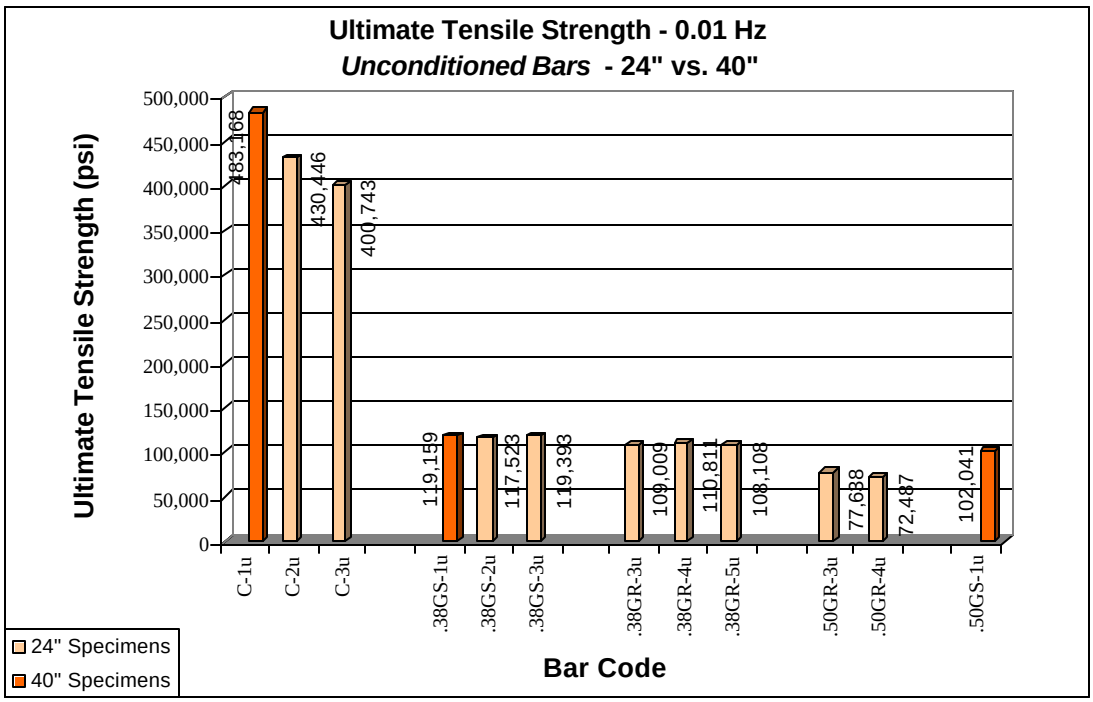

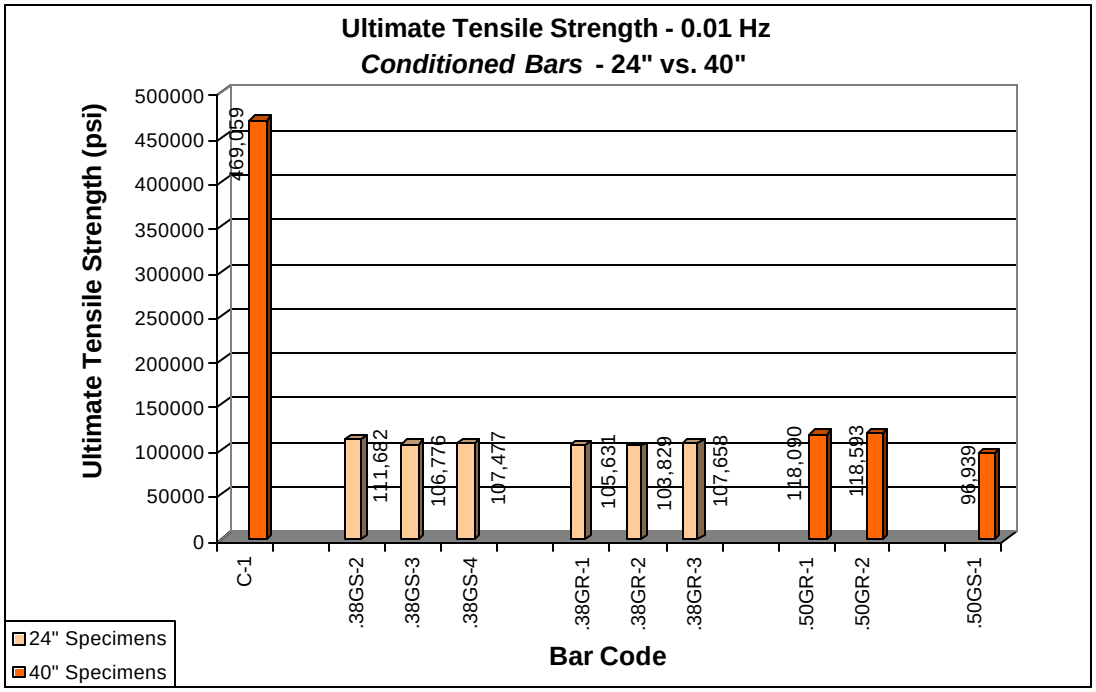

Table B1: Axial Tension, All Type Bars, Load Control, 0.01 Hz

Pre-Conditioning: UNCONDITIONED

Test Environment:
Room temperature, RH = 13%, Load Rate ~ 250 lb/sec ~ .01 Hz

				Tensile Load	24"	Tensile Strength				Tensile Load	40"	Tensile Strength		
Bar #	**Code**	**Type**	Extension (in)	Maximum (lbs)		Nominal (psi)	COV (%)	SD	Extension (in)	Maximum (lbs)		Nominal (psi)	COV (%)	SD
A	C-1u	3/8" CFRP							N/A	48,800		483,168	0	
8[2]	*C-2u*	*3/8" CFRP*		*43,475*		*430,446*	*14,851*							
9[2]	*C-3u*	*3/8" CFRP*		*40,475*		*400,743*	*-14,851*							
				41,975	**Avg.**	**415,594**	**5.054%**	21003		**48,800**	**Avg.**	**483,168**	**0.000%**	0
B	.38GS-1u	3/8" $GFRP_S$							N/A	12,750		119,159	0	
6	.38GS-2u	3/8" $GFRP_S$	N/A	12,575		117,523	-935							
12	.38GS-3u	3/8" $GFRP_S$	N/A	12,775		119,393	935							
				12,675	**Avg.**	**118,458**	**1.116%**	1322		**12,750**	**Avg.**	**119,159**	**0.000%**	0
28	.38GR-3u	3/8" $GFRP_R$	0.500	12,100		109,009	-300							
29	.38GR-4u	3/8" $GFRP_R$	0.000	12,300		110,811	1,502							
37	.38GR-5u	3/8" $GFRP_R$	0.380	12,000		108,108	-1,201							
				12,133	**Avg.**	**109,309**	**1.259%**	1376						
41	.50GR-3u	1/2" $GFRP_R$	0.500	15,450		77,638	2,575							
42	.50GR-4u	1/2" $GFRP_R$	0.440	14,425		72,487	-2,575							
				14,938	**Avg.**	**75,063**	**4.852%**	3642						
C	.50GS-1u	1/2" $GFRP_S$							N/A	20,000		102,041	0	
										20,000	**Avg.**	**102,041**	**0.000%**	0

[1] Graph Included
[2] *Bar slipped in end grip anchor.*

Table B2: Axial Tension, All Type Bars, Load Control, 0.01 Hz

Cycle Temperature	Cycle Time	# of Cycles	Test Environment:
-20 °F to 68 °F	3 hr/cycle; 8 cycles/day	250	Room temperature, RH = 13%, Load Rate ~ 200 lb/sec ~ .01 Hz

Bar #	Code	Type	24" Extension (in)	24" Tensile Load Maximum (lbs)		24" Tensile Strength Nominal (psi)	24" COV (%)	24" SD	40" Extension (in)	40" Tensile Load Maximum (lbs)		40" Tensile Strength Nominal (psi)	40" COV (%)	40" SD
1	C-1	3/8" CFRP							N/A	47,375		469,059	0	
										47,375	**Avg.**	**469,059**	**0.000%**	0
19	.38GS-2	3/8" $GFRP_S$	0.56	11,950		111,682	3,037							
20	.38GS-3	3/8" $GFRP_S$	0.00	11,425		106,776	-1,869							
21	.38GS-4	3/8" $GFRP_S$	0.00	11,500		107,477	-1,168							
				11,625	**Avg.**	**108,645**	**2.443%**	2654						
17	.38GR-1	3/8" $GFRP_R$	0.56	11,725		105,631	-75							
18	.38GR-2	3/8" $GFRP_R$	0.50	11,525		103,829	-1,877							
25	.38GR-3	3/8" $GFRP_R$	0.25	11,950		107,658	1,952							
				11,733	**Avg.**	**105,706**	**1.812%**	1916						
4	.50GR-1	1/2" $GFRP_R$							N/A	23,500		118,090	-251	
5	.50GR-2	1/2" $GFRP_R$							N/A	23,600		118,593	251	
										23,550	**Avg.**	**118,342**	**0.300%**	355
3	.50GS-1	1/2" $GFRP_S$							N/A	19,000		96,939	0	
										19,000	**Avg.**	**96,939**	**0.000%**	0

[1] Graph Included

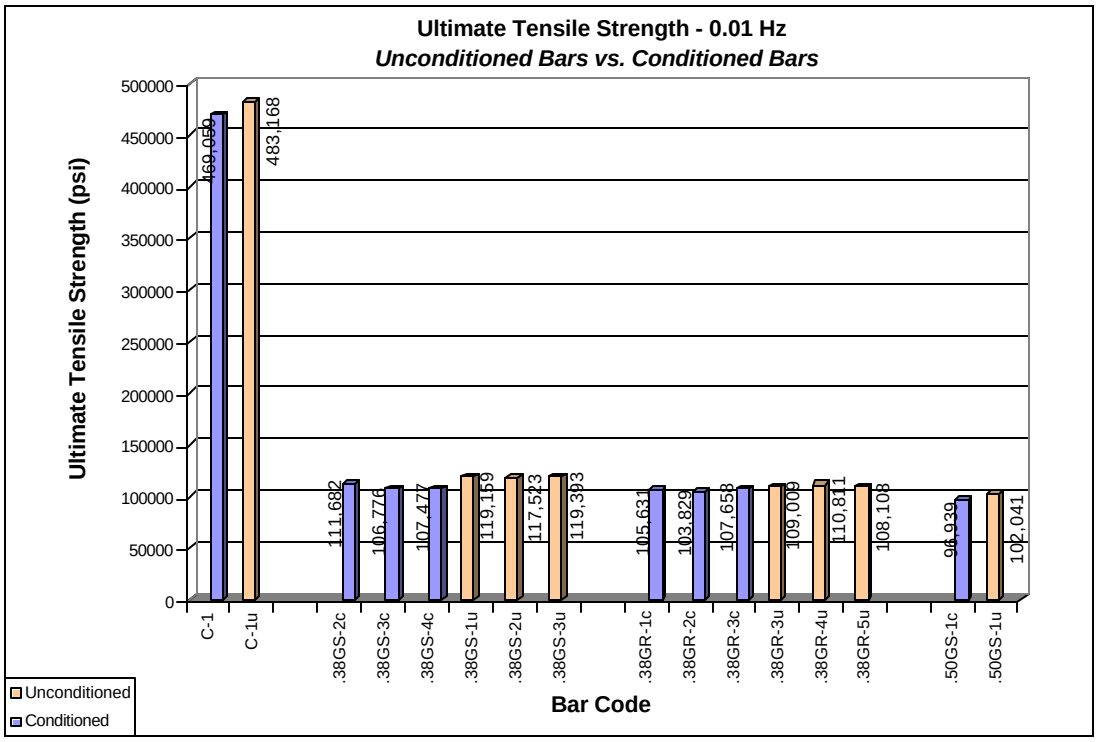
Ultimate Tensile Strength - 0.01 Hz
Unconditioned Bars vs. Conditioned Bars
Ultimate Tensile Strength (psi)
500000
450000
400000
350000
300000
250000
200000
150000
100000
50000
0
469,059
483,168
111,682
106,776
107,477
119,159
117,523
119,393
105,631
103,829
107,653
109,009
110,811
108,108
96,939
102,041
C-1
C-1u
.38GS-2c
.38GS-3c
.38GS-4c
.38GS-1u
.38GS-2u
.38GS-3u
.38GR-1c
.38GR-2c
.38GR-3c
.38GR-3u
.38GR-4u
.38GR-5u
.50GS-1c
.50GS-1u
Bar Code
Unconditioned
Conditioned

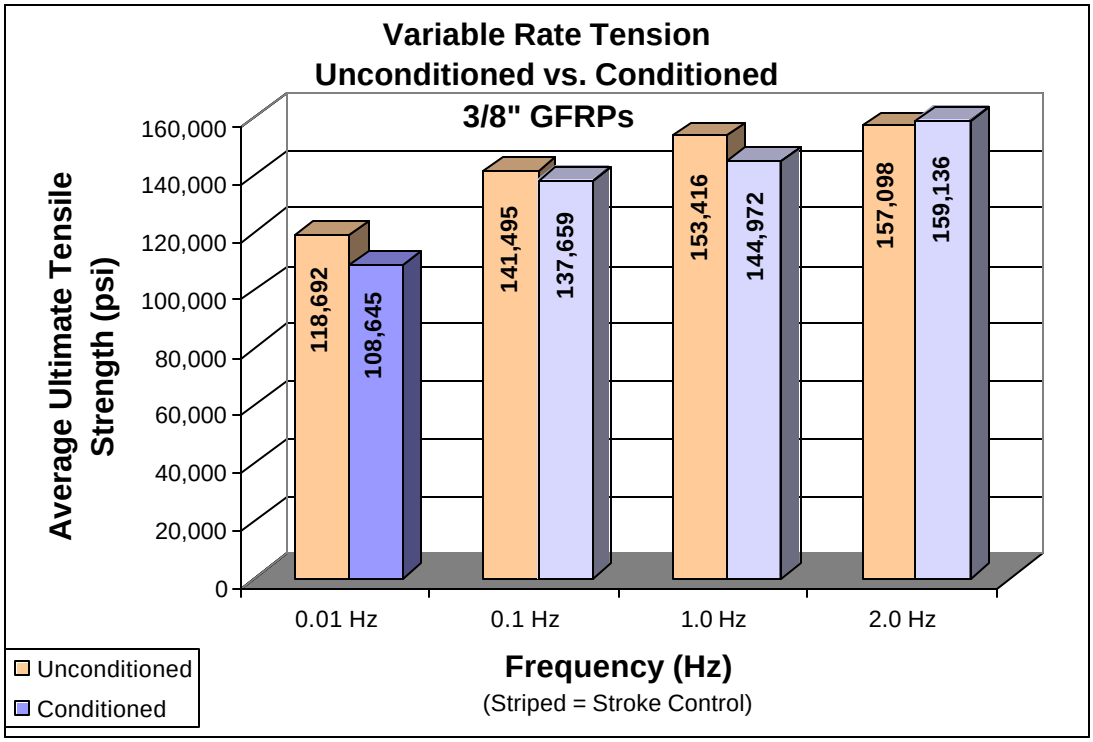
Variable Rate Tension
Unconditioned vs. Conditioned
3/8" GFRPs
Average Ultimate Tensile Strength (psi)
160,000
140,000
120,000
100,000
80,000
60,000
40,000
20,000
0
118,692
108,645
141,495
137,659
153,416
144,972
157,098
159,136
0.01 Hz
0.1 Hz
1.0 Hz
2.0 Hz
Frequency (Hz)
(Striped = Stroke Control)
Unconditioned
Conditioned

Table B3: Axial Tension, Variable Load Rate, 3/8”GFRPs

Pre-Conditioning: UNCONDITIONED

Test Environment: Room temperature, RH = 13%, Load Rate ~ Variable

Bar #	Code	Type	Extension (in)	Tensile Load Maximum (lbs)	24"	Tensile Strength Nominal (psi)	COV (%)	SD	Load Type	Actual/Prog Frequency	# Cyc/ Fail	End Level 1	End Level 2	Fail Time (sec)
0.01 Hz frequency, 50.00 sec failure:									Load Control					
B	.38GS-1u	3/8" $GFRP_S$	-	12,750		119,159	467		Rate	250 lb/sec	0.5	0 lbs	-	51.00
6	.38GS-2u	3/8" $GFRP_S$	-	12,575		117,523	-1,168		Rate	250 lb/sec	0.5	0 lbs	-	50.00
12	.38GS-3u	3/8" $GFRP_S$	-	12,775		119,393	701		Rate	250 lb/sec	0.5	0 lbs	-	51.00
				12,700	**Avg.**	**118,692**	**0.858%**	1018						
0.1 Hz frequency, 5.00 sec failure:									Load Control					
52	.38GS-7u	3/8" $GFRP_S$	0.397	14,951		139,729	-1,766		Rate	2450/2600 lb/s	0.5	0 lbs	-	5.90
53	.38GS-8u	3/8" $GFRP_S$	0.437	15,725		146,963	5,467		Rate	2800/3000 lb/s	0.5	0 lbs	-	5.40
54	.38GS-9u	3/8" $GFRP_S$	0.465	14,744		137,794	-3,701		Rate	2900/3200 lb/s	0.5	0 lbs	-	4.90
				15,140	**Avg.**	**141,495**	**3.415%**	4833						
1 Hz frequency, 0.50 sec failure:									Load Control					
58	.38GS-13u	3/8" $GFRP_S$	0.453	16,734		156,393	2,977		Ramp	0.66/10 Hz	0.5	20000 lbs	10000 lbs	0.76
59	.38GS-14u	3/8" $GFRP_S$	0.440	16,097		150,439	-2,977		Ramp	0.68/10 Hz	0.5	18000 lbs	16000 lbs	0.74
				16,416	**Avg.**	**153,416**	**2.744%**	4210						
2 Hz frequency, 0.25 sec failure:									Load Control					
57	.38GS-12u	3/8" $GFRP_S$	0.448	16,345		152,757	-4,341		Ramp	1.43/2 Hz	0.5	33000 lbs	0 lbs	0.35
39	.38GS-4u	3/8" $GFRP_S$	0.452	17,274		161,439	4,341		Ramp	1.6/2 Hz	0.5	25,000 lbs	0 lbs	0.31
				16,810	**Avg.**	**157,098**	**3.908%**	6139						

[1]Graph Included

Table B4: Axial Tension, Variable Load Rate, 3/8”GFRPs

Cycle Temperature	Cycle Time	# of Cycles	Test Environment:
-20 °F to 68 °F	3 hr/cycle; 8 cycles/day	250	Room temperature, RH = 13%, Load Rate ~ 200 lb/sec ~ .01 Hz

Bar #	Code	Type	Tensile Load Extension (in)	Tensile Load Maximum (lbs)	24"	Tensile Strength Nominal (psi)	COV (%)	SD	Load Type	Program Frequency	# Cyc/ Fail	End Level 1	End Level 2	Fail Time (sec)
0.01 Hz frequency, 50.00 sec failure:									Load Control					
19	.38GS-2	3/8" $GFRP_S$	0.56	11,950		111,682	3.037		Rate	250 lb/sec	0.5	0 lbs	-	48.00
20	.38GS-3	3/8" $GFRP_S$	0.00	11,425		106,776	-1,869		Rate	250 lb/sec	0.5	0 lbs	-	46.00
21	.38GS-4	3/8" $GFRP_S$	0.00	11,500		107,477	-1,168		Rate	250 lb/sec	0.5	0 lbs	-	46.00
				11,625	**Avg.**	**108,645**	**2.443%**	2654						
0.1 Hz frequency, 5.00 sec failure:									Stroke Control					
30	.38GS-6	3/8" $GFRP_S$	0.387	14,482		135,346	-2,313		Rate	0.1 in/sec	0.5	0 in	1 in	3.91
31	.38GS-7	3/8" $GFRP_S$	0.408	14,493		135,449	-2,210		Rate	0.1 in/sec	0.5	0 in	1 in	4.58
32	.38GS-8	3/8" $GFRP_S$	0.411	15,216		142,206	4,547		Rate	0.1 in/sec	0.5	0 in	1 in	4.16
33	.38GS-9	3/8" $GFRP_S$	0.434	14,727		137,636	-23		Rate	0.1 in/sec	0.5	0 in	1 in	4.40
				14,730	**Avg.**	**137,659**	**2.332%**	3210						
1 Hz frequency, 0.50 sec failure:									Stroke Control					
36	.38GS-12	3/8" $GFRP_S$	0.446	15,636		146,131	1,159		Rate	1 in/sec	0.5	0 in	1 in	0.43
27	.38GS-5	3/8" $GFRP_S$	0.427	15,388		143,813	-1,159		Rate	1 in/sec	0.5	0 in	1 in	0.48
				15,512	**Avg.**	**144,972**	**1.130%**	1639						
2 Hz frequency, 0.25 sec failure:									Stroke Control					
34	.38GS-10	3/8" $GFRP_S$	0.445	16,538		154,561	-4,575		Rate	10 in/sec	0.5	0 in	1 in	0.24
46	.38GS-13	3/8" $GFRP_S$	0.499	17,095		159,766	631		Rate	10 in/sec	0.5	0 in	1 in	0.26
47	.38GS-14	3/8" $GFRP_S$	0.479	16,665		155,748	-3,388		Rate	10 in/sec	0.5	0 in	1 in	0.25
48	.38GS-15	3/8" $GFRP_S$	0.520	17,812		166,467	7,332		Rate	10 in/sec	0.5	0 in	1 in	0.28
				17,028	**Avg.**	**159,136**	**3.375%**	5371						

[1]Graph Included

Table B5: Axial Tension, Variable Load Rate, 3/8”GFRPr

Pre-Conditioning: UNCONDITIONED

Test Environment: Room temperature, RH = 13%, Load Rate ~ Variable

Bar #	Code	Type	Extension (in)	Tensile Load Maximum (lbs)	24"	Tensile Strength Nominal (psi)	COV (%)	SD	Load Type	Program Frequency	# Cyc/ Fail	End Level 1	End Level 2	Fail Time (sec)
0.01 Hz frequency, 50.00 sec failure:									Load Control					
28	.38GR-3u	3/8" $GFRP_R$	0.500	12,100		109,009	-300		Rate	250 lb/sec	0.5	0 lbs	-	48.00
29	.38GR-4u	3/8" $GFRP_R$	0.000	12,300		110,811	1,502		Rate	250 lb/sec	0.5	0 lbs	-	49.00
37	.38GR-5u	3/8" $GFRP_R$	0.380	12,000		108,108	-1,201		Rate	250 lb/sec	0.5	0 lbs	-	48.00
				12,133	**Avg.**	**109,309**	**1.259%**	1376						
0.1 Hz frequency, 5.00 sec failure:									Stroke Control					
78[23]	*.38GR-13u*	*3/8" $GFRP_R$*	*0.474*	*16,317*		*147,000*	*-901*		*Ramp Rate*	*0.1 in/sec*	*0.5*	*0 in*	*1 in*	*4.77*
79[23]	*.38GR-14u*	*3/8" $GFRP_R$*	*0.644*	*16,648*		*149,982*	*2,081*		*Ramp Rate*	*0.1 in/sec*	*1.5*	*0 in*	*1 in*	*3.28*
80[23]	*.38GR-15u*	*3/8" $GFRP_R$*	*0.664*	*16,286*		*146,721*	*-1,180*		*Ramp Rate*	*0.1 in/sec*	*1.5*	*0 in*	*1 in*	*3.24*
				16,417	**Avg.**	**147,901**	**1.222%**	1808						
1 Hz frequency, 0.50 sec failure:									Stroke Control					
60	.38GR-9u	3/8" $GFRP_R$	0.423	15,346		138,252	-16,276		Haversine	1 in/sec	0.5	0 in	1 in	0.55
81[23]	*.38GR-16u*	*3/8" $GFRP_R$*	*0.544*	*17,794*		*160,306*	*5,778*		*Ramp Rate*	*1 in/sec*	*0.5*	*0 in*	*1 in*	*0.58*
82[23]	*.38GR-17u*	*3/8" $GFRP_R$*	*0.543*	*18,318*		*165,027*	*10,498*		*Ramp Rate*	*1 in/sec*	*0.5*	*0 in*	*1 in*	*0.60*
				17,153	**Avg.**	**154,529**	**9.249%**	14292						
2 Hz frequency, 0.25 sec failure:									Stroke Control					
62	.38GR-11u	3/8" $GFRP_R$	0.424	15,983		143,991	-12,060		Ramp Rate	5 in/sec	0.5	0 in	1 in	0.23
63	.38GR-12u	3/8" $GFRP_R$	0.494	16,810		151,441	-4,610		Ramp Rate	10 in/sec	0.5	0 in	1 in	0.27
83[23]	*.38GR-18u*	*3/8" $GFRP_R$*	*0.574*	*19,172*		*172,721*	*16,670*		*Ramp Rate*	*5 in/sec*	*0.5*	*0 in*	*1 in*	*0.29*
				17,322	**Avg.**	**156,051**	**9.554%**	14909						

[1] Graph Included

[2] Epoxy filled grip anchor.

[3] *Bar slipped in end grip anchor.*

Table B6: Axial Tension, Variable Load Rate, 3/8”GFRPr

Cycle Temperature	Cycle Time	# of Cycles	Test Environment:
-20 °F to 68 °F	3 hr/cycle; 8 cycles/day	250	Room temperature, RH = 13%, Load Rate ~ Variable

Bar #	Code	Type	Tensile Load 24" Extension (in)	Tensile Load 24" Maximum (lbs)	Tensile Strength Nominal (psi)	Tensile Strength COV (%)	Tensile Strength SD	Load Type	Program Frequency	# Cyc/ Fail	End Level 1	End Level 2	Fail Time (sec)
0.01 Hz frequency, 50.00 sec failure:								Load Control					
17	.38GR-1	3/8" $GFRP_R$	0.56	11,725	105,631	-75		Rate	250 lb/sec	0.5	0 lbs	-	47.00
18	.38GR-2	3/8" $GFRP_R$	0.50	11,525	103,829	-1,877		Rate	250 lb/sec	0.5	0 lbs	-	46.00
25	.38GR-3	3/8" $GFRP_R$	0.25	11,950	107,658	1,952		Rate	250 lb/sec	0.5	0 lbs	-	48.00
				11,733	**Avg. 105,706**	**1.812%**	1916						

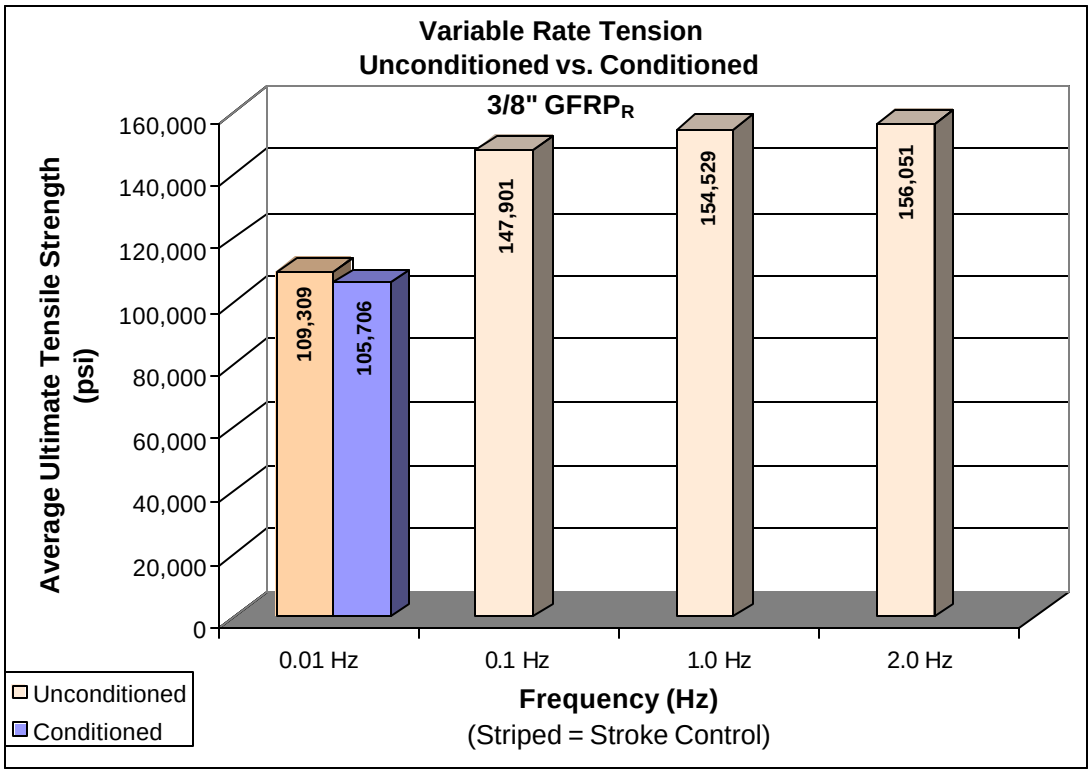
Variable Rate Tension
Unconditioned vs. Conditioned
3/8" GFRP$_R$
Average Ultimate Tensile Strength (psi)
160,000
140,000
120,000
100,000
80,000
60,000
40,000
20,000
0
109,309
105,706
147,901
154,529
156,051
0.01 Hz
0.1 Hz
1.0 Hz
2.0 Hz
Frequency (Hz)
(Striped = Stroke Control)
Unconditioned
Conditioned

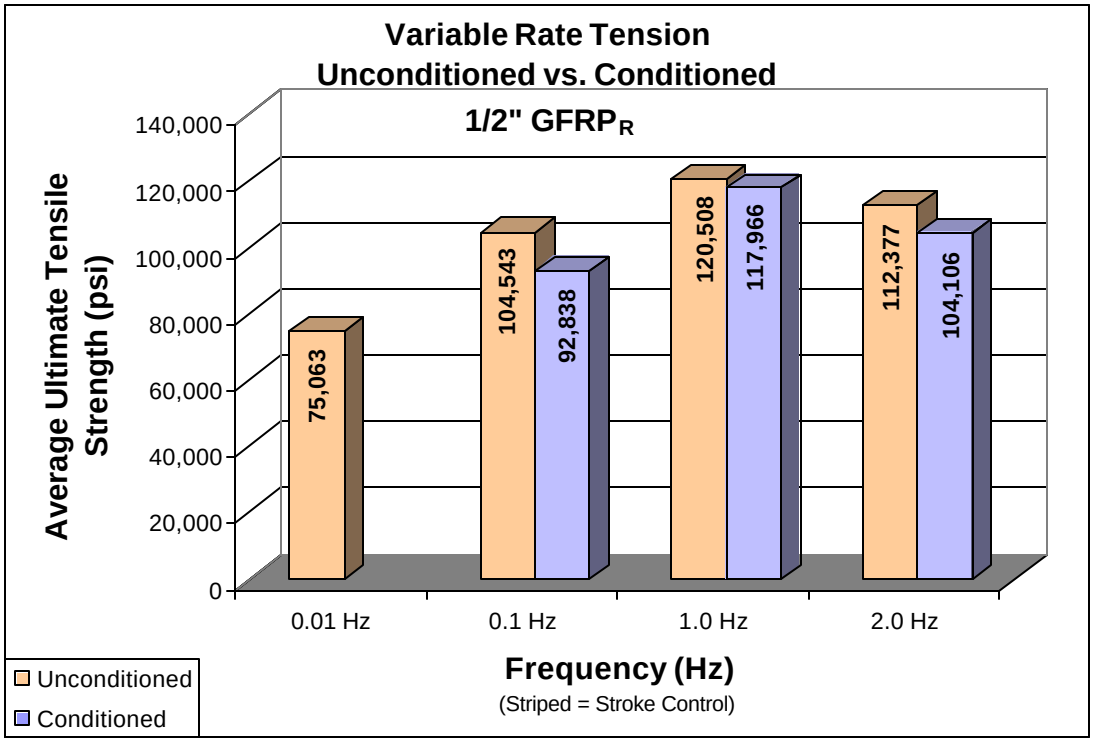
Variable Rate Tension
Unconditioned vs. Conditioned
1/2" GFRP$_R$
Average Ultimate Tensile Strength (psi)
140,000
120,000
100,000
80,000
60,000
40,000
20,000
0
75,063
104,543
92,838
120,508
117,966
112,377
104,106
0.01 Hz
0.1 Hz
1.0 Hz
2.0 Hz
Frequency (Hz)
(Striped = Stroke Control)
Unconditioned
Conditioned

Table B7: Axial Tension, Variable Load Rate, 1/2"GFRPr

Pre-Conditioning: UNCONDITIONED

Test Environment:
Room temperature, RH = 13%, Load Rate ~ Variable

Bar #	Code	Type	Extension (in)	Tensile Load Maximum (lbs)	24"	Tensile Strength Nominal (psi)	COV (%)	SD	Load Type	Actual/Prog Frequency	# Cyc Fail / Tot Cyc	End Level 1	End Level 2	Fail Time (sec)
0.01 Hz frequency, 50.00 sec failure:									Load Control					
41	.50GR-3u	1/2" $GFRP_R$	-	15,450		77,638	2,575		Rate	250 lb/sec	0.5	0 lbs	-	62.00
42	.50GR-4u	1/2" $GFRP_R$	-	14,425		72,487	-2,575		Rate	250 lb/sec	0.5	0 lbs	-	58.00
				14,938	**Avg.**	**75,063**	**4.852%**	3642						
0.1 Hz frequency, 5.00 sec failure:									Load Control					
64	.50GR-5u	1/2" $GFRP_R$	0.378	20,804		104,543	-1,470		Ramp Rate	5000 lb/sec	0.5	25,000 lbs	-	4.29
65[2]	*.50GR-6u*	*1/2" GFRP R*	*0.670*	*22,615*		*113,643*	*7,631*		*Ramp Freq*	*0.1/0.1 Hz*	*1.5/3*	*25,000 lbs*	*20,000 lbs*	*5.06*
66[2]	*.50GR-7u*	*1/2" GFRP R*	*0.559*	*21,258*		*106,824*	*812*		*Ramp Freq*	*0.13/0.1 Hz*	*1.5/3*	*30,000 lbs*	*25,000 lbs*	*3.97*
77[2]	*.50GR-18u*	*1/2" GFRP R*	*0.553*	*19,709*		*99,040*	*-6,972*		*Stroke: Ramp Rate*	*.1in/sec*	*1.5/3*	*0"*	*1"*	*5.58*
				21,097	**Avg.**	**106,013**	**5.703%**	6046						
1 Hz frequency, 0.50 sec failure:									Load Control					
67	.50GR-8u	1/2" $GFRP_R$	0.472	23,981		120,508	11,560		Ramp Freq	0.97/1.0 Hz	2.5/3	25,000 lbs	20,000 lbs	2.58
68[2]	*.50GR-9u*	*1/2" GFRP R*	*0.418*	*22,983*		*115,492*	*6,545*		*Ramp Freq*	*0.85/1.0 Hz*	*.5/2*	*30,000 lbs*	*25,000 lbs*	*0.59*
69[2]	*.50GR-10u*	*1/2" GFRP R*	*0.503*	*19,268*		*96,824*	*-12,123*		*Ramp Freq*	*0.82/1.0 Hz*	*.5/2*	*30,000 lbs*	*25,000 lbs*	*0.61*
76[2]	*.50GR-17u*	*1/2" GFRP R*	*0.532*	*20,490*		*102,965*	*-5,982*		*Stroke: Ramp Rate*	*1in/sec*	*1.5/2*	*0"*	*1"*	*0.58*
				21,681	**Avg.**	**108,947**	**10.044%**	10943						
2 Hz frequency, 0.05 sec failure:									Load Control					
70[2]	*.50GR-11u*	*1/2" GFRP R*	*0.411*	*22,363*		*112,377*	*0*		*Ramp Freq*	*1.4/10 Hz*	*.5/2*	*30,000 lbs*	*25,000 lbs*	*0.36*
				22,363	**Avg.**	**112,377**	**0.000%**	0						

[1]Graph Included
[2]*Bar slipped in end grip anchor.*

Table B8: Axial Tension, Variable Load Rate, 1/2”GFRPr

Cycle Temperature	Cycle Time	# of Cycles	Test Environment:
-20 °F to 68 °F	3 hr/cycle; 8 cycles/day	250	Room temperature, RH = 13%, Load Rate ~ Variable

Bar #	Code	Type	Tensile Load 24" Extension (in)	Tensile Load Maximum (lbs)		Tensile Strength Nominal (psi)	COV (%)	SD	Load Type	Program Frequency	# Cyc-Fail	End Level 1	End Level 2	Fail Time (sec)
0.01 Hz frequency, 50.00 sec failure:														
0.1 Hz frequency, 5.00 sec failure:									Stroke Control					
14	.50GR-4	1/2" $GFRP_R$	0.285	17,653		88,709	-4,129		Ramp Rate	.1 in/sec	0.5	0"	1"	2.89
15	.50GR-5	1/2" $GFRP_R$	0.233	18,414		92,533	-305		Ramp Rate	.1 in/sec	0.5	0"	1"	4.81
23	.50GR-7	1/2" $GFRP_R$	0.338	19,357		97,271	*4,434*		Ramp Rate	.1 in/sec	0.5	0"	1"	5.06
				18,475	**Avg.**	**92,838**	**4.620%**	4290						
1 Hz frequency, 0.50 sec failure:									Stroke Control					
43	.50GR-9	1/2" $GFRP_R$	0.391	23,059		115,874	-2,092		Ramp Rate	1 in/sec	0.5	0"	1"	0.45
44	.50GR-10	1/2" $GFRP_R$	0.407	24,109		121,151	3,184		Ramp Rate	1 in/sec	0.5	0"	1"	0.46
45	.50GR-11	1/2" $GFRP_R$	0.390	23,258		116,874	*-1,092*		Ramp Rate	1 in/sec	0.5	0"	1"	0.44
				23,475	**Avg.**	**117,966**	**2.376%**	2803						
2 Hz frequency, 0.25 sec failure:									Stroke Control					
24	.50GR-8	1/2" $GFRP_R$	0.362	20,717		104,106	0		Ramp Rate	10 in/sec	0.5	0"	1"	0.20
				20,717	**Avg.**	**104,106**	**0.000%**	0						

[1]Graph Included

Table B9: Fatigue Test, Variable Load Rate

			Pre-Conditioning: VARIABLE						Test Environment: Room temperature, RH = 13%, Load Rate ~ Variable					
				Residual Load	**24"**	**Residual Strength**			Load Type	Prog/Actual Frequency	Cycle End Level 1		Cycle End Level 2	
Bar #	**Code**	**Type**	Extension (in)	Maximum (lbs)		Nominal (psi)	Cycles #	Cycled Failure						
											5 Hz: Projected Average Max~17,500 lbs			
Unconditioned:											30%	Prog:5,000	Prog:10,000	60%
49	.38GS-5u	3/8" $GFRP_S$	0.436	14,696	0.01Hz	137,346	985,000	No	Haversine	5Hz / 5Hz	42%	7,350 lbs	8,000 lbs	46%
50	.38GS-6u	3/8" $GFRP_S$	0.419	13,081	0.01Hz	122,252	765,374	No	Haversine	5Hz / 5Hz		Actual Mean = 7,265 lbs		
51[1] -1	*.38GS-7u*	*3/8" GFRP s*	*0.277*	*-*		*-*	*598,817*	***No***	*Haversine*	*5Hz / 5Hz*	*47%*	*8,250 lbs*	*9,150 lbs*	*52%*
51[1] -2			*0.244*	*-*		*-*	*47,130*	***Yes***	*Haversine*	*4.99Hz / 5Hz*	*47%*	*~8,250 lbs*	*~9,150 lbs*	*52%*
											2 Hz: Average Maximum~17,000 lbs			
											30%	Prog:5,000	Prog:10,000	60%
11	.38GR-1u	3/8" $GFRP_R$	0.229	-		-	3000	No	Ramp	5Hz /1.7Hz	36%	6,130 lbs	9,951 lbs	59%
											5 Hz: Proj Avg Max ~18,000-20,000 lb			
											7%	Prog:1,250	Prog:6,250	35%
38	.38GR-6u	3/8" $GFRP_R$	0.468	17,150	2 Hz	154,505	500	No	Ramp	5Hz / 4.5Hz	19%	3,677 lbs	4,193 lbs	22%
				Failure Load @ 6.5 Cycles:										
72	.50GR-13u	1/2" $GFRP_R$	0.594	25,031		125,784	6.5	**Yes**	Haversine	5Hz / 4.8Hz	-	-	-	-
				Maximum Load @ 0.5 cycles:								Prog: 10,600	Prog: 20,000	
10	.50GR-2u	1/2" $GFRP_R$	0.287	19,805		99,523	449	**Yes**		5Hz / 1.74Hz		13,769 lbs	17,070 lbs	
											5 Hz: Projected Average Max~25,000 lbs			
				Failure Load @ 77 Cycles:							35%	Prog: 9050	Prog: 18105	70%
75-1	.50GR-16u	1/2" $GFRP_R$		-		-	2,682	No	Haversine	5Hz/4.95Hz				
75-2			0.850	19,216		96,563	77	**Yes**	Haversine	5Hz/3.43Hz	42%	9,598 lbs	17,465 lbs	77%

[1]Italic: *Bar slipped in end grip anchor.*

Table B10: Creep Tests, Variable Load Rate

Bar #	Code	Type	Max Load Extension (in)	**Tensile Load** Maximum (lbs)	**24" Tensile Strength** Nominal (psi)	Average Extension (in)	Average Sustained Load (lbs)	Time Load Sustained (sec)	Time to Load (sec)	Load Rate	Load Type
Unconditioned:											
7	.50GR-1u	1/2" $GFRP_R$	0.304	20,252	101,769	0.307	20,226	23.19	10.65	1900 lb/sec	Ramp
73	.50GR-14u	1/2" $GFRP_R$	0.929	23,386	117,518	0.575	21,938	6.81	0.51	1 Hz	Haversine
74	.50GR-15u	1/2" $GFRP_R$	0.560	22,904	115,095	0.561	22,863	44.65	0.96	0.5 Hz	Haversine

[1] Graph Included

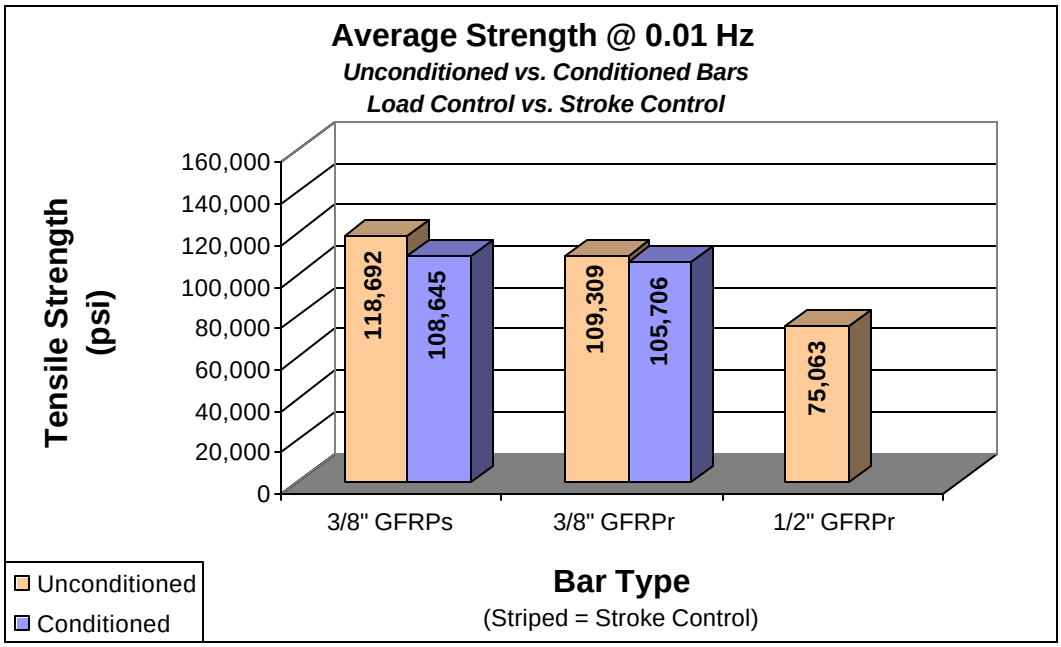
Average Strength @ 0.01 Hz
Unconditioned vs. Conditioned Bars
Load Control vs. Stroke Control
Tensile Strength (psi)
160,000
140,000
120,000
100,000
80,000
60,000
40,000
20,000
0
118,692
108,645
109,309
105,706
75,063
3/8" GFRPs
3/8" GFRPr
1/2" GFRPr
Bar Type
(Striped = Stroke Control)
Unconditioned
Conditioned

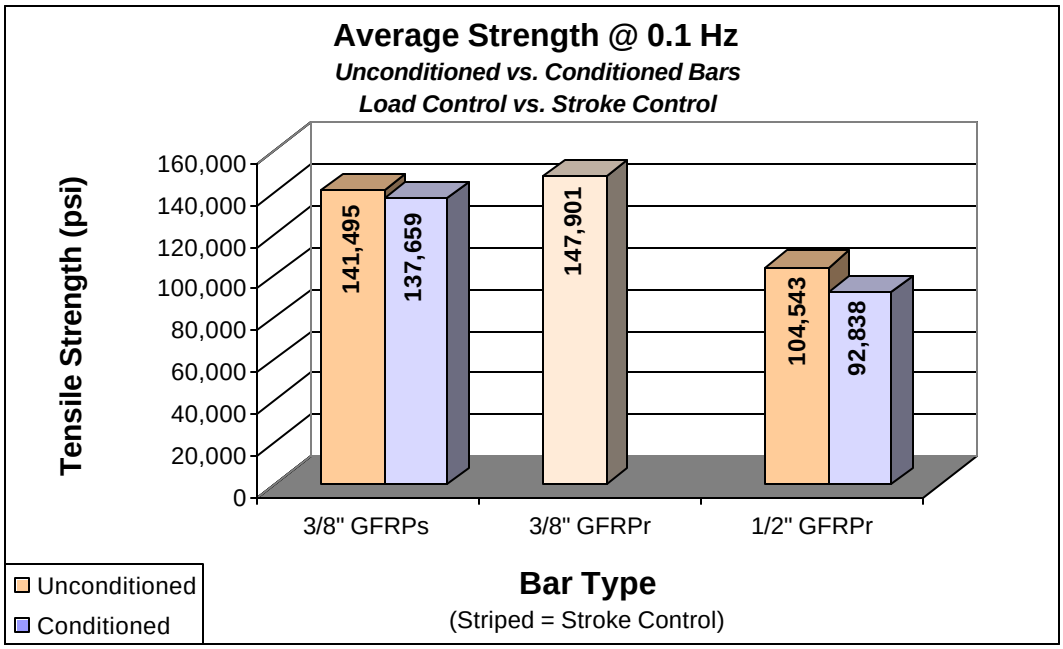
Average Strength @ 0.1 Hz
Unconditioned vs. Conditioned Bars
Load Control vs. Stroke Control
Tensile Strength (psi)
160,000
140,000
120,000
100,000
80,000
60,000
40,000
20,000
0
141,495
137,659
147,901
104,543
92,838
3/8" GFRPs
3/8" GFRPr
1/2" GFRPr
Bar Type
(Striped = Stroke Control)
Unconditioned
Conditioned

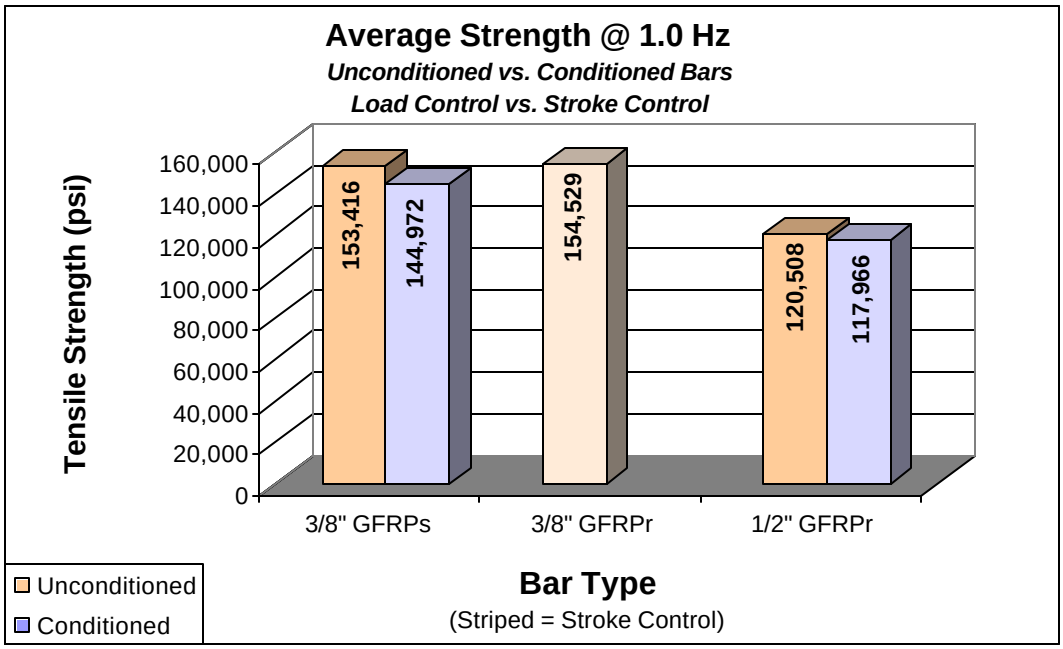
Average Strength @ 1.0 Hz
Unconditioned vs. Conditioned Bars
Load Control vs. Stroke Control
Tensile Strength (psi)
160,000
140,000
120,000
100,000
80,000
60,000
40,000
20,000
0
153,416
144,972
154,529
120,508
117,966
3/8" GFRPs
3/8" GFRPr
1/2" GFRPr
Unconditioned
Conditioned
Bar Type
(Striped = Stroke Control)

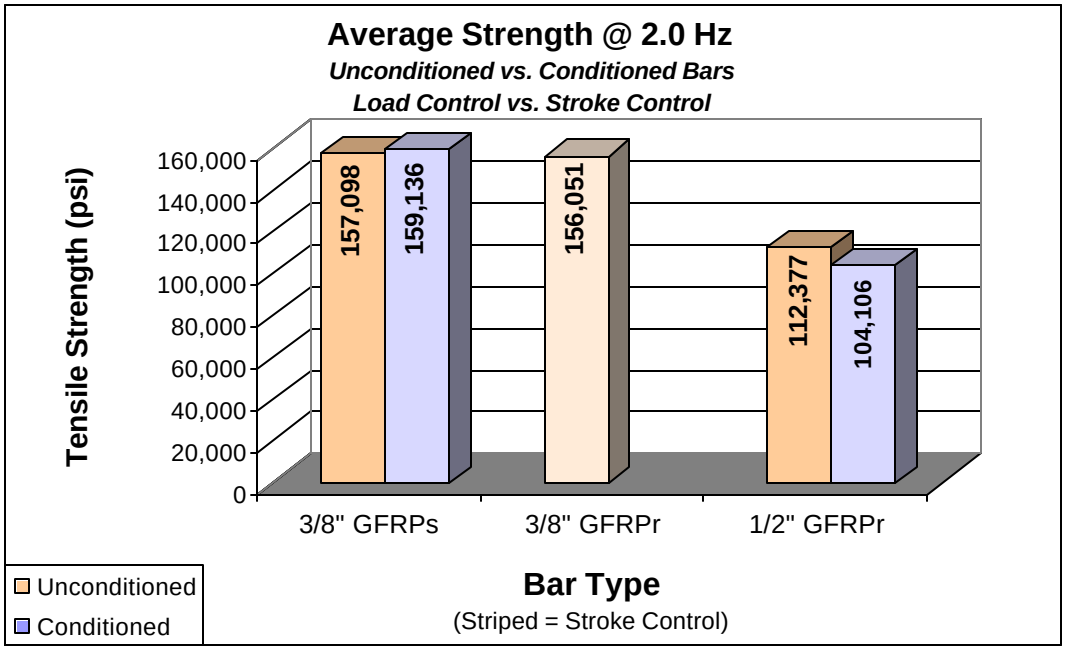
Average Strength @ 2.0 Hz
Unconditioned vs. Conditioned Bars
Load Control vs. Stroke Control
Tensile Strength (psi)
160,000
140,000
120,000
100,000
80,000
60,000
40,000
20,000
0
157,098
159,136
156,051
112,377
104,106
3/8" GFRPs
3/8" GFRPr
1/2" GFRPr
Unconditioned
Conditioned
Bar Type
(Striped = Stroke Control)

Table B11: Axial Tension, Variable Load Rate, 3/8"GFRPs

Bar #	Code	Type	Failure Load	Failure Stress		Extension at Rupture	Original Length			Elongation	Corr. Coef.	Average Displacement Stiffness	Average Tensile Modulus	Corr. Coef.
			Maximum	Nominal				SD	COV		R^2		Slope, M	R^2
UNCONDITIONED			(lbs)	(psi)		(in)	(in)		(%)	(%)		(lb/in)	(ksi)	
0.1 Hz frequency:														
52	.38GS-7u	3/8" $GFRP_S$	14,951	139,729		0.397	23.69		-0.14	1.68%				
53	.38GS-8u	3/8" $GFRP_S$	15,725	146,963		0.437	23.88		0.01	1.83%				
54	.38GS-9u	3/8" $GFRP_S$	14,744	137,794		0.465	23.69		0.14	1.96%				
1 Hz frequency:					**Avg.**	**0.433**	**23.75**	0.1402	**7.70%**	**1.82%**	0.990	35.910	8006.3	0.990
58	.38GS-13u	3/8" $GFRP_S$	16,734	156,393		0.453	23.63		0.04	1.92%				
59	.38GS-14u	3/8" $GFRP_S$	16,097	150,439		0.440	23.75		-0.03	1.85%				
2 Hz frequency:					**Avg.**	**0.447**	**23.69**	0.0500	**2.66%**	**1.88%**	0.997	35.885	7999.0	0.996
57	.38GS-12u	3/8" $GFRP_S$	16,345	152,757		0.448	23.69		-0.01	1.89%				
39	.38GS-4u	3/8" $GFRP_S$	17,274	161,439		0.452	23.80		0.00	1.90%				
CONDITIONED					**Avg.**	**0.450**	**23.75**	0.0100	**0.53%**	**1.90%**	0.998	37.274	8283.6	0.998
0.1 Hz frequency:										**3/8" GFRPs Average:**		**35.951**	**8016.4**	
30	.38GS-6	3/8" $GFRP_S$	14,482	135,346		0.387	23.94		-0.11	1.62%				
31	.38GS-7	3/8" $GFRP_S$	14,493	135,449		0.408	23.06		0.04	1.77%				
32	.38GS-8	3/8" $GFRP_S$	15,216	142,206		0.411	23.81		0.00	1.73%				
33	.38GS-9	3/8" $GFRP_S$	14,727	137,636		0.434	23.75		0.10	1.83%				
1 Hz frequency:					**Avg.**	**0.410**	**23.64**	0.0889	**5.14%**	**1.73%**	0.987	34.910	7694.1	0.985
36	.38GS-12	3/8" $GFRP_S$	15,636	146,131		0.446	23.75		0.05	1.88%				
27	.38GS-5	3/8" $GFRP_S$	15,388	143,813		0.427	23.94		-0.05	1.78%				
2 Hz frequency:					**Avg.**	**0.437**	**23.85**	0.0707	**3.86%**	**1.83%**	0.993	35.281	7874.3	0.992
34	.38GS-10	3/8" $GFRP_S$	16,538	154,561		0.445	23.69		-0.09	1.88%				
46	.38GS-13	3/8" $GFRP_S$	17,095	159,766		0.499	23.81		0.13	2.10%				
47	.38GS-14	3/8" $GFRP_S$	16,665	155,748		0.479	23.63		0.06	2.03%				
48	.38GS-15	3/8" $GFRP_S$	17,812	166,467		0.452	23.88		-0.08	1.89%				
					Avg.	**0.469**	**23.75**	0.1080	**5.48%**	**1.97%**	0.990	34.058	7570.1	0.990
										3/8" GFRPs Average:		**34.968**	**7736.5**	

[1] Graph Included

Table B12: Axial Tension, Variable Load Rate, 3/8"GFRPr

Bar #	Code	Type	Failure Load Maximum (lbs)	Failure Stress Nominal (psi)		Extension at Rupture (in)	Original Length (in)	SD	COV (%)	Elongation (%)	Corr. Coef. R^2	Average Displacement Stiffness (lb/in)	Average Tensile Modulus Slope, M (ksi)	Corr. Coef. R^2
UNCONDITIONED														
0.1 Hz frequency:														
78[23]	*.38GR-13u*	*3/8" GFRP R*	*16,317*	*147,000*		*0.474*	*23.75*		*-0.51*	*2.00%*				
79[23]	*.38GR-14u*	*3/8" GFRP R*	*16,648*	*149,982*		*0.644*	*23.63*		*0.22*	*2.73%*				
80[23]	*.38GR-15u*	*3/8" GFRP R*	*16,286*	*146,721*		*0.664*	*23.75*		*0.29*	*2.80%*				
1 Hz frequency:					**Avg.**	**0.594**	**23.71**	0.4431	**17.65%**	**2.51%**	0.989	34.456	7371.8	0.989
60	.38GR-9u	3/8" $GFRP_R$	15,346	138,252		0.423	23.75		-0.33	1.78%				
81[23]	*.38GR-16u*	*3/8" GFRP R*	*17,794*	*160,306*		*0.544*	*24.13*		*0.14*	*2.25%*				
82[23]	*.38GR-17u*	*3/8" GFRP R*	*18,318*	*165,027*		*0.543*	*23.69*		*0.18*	*2.29%*				
2 Hz frequency:					**Avg.**	**0.503**	**23.86**	0.2836	**13.44%**	**2.11%**	0.988	35.199	7580.5	0.988
62	.38GR-11u	3/8" $GFRP_R$	15,983	143,991		0.424	23.81		-0.31	1.78%				
63	.38GR-12u	3/8" $GFRP_R$	16,810	151,441		0.494	23.75		-0.01	2.08%				
83[23]	*.38GR-18u*	*3/8" GFRP R*	*19,172*	*172,721*		*0.574*	*23.88*		*0.31*	*2.40%*				
					Avg.	**0.497**	**23.81**	0.3101	**14.84%**	**2.09%**	0.988	32.129	6919.0	0.988
										3/8" GFRPr Average:		**34.456**	**7389.5**	

[1]Italic: *Bar slipped in end grip anchor.*

Table B13: Axial Tension, Variable Load Rate, 1/2"GFRPr

Bar #	Code	Type	Failure Load Maximum (lbs)	Failure Stress Nominal (psi)		Extension at Rupture (in)	Original Length (in)	SD	COV (%)	Elongation (%)	Corr. Coef. R^2	Average Displacement Stiffness (lb/in)	Average Tensile Modulus Slope, M (ksi)	Corr. Coef. R^2
UNCONDITIONED														
0.1 Hz frequency:														
64	.50GR-5u	1/2" $GFRP_R$	20,804	104,543		0.378	23.75		-0.69	1.59%				
65	.50GR-6u	1/2" $GFRP_R$	22,615	113,643		0.67	23.69		0.55	2.83%				
66	.50GR-7u	1/2" $GFRP_R$	21,258	106,824		0.559	23.75		0.07	2.35%				
77	.50GR-18u	1/2" $GFRP_R$	19,709	99,040		0.553	23.69		0.05	2.33%				
1 Hz frequency:					**Avg.**	**0.540**	**23.72**	0.5119	**22.45%**	**2.28%**	0.990	52.229	6229.9	0.990
67	.50GR-8u	1/2" $GFRP_R$	23,981	120,508		0.472	23.69		-0.04	1.99%				
68	.50GR-9u	1/2" $GFRP_R$	22,983	115,492		0.418	23.63		-0.26	1.77%				
69	.50GR-10u	1/2" $GFRP_R$	19,268	96,824		0.503	23.75		0.09	2.12%				
76	.50GR-17u	1/2" $GFRP_R$	20,490	102,965		0.532	23.81		0.20	2.23%				
2 Hz frequency:					**Avg.**	**0.481**	**23.72**	0.1977	**9.74%**	**2.03%**	0.981	48.146	5729.1	0.980
70	.50GR-11u	1/2" $GFRP_R$	22,363	112,377		0.411	23.88		0.00	1.72%				
					Avg.	**0.411**	**23.88**	0.0000	**0.00%**	**1.72%**	0.992	51.126	6135.1	0.992
										1/2" GFRPr Average:		**50.818**	**6062.2**	
CONDITIONED														
0.1 Hz frequency:														
14	.50GR-4	1/2" $GFRP_R$	17,653	88,709		0.285	23.38		0.02	1.22%				
15	.50GR-5	1/2" $GFRP_R$	18,414	92,533		0.233	24.00		-0.23	0.97%				
23	.50GR-7	1/2" $GFRP_R$	19,357	97,271		0.338	23.75		0.22	1.42%				
1 Hz frequency:					**Avg.**	**0.285**	**23.71**	0.2255	**18.79%**	**1.20%**	0.991	56.900	6776.0	0.992
43	.50GR-9	1/2" $GFRP_R$	23,059	115,874		0.391	23.81		-0.02	1.64%				
44	.50GR-10	1/2" $GFRP_R$	24,109	121,151		0.407	23.81		0.05	1.71%				
45	.50GR-11	1/2" $GFRP_R$	23,258	116,874		0.390	23.81		-0.02	1.64%				
2 Hz frequency:					**Avg.**	**0.396**	**23.81**	0.0406	**2.45%**	**1.66%**	0.990	59.135	7075.4	0.985
24	.50GR-8	1/2" $GFRP_R$	20,717	104,106		0.362	23.75		0.00	1.52%				
					Avg.	**0.362**	**23.75**	0.0000	**0.00%**	**1.52%**	0.996	55.044	6569.4	0.996
										1/2" GFRPr Average:		**57.463**	**6850.1**	

[1]Graph Included

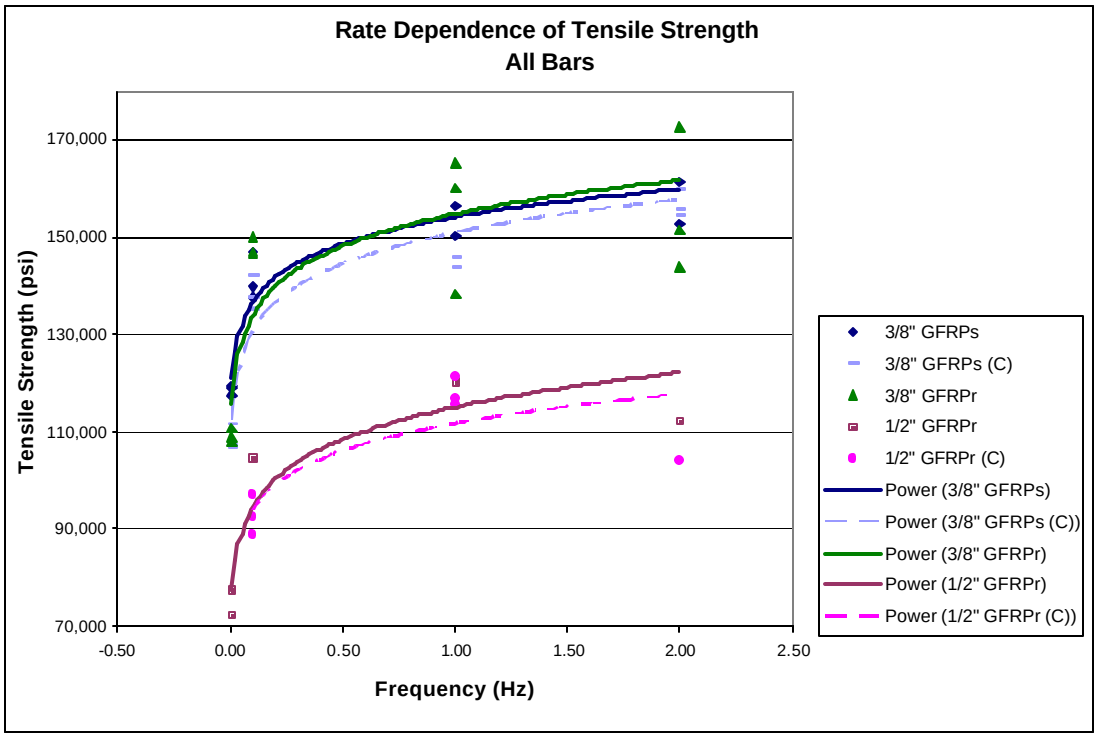
Rate Dependence of Tensile Strength
All Bars
Tensile Strength (psi)
170,000
150,000
130,000
110,000
90,000
70,000
-0.50
0.00
0.50
1.00
1.50
2.00
2.50
Frequency (Hz)
3/8" GFRPs
3/8" GFRPs (C)
3/8" GFRPr
1/2" GFRPr
1/2" GFRPr (C)
Power (3/8" GFRPs)
Power (3/8" GFRPs (C))
Power (3/8" GFRPr)
Power (1/2" GFRPr)
Power (1/2" GFRPr (C))

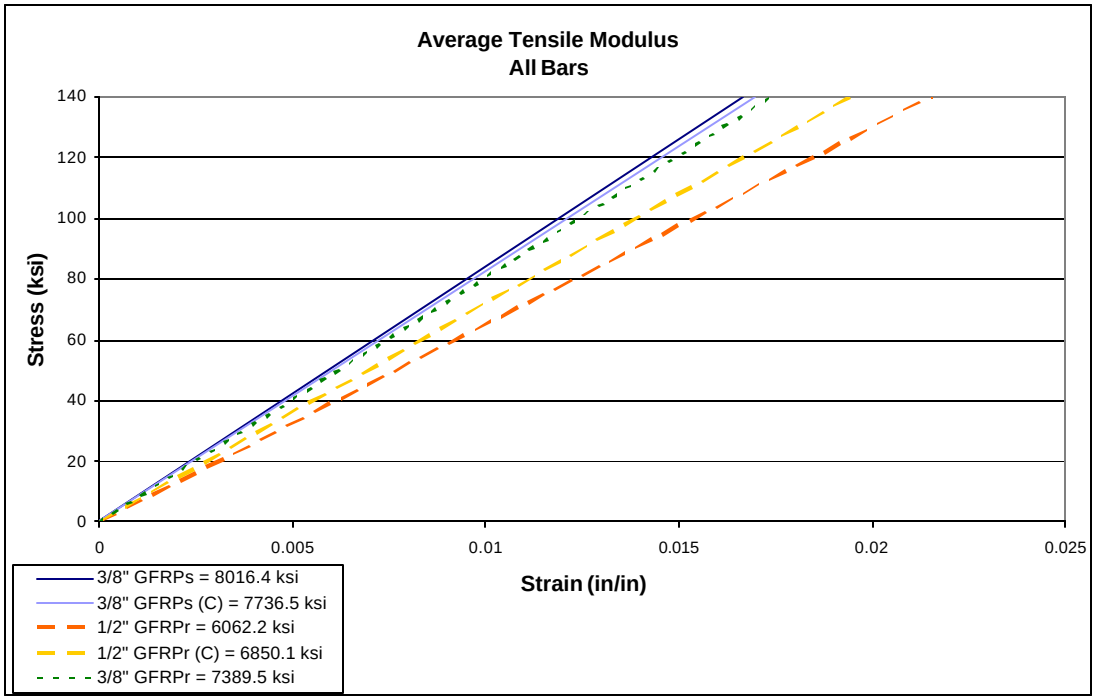
Average Tensile Modulus
All Bars
Stress (ksi)
140
120
100
80
60
40
20
0
0
0.005
0.01
0.015
0.02
0.025
Strain (in/in)
3/8" GFRPs = 8016.4 ksi
3/8" GFRPs (C) = 7736.5 ksi
1/2" GFRPr = 6062.2 ksi
1/2" GFRPr (C) = 6850.1 ksi
3/8" GFRPr = 7389.5 ksi

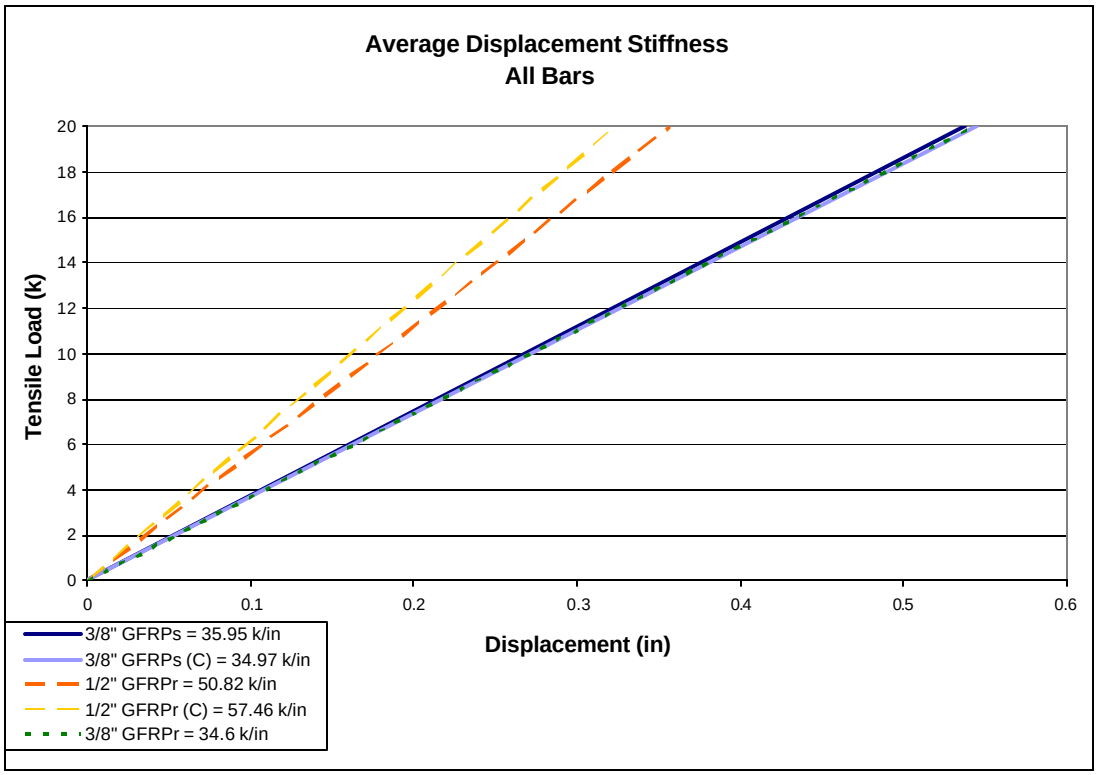
Average Displacement Stiffness
All Bars
Tensile Load (k)
20
18
16
14
12
10
8
6
4
2
0
0
0.1
0.2
0.3
0.4
0.5
0.6
Displacement (in)
3/8" GFRPs = 35.95 k/in
3/8" GFRPs (C) = 34.97 k/in
1/2" GFRPr = 50.82 k/in
1/2" GFRPr (C) = 57.46 k/in
3/8" GFRPr = 34.6 k/in